2022-11-02

EVALUATION OF THE HYDRAULIC PERFORMANCE OF STORMWATER DRAINAGE STRUCTURES IN WORETA TOWN, AMHARA, ETHIOPIA.

MEZMUR, HAWAZ FEKADU

BAHIRDAR UNIVERSITY

BAHIRDAR UNIVERSITY INSTITUTE OF TECHNOLOGY

SCHOOL OF GRADUATE STUDIES

FACULTY OF CIVIL AND WATER RESOURCES ENGINEERING

MASTER OF SCIENCE IN HYDRAULIC ENGINEERING

EVALUATION OF THE HYDRAULIC PERFORMANCE OF STORMWATER DRAINAGE STRUCTURES IN WORETA TOWN, AMHARA, ETHIOPIA.

BY

MEZMUR HAWAZ FEKADU

NOVEMBER 2, 2022

BAHIR DAR, ETHIOPIA

BAHIRDAR UNIVERSITY

BAHIRDAR INSTITUTE OF TECHNOLOGY

SCHOOL OF GRADUATE STUDIES

FACULTY OF CIVIL AND WATER RESOURCES ENGINEERING

EVALUATION OF THE HYDRAULIC PERFORMANCE OF STORMWATER DRAINAGE STRUCTURES IN WORETA TOWN, AMHARA, ETHIOPIA.

BY

MEZMUR HAWAZ FEKADU

A THESIS SUBMITTED IN PARTIAL FULFILLMENT OF THE

REQUIREMENTS FOR THE DEGREE OF MASTER OF SCIENCE

IN HYDRAULIC ENGINEERING

ADVISOR NAME: DR. ASEGDEW GASHAW

NOVEMBER 2, 2022

BAHIR DAR, ETHIOPIA

DECLARATION

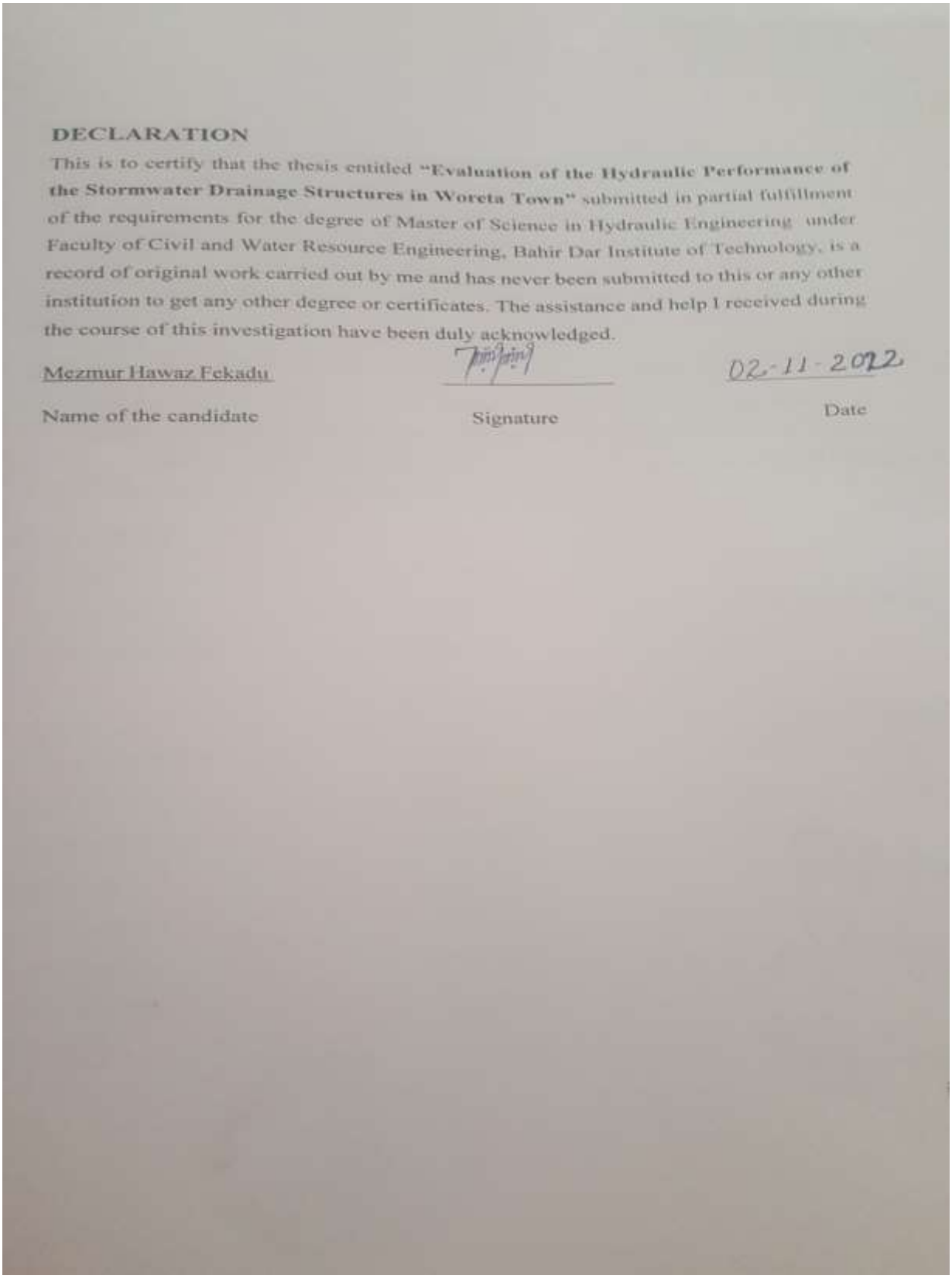

DECLARATION

This is to certify that the thesis entitled **"Evaluation of the Hydraulic Performance of the Stormwater Drainage Structures in Woreta Town"** submitted in partial fulfillment of the requirements for the degree of Master of Science in Hydraulic Engineering under Faculty of Civil and Water Resource Engineering, Bahir Dar Institute of Technology, is a record of original work carried out by me and has never been submitted to this or any other institution to get any other degree or certificates. The assistance and help I received during the course of this investigation have been duly acknowledged.

Mezmur Hawaz Fekadu — Name of the candidate

Signature

02-11-2022 — Date

BAHIR DAR UNIVERSITY
BAHIR DAR INSTITUTE OF TECHNOLOGY
SCHOOL OF GRADUATE STUDIES
FACULTY OF CIVIL AND WATER RESOURCE ENGINEERING

Approval of thesis for defense result

I hereby confirm that the changes required by the examiners have been carried out and incorporated in the final thesis.

Name of Student: Meznur Hawaz Fekadu Signature _____ Date Nov-01-2022

As members of the board of examiners, we examined this thesis entitled **Evaluation of the Hydraulic Performance of the Stormwater Drainage Structures in Woreta Town** by Meznur Hawaz Fekadu. We hereby certify that the thesis is accepted for fulfilling the requirements for the award of the degree of Masters of Science in Hydraulic Engineering.

Board of Examiners

Name of Advisor	Signature	Date
Dr. Asegdew Gashaw		02/11/2022
Name of External examiner	Signature	Date
Dr. Wubneh Belete		Nov. 01-2022
Name of Internal Examiner	Signature	Date
Dr. Fasikaw Atanaw		Nov 2, 2022
Name of Chairperson	Signature	Date
Mr. Setegn Abate		2/11/2022
Name of Chair Holder	Signature	Date
Dr. Asegdew Gashaw		02/11/2022
Name of Faculty Dean	Signature	Date
Dr. Mitiku Damte		03/11/2022

Faculty Stamp

ACKNOLEDGMENT

First of all, I would like to thank the almighty God for his unspeakable gift, help, and protection during all my work and in my life. I would like to express my honest thankfulness and appreciation to Bahirdar University for giving a scholarship to me and to Dr. Asegdew Gashaw for his encouragement, guidance, and support from the initial to this level of this thesis. He enabled me to develop and understand the subject matter as well as the way of writing this research.

I am grateful to my family for their unending love, moral, and financial support, which has greatly aided in the completion of this thesis.

And also, I am very grateful to my lecturers and my friends who helped me at all stages and all my class members who supported me during the research.

ABSTRACT

The challenges that managers and urban planners have long observed are preventing urban flooding, and failure of drainage structures. Only stormwater drainage systems hydraulically with high reliability can accomplish this. The objective of this study was to evaluate the hydraulic performance of the existing stormwater drainage systems in Woreta Town. Maximum annual rainfall data from 1987 to 2016 were used. The intensity duration frequency curves of the study area was developed using the Log-person type III. The physical parameters of the sub-catchments, especially the terrain of the catchments of the study area, were examined using Google Earth and ArcGIS. The SCS TR-20 method was utilized in HydroCAD to determine the culvert catchment peak discharge. The analysis of the culvert flow overtopping was performed using HY-8. The maximum channel flow rate, maximum velocity, and maximum water level were assessed using a stormwater management model. The 213-hectare region was chosen for the SWMM area because it has drainage problems and has historically been prone to flooding. 42 sub-catchments make up the model's area, and its drainage system consists of 56 conduits, 57 junctions, and 7 outfalls. The two most sensitive parameters N-pervious and N-impervious were calibrated using ten channel flow depth observations in 2021 until the simulated and observed flow depth values reached an acceptable threshold, and seven events in 2022 to verify the model. The SWMM model performs best at C21 (R^2=0.95, d=0.97, and NSE =0.84), C36 (R^2=0.93, d=0.96, and NSE =0.85), and C21 (R^2=0.79, d=0.94, and NSE =0.78), and C36 (R^2=0.71, d=0.82, and NSE =0.58), respectively, in terms of calibration and validation. According to the SWMM finding, the research area has poor freeboard performance on several channels. But there is high velocity performance on almost all channels except C39. The weighted System reliability is 68%. This shows that while the all over system's performance is acceptable, it is not exceptional. The HY-8 model's findings show that culverts 1 and 3 have overtopping problems. This study suggests redesigning road culverts that have issues with overtopping and storm drainage to meet the minimum freeboard standard.

Key Words: *HydroCAD, HY-8, SWMM, Reliability*

TABLE OF CONTENTS

LIST OF FIGURES

LIST OF TABLES

LIST OF ABBRIBATIONS

AASHTO	American Association of State Highway and Transportation Officials
ANN	Artificial Neural Network
BC	Before Christ
CN	Curve Number
DEM	Digital Elevation Model
EPA	Environmental Protection Agency
ERA	Ethiopian Road Authority
ESRI.	Environmental Systems Research Institute
FHWA	Federal Highway Administration
GIS	Geographic Information System
IDF	Intensity Duration Frequency Curve
IDR	Intensity Duration Recurrence
LID	Low Impact Development
MI	Multiple Imputation
MUSIC	Model for Urban Stormwater Improvement Conceptualization
NSC	Nash– Sutcliffe Coefficient
PIF	Performance Index of Freeboard
PIV	Performance Index of Velocity
PURRS	Probabilistic Urban Rainwater and Wastewater Reuse Simulator
SCS	Soil Conservation Service
SUDS	Sustainable Urban Drainage Systems
SWMM	Storm Water Management Model
USEPA	United States Environmental Protection Agency
USBR	United States Bureau of Reclamation
USWD	Urban Storm Water Drainage
WMO	World Meteorological Organization

1 INTRODUCTION

1.1 Background

Infrastructure is one of the key elements in the process of urbanization and emergence and continuity of an urban growth (Kim et al., 2020). It is consider as motor/engine for economic development (World Bank, 2006). Urban infrastructure (UI) is a broad notion that encompasses more than just a collection of constructed facilities, utilities, and systems (Bajracharya et al., 2016). It is also a venue for local government, tying together concerns about economic development, climate change, and municipal trash (Ferrer et al., 2018).

Urban drainage is that part of the water infrastructure, which seeks to avoid interruption to the free movement of pedestrians and vehicles, material damage from torrential flows, and peril to health and terrain from rainfall in urban areas (Silveira,2002). Drainage is an important feature in determining the ability of a given pavement to withstand the effects of traffic and the environment (Abhijit, 2011).

The drainage system is a process of removing and controlling excess surface water with in right of way (Mukherjee, 2014). Highways must have adequate drainage since it impacts how well they function and how long they can be used (Ponnurangam, 2019). If there is ponding on the traveled road, hydroplaning becomes a serious safety issue (Spitzhüttl et al., 2020). Drainage design involves providing facilities that collect, transport and removes stormwater from the highway (O'Flaherty, 2020). Culvert is simply described as a closed conduit carrying a watercourse under an obstruction such as a road, railway or canal (Balkham et al., 2010).

According to Azari & Tabesh (2022) stormwater network performance can be described as the system ability to convey sewerage and stormwater without hydraulic overload, beside minimizing the environmental impacts and retaining good structural integrity as well. The performance of a specific urban area's road infrastructure may be hindered by improperly provided or integrated road and drainage facilities (Tingsanchali, 2012). Problems like flooding and erosion when continuously can minimize the life span of road infrastructures and other urban utilities (Dagnachew, 2011).

Urban drainage issues result in flooding, deteriorated roadways, degraded soil, sedimentation, and water logging (Shaaban, 2022). A challenging issue in a nation with relatively little financial resources is stormwater runoff (Boguniewicz-Zabłocka & Capodaglio, 2020). With urbanization, impermeability increases because of the increase in impervious surfaces, and this the drainage pattern changes increase overland flow resulting in flooding and related environmental problems (Parkinson and Mark, 2015). Overtopping of flow over the roads by the cause of inadequacy of culvert cross-section and cause of sedimentation at the face and inside of the culvert (Balkham et al. ,2010). The impact of this is severe on spatial structures like roads and houses. This is because, flooding and its related environmental problems like sheet and gulley erosion, surface flood tends to affect road services and its life span (Adisu & Hailemikael, 2017). According to World Development Report (2006), infrastructure development in Africa is abysmal, lagging behind the rest of the world in terms of quality, quantity and access.

Ethiopia is a developing country with a high rate of urbanization and industrialization. This has led to an increase in the civic population and physical structures such as buildings, roads, and industries (Taka et al., 2020). These developments lead to challenges in the control of urban floods since it results in further surface flow (Ababa and Chen, 2020). In the Ethiopian context, where watersheds of many urban centers receive a significant amount of annual rainfall and where rainfall intensity is generally high, control of runoff at the source, flood protection, and safe disposal of redundant water/ runoff through proper drainage facilities becomes essential (Loudyi et al., 2022).

Woreta Town like other towns in Ethiopia has many drainage problems including inadequacy and poor quality drainage infrastructure. Therefore, this research is done for evaluating the hydraulic performance of selected stormwater networks and roadway culverts in the town by evaluating the hydrological response of the watershed and then modeling the structures to handle the yearly repeating problems and the serious consequences on the environment.

1.2 Statement of the Problem

One of the most frequent complaints from residents in many Ethiopian urban centers is to poor urban stormwater drainage (USWD) design and management, a problem that only worsens with the rate of urbanization. Failures of drainage structures and hydraulically inadequate culverts are frequently caused by poor hydrologic and hydraulic analysis combined with a lack of suitable data (Nagappa et al., 2020).

In other words, the feasibility of the projects is determined by the hydrologic and hydraulic study used during the planning stage. Unexpected flooding that results from the town's expanding urbanization and impermeability, which increases the rate of runoff per year, has made the problem even worse (Gupta & Nair, 2011).

In recent years, Woreta Town has seen a large increase in the construction of hydraulic structures for use in expensive drainage systems. But a number of the problems from the study region, such as bed material scoring, sedimentation, flooding in drainage lines, and overtopping of floods over culverts, are still present today (see Appendix A1). During the wet season, this has led to significant property damage. Even though this municipality has had a problem for a long time, no study has been done to evaluate the state of the current drainage facilities' hydraulic performance.

Therefore, the goal of this study is to identify this issue. A cornerstone should be laid for the future construction of stormwater networks and culverts for the town after the hydraulic performance of storm drainage facilities in the town is evaluated and improvement measures are offered for their sustainable and proper operation.

1.3 Objectives of the Study

1.3.1 General Objective

To evaluate the hydraulic performance of the existing stormwater drainage structures in Woreta Town.

1.3.2 Specific Objectives

- ✓ To assess the the existing condition of stormwater drainages structures.

- ✓ To determine the runoff quantity of the catchments of roadway culverts and sub-catchments of drainage lines.
- ✓ To model the drainage structures and evaluate the PIV, PIF and reliability of the existing stormwater networks and overtopping of roadway culverts.
- ✓ To recommend appropriate measure.

1.4 Research Questions

- ✓ What is the status of current stormwater drainage structures in the town?
- ✓ What is the runoff quantity of the catchments of the study area?
- ✓ What is the hydraulic performance index, and the reliability of the existing stormwater networks?
- ✓ What is the hydraulic performance of stormwater drainage networks and roadway culverts in the town?
- ✓ What are the recommended measurements?

1.5 Significance of the Study

This study is expected to be highly significant and plays a vital role in the following aspects:

- ✓ It is important to identify the existing conditions of drainage structures in the study area.
- ✓ It gives information about the hydraulic performance of each drainage channel and their all-over reliability and overtopping of roadway culverts.
- ✓ It will serve as an input for researchers on this topic, planners and decision-makers in the town, and help understand the errors.

1.6 Scope and Limitation of the Study

The scope of evaluation is spatially constrained and limited to Woreta Town. The purpose of this study include investigating the functionality of the existing stormwater networks and roadway culverts and evaluating hydraulic performance reliability of overall storm drainage networks and overtopping of culverts. To achieve the study's objectives, historical rainfall depth data is gathered from the National Metrological Agency, and the data is

processed to develop an intensity duration frequency curve. The soil map is from Amhara Design and Supervision Works, and the land use map was collected from ESRI for the study area. The locations of culvert inlets and outlets, river cross sections, road elevations, drainage junctions, and outfalls were determined using a handheld GPS. A tape meter was used to measure the cross sections of drainage structures and flow depths. Asphalt roads and roofs were taken as impervious surfaces of the study area during the calculation of the percentage of impervious surface. The curve number method of infiltration computation is used to calculate the infiltration of sub-catchments in the research region, and SWMM is utilized to compute the surface runoff of sub-catchments. I determined the flow velocity of the observed discharge at the chosen channels using the Manning roughness method.

1.7 Outline of the Thesis

The study structure is dependent on five chapters. Introduction or background with related study, problem statement, objectives of study, questions of study, significance of study, scope and limitations of study, and study outline are all included in the first chapter.

The second chapter reviews the literature that is related to studies on stormwater and drainage system performance, hydraulic and hydrologic models.

The third chapter material and methodology used starts from the description of the study area, material used for study, and methodology used to address the objectives.

The fourth chapter contains the results and discussion sections. The final chapter includes a conclusion and recommendations.

2 LITRATURE REVIEW

2.1 History of Urban Stormwater Drainage System

According to historical records of ancient civilizations (such as Indus and Minoan), urban drainage systems were built under guardianship with the goals of collecting rainwater, preventing nuisance flooding, and transporting trash (Shimabuku et al., 2018). The systems that eventually met their objectives likely did so after trial-and-error modifications. In general, planning and design were limited. Urban drainage had few numerical standards, and design didn't involve engineering calculations (Schäfer, 2019). Despite the lack of optimization and the use of trial-and-error construction methods, numerous ancient urban drainage systems can be rated as very successful (Jayasooriya et al., 2020). Lewis Mumford summarized the state of ancient urban infrastructure when he stated that ancient sewer systems were an uneconomic combination of refined technical devices and primitive social planning (Burian and Edwards, 2002)

According to Mays (2001) a highly rich history of hydraulics has developed since the first successful attempts to control the flow of water by the Egyptians and Mesopotamians thousands of years ago. Since the remains of ancient irrigation systems may still be seen in Mesopotamia and Egypt, the earliest effective attempts to regulate the flow of water were likely made there. Urban drainage systems have been put in place in cities all over the world for more than a century in an effort to stop flooding by quickly removing runoff from populated areas (Gichuhi & Gitahi, 2021). In several regions of the world, combined stormwater and wastewater drainage systems are offered with a similar goal (Naserisafavi et al., 2022). Construction of drainage systems can be traced back to the Indus civilization in the early third millennium BC (Valipour et al., 2020). Open channels were used in public areas for the purpose of runoff drainage in ancient practices that the Romans started (Angelakis et al., 2020). With the development of underground combined sewer systems, which were intended to eliminate sanitary waste and urban surface runoff, these procedures were further improved (Arden & Jawitz, 2019).

In the late 18th century, a progressive attention was provide to wet-weather flow management, intending to transfer the increased runoff further away from urban area, which required larger stormwater collection systems (interceptors) with respect to the

growing population. It resulted in higher investment cost for overall urban drainage systems. By the middle to late 19th century, anthropogenic pollutants in watercourses were identified as the combined systems transported sewage from the urban area to receiving water bodies (Turner et al., 2019). This problem was further aggravated by rapid urbanization (Yazdanfar & Sharma, 2015).

2.2 Stormwater

Stormwater is generate by rainfall, and consists of that proportion of rainfall that runs off from urban surfaces. Hence, the properties of stormwater, in terms of quantity and quality, are intrinsically linked to the nature and characteristics of both the rainfall and the catchment (David, Butler and John, 2004) . Stormwater (surface runoff) is the second major urban flow of concern to the drainage engineer (Qin et al., 2019).

Urban regions have a higher percentage of impermeable surfaces than rural areas, which causes more runoff and higher stormwater volumes and discharges (Bajracharya et al., 2016). It is preferable to characterize rain in urban or built-up areas as falling on nonporous surfaces like roofs, driveways, and roads (Sobieraj et al., 2022). The stormwater drainage network, a system of pipes, transports it to our natural water bodies, including creeks, rivers, and the sea. In some places, subsurface water is directly contacted with stormwater flow (Walsh et al., 2004).

Stromwater management is important in consideration of modeling the urban drainage system (Rangari & Sai Prashanth, 2018). When stormwater management practices, are properly selected, modeled, and applied, can be utilized to mitigate the adverse hydrologic and hydraulic impacts caused by drainage facilities, thus protecting downstream areas from flooding and erosion (Saraswat et al., 2016).

2.3 Urban Drainage System

City drainage systems have been viewed as a dynamic natural resource, a discarded mode of transportation, and a flooding problem. (Alves et al., 2020). The drainage system's functions include gathering surface water and/or groundwater and directing it elsewhere to keep the bed's strength depleted (Uppala & Dey, 2021). Drainage systems, particularly in the network of minor systems, may consist of canals, open channels, and natural surface

channels (Hanumanthanaik & Gowda, 2022). The major drainage system would almost certainly include open channels and natural watercourses within an urbanized (or urbanizing) catchment. The main parts of an urban drainage system are:

- ✓ Property drainage
- ✓ Street drainage
- ✓ Trunk drainage
- ✓ Retention and Detention Basins
- ✓ Receiving Water Bodies

The culvert is small structures that are required for the under roads and its uses for the crossing of water like streams under the roads (Brunen et al., 2020). The culvert structure protects and balances the embankment to lower the water flow level, as well as balancing the water flow on both sides of the highways (Marijnissen et al., 2021). There are different types of culverts shapes, and they are circle, arch, Slap & box; therefore, these can be construct by using different materials like; stones, bricks, reinforced cement concrete. Since the culvert crossing under the earthen embankment, so the culvert is subjecting a traffic load similarly as the roads carry; therefore, they required being design for such loads the acting on the surface of the culvert (Ali, 2020).

Safe and efficient drainage of stormwater is particularly important to maintain public health and safety (due to the potential impact of flooding on life and property) and to protect the receiving water environment (Lourenço et al., 2020). A proper design of stormwater system is a vital part of risk management practice. It helps to discharge runoff safely into environment (Teshome, 2020)

The indication with Sustainable Urban Drainage Systems (SUDS) is that in the best potential way redevelop the natural system of stormwater handling, in order to reduce peak flows and deliver treatment for the stormwater on its way to the recipients. The consequences of high peak flows, which arrive quickly after the storm starts. Since the traditional pipe-systems in the cities normally aren´t designed to handle these infrequent peak flows, flooding is often the result (Hoang and Fenner ,2016).

2.4 Urbanization Effect on Surface Water Flow

During the past 15 to 20 years, hydrologists have paid considerable attention to the effects of urbanization. Early works in urban hydrology were concerned with the effects of urbanization on the flood potential of small urban watersheds. The effects of urbanization on the flood hydrograph include increased total runoff volumes and peak flow rates (Chow, 1988). According to (Jacobson, 2011; Tsihrintzis and Hamid, 1998) urbanization has several impacts such as:

- ✓ reduction of rainfall interception by vegetation;
- ✓ reduction of infiltration;
- ✓ higher flow velocities as roughness decreases;
- ✓ faster response times;
- ✓ increase of runoff volume;
- ✓ higher peak flows in rivers and in stormwater drainage systems;
- ✓ increase of pluvial, flash and urban flooding;
- ✓ more frequent combined sewer overflows;
- ✓ alteration of flow paths; and
- ✓ Increased pollutant loads.

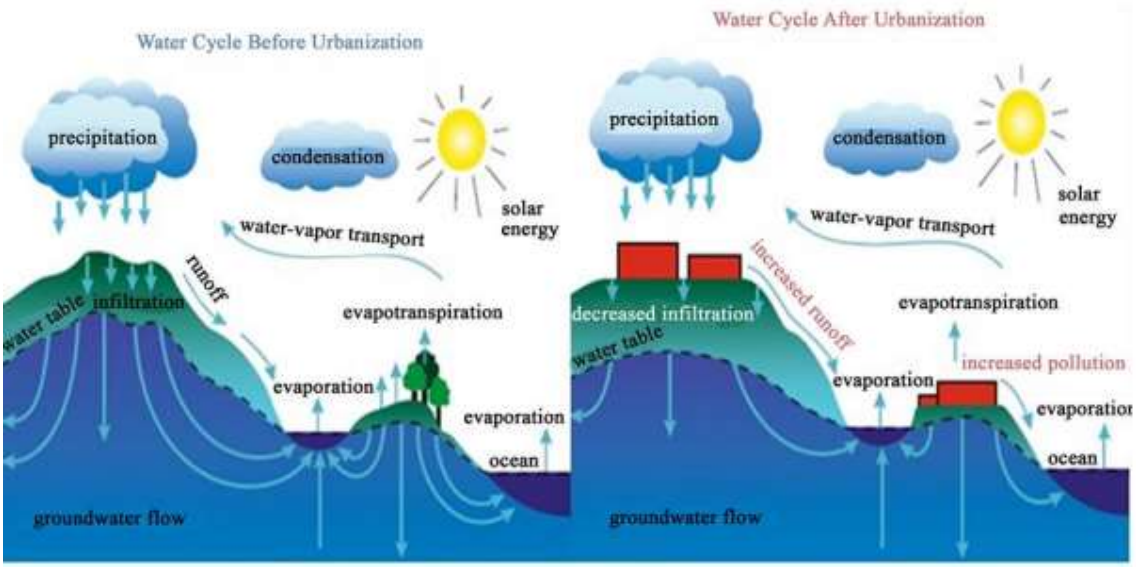

Figure 2.1 Water cycle diagram showing different processes involved before and after urbanization: Source (UNCE, 2015)

2.5 Flooding

Flood is a natural phenomenon, which has certain positive consequences but when it occurs in an urban area then it may results into great devastation to people (Agarwal & Kumar, 2019) . Due to high intensity rainfall events in urban areas prevention of flooding is very difficult due to lack of adequate drainage systems (Ribas et al., 2020). According to Wali et al. (2021) when a body of water, such as a river, lake, or ocean, overflows and breaches levees, allowing part of the water to escape its usual boundaries, flooding will occur. It may also occur when precipitation accumulates on wet ground, flooding the nearby region. Flooding, by its very nature, frequently results from both meteorological and hydrologic strategies; the characteristics of a flood are dictated by both the nature of the setting in which the occurrence is likely to occur and the precise conduct of the precipitation. (Erena et al., 2018).

2.5.1 Factors Affecting Flood Runoff

For all hydrologic analyses, the following factors will be evaluated and included if they have an enormous impact on the final outcomes:-

- ✓ Drainage basin characteristics including length, shape, slope, land use, geology, soil kind, surface infiltration, and storage;
- ✓ movement channel characteristics including geometry and configuration, natural and artificial controls, channel modification, aggradation/degradation, and particles;
- ✓ Flood plain characteristics; and

Meteorological characteristics along with precipitation amounts and sort (rain, hail, or combinations thereof), hurricane mobile size and distribution traits, storm route, and time charge of precipitation (Ethiopian Roads Authority, 2013).

2.6 Hydraulics of Stormwater Drainage System

Understanding fundamental hydraulic ideas and principles is necessary for the hydraulic design of stormwater drainage systems (Šuvalija et al., 2021). Important hydraulic principles include flow classification, conservation of mass, conservation of momentum, and conservation of energy (Brown et al., 2013). Conditions upstream, downstream, and the culvert's hydraulic features can all have an impact on a culvert's capacity (Karimpour

& Gohari, 2020). Combinations of these factors can be grouped into two types of flow conditions in culverts, inlet control and outlet control. The placement of the control section at the culvert inlet or outlet can also serve to distinguish these types of flow control (Muste & Xu, 2022). Inlet control occurs when the culvert barrel is capable of conveying more flow than the culvert inlet will accept. The culvert allows water to exit more quickly than it can enter the inlet (Jaeger et al., 2019). The culvert's entry or a nearby area experiences critical depth, and the flow downstream from the intake is supercritical (Karimpour & Gohari, 2020). Hydraulic characteristics of the downstream channel do not affect culvert capacity (Le et al., 2022). Most culverts, except those in flat terrain (less than 3 percent), are designed to operate under inlet controlled conditions (Yan et al., 2020). Culvert design is iterative and consists of the following steps:

- ✓ Determine the flow rate of water the culvert must carry.
- ✓ Select a culvert shape, type, and size with a particular inlet end treatment.
- ✓ Determine a headwater depth from the relevant charts for both inlet and outlet control for the design discharge, the grade and length of culvert, and the depth of water at the outlet (tail water).
- ✓ Compare the largest depth of headwater (as determined from either inlet or outlet control) to the design criteria. If the design criteria are not met, continue trying other culvert configurations until one or more configurations are found to satisfy the design parameters.
- ✓ Estimate the culvert outlet velocity and determine if there is a need for any special features such as energy dissipaters or armoring of the downstream channel.

2.7 Hydraulic Performance

The factors to be considered in the design are: the kind of material forming the channel body, which determines the roughness coefficient; the minimum permissible velocity, to avoid deposition if the water carries silt or debris; the channel bottom slope and side slopes; the freeboard; and the most efficient section, either hydraulically or empirically determined (Chow, 2007). Transporting a flow from one side of the road to the other is how culverts work (Starnes et al., 2022). It's crucial to analyze the flow frequency

during design and then estimate the discharge frequency to calculate the permitted head water elevation (Lombardi & Davis, 2022). The intensity of the discharge flow, the permitted outlet velocity, and the controlling headwater design all affect the type of culvert that is used (Jaeger et al., 2019).

Flow velocity and channel freeboard are two important parameters in designing urban drainage network channels (Tabesh et al., 2016).

2.7.1 Performance Index of Velocity (PIV)

The flow velocity in the drainage channel system should have a minimum value in order to prevent sedimentation. Several standard codes have announced different values for velocity in evaluating the performance or designing channels.

2.7.2 Performance Index Freeboard (PIF)

Freeboard of a channel is define as the vertical distance from the water surface to the top of the channel at the design condition. The distance should be sufficient to prevent water from overflowing the sides by waves and fluctuations (Chow, 2007). Due to erratic phenomena such as embankment settlement, silt accumulation, trash and debris in the channel, aquatic or other growth in the channels, and various assumptions in estimating the roughness, there is no definite rule for freeboard distance determination Generally, 5 to 30 percent of the flow depth can be consider as the design freeboard experimentally. According to USBR standard, for low depth flow rate channel and for channels with a flow rate of 85 m3/s freeboard distance is suggested to be 30 cm and 1.2 m respectively (Tabesh et al., 2016).

2.8 Hydraulic and Hydrologic Models

A model is a simplified explanation of a phenomenon, theory, or system that takes into account its known or inferred attributes and may be used to further investigate its features. (Haslbeck et al., 2021). Every model is a simplification of the real system (Batty, 2018). The applicability of a given model depends on the degree of simplification that can be apply while still representing the system in a meaningful way to solve a problem (Devia et al., 2015). Stormwater computer simulation models are well-established methods for anticipating a watershed's hydrologic response and assessing the capacity of related hydraulic conveyance systems (Alamdari & Hogue, 2022). Their usefulness extends from

the capacity to model complicated drainage systems to the ability to quickly analyze the impact of various storms and land use conditions (Sangal & Bonema, 1994).

Model inputs, model parameters, and the extent to which physical principles are utilized in the model are used to categorize rainfall-runoff models. It can take the form of deterministic and stochastic models based on the other criteria, as well as lumped and distributed models depending on the model parameters as a function of space and time (Devia et al., 2015).. One of the most important classifications is empirical model, conceptual models and physically based models as shown in Table 2.1.

Table 2.1 Characteristics of three models: (Devia et al. 2015)

Empirical model	Conceptual model	Physical based model
Data based or metric or black box model	Parametric or grey box model	Mechanistic or white box model
Involve mathematical equation, drive value from available time series	Based on modeling of reservoir and include semi empirical equation with a physical basis	Based on spatial distribution, Evaluation of parameter describing physical characteristics
Little consideration of features and process of system	Parameter are derived from field data and calibration	Require data about initial state of model and morphology of catchment
High productive power, low explanatory depth	Simple and can be easily implemented in computer code	Complex model. Requires human expertise and computation capability.
Cannot be generated to other catchments	Require large hydrologic and metrological data	Suffer from scale related problems
ANN unit hydrograph	HBV model TOPMODEL	SHE or MIKESHE model SWAT
Valid within the boundary of given domain	Calibration involves curve fitting make difficult physical interpretation	Valid for wide range of situations.

A runoff model can be define as a set of equations that helps in the estimation of runoff as a function of various parameters used for describing watershed characteristics. The two

important inputs required for all models are rainfall data and drainage area. Along with these, watershed characteristics like soil properties, vegetation cover, watershed topography, soil moisture content, characteristics of ground water aquifer are also considered. Hydrological models are now a day consider as an important and necessary tool for water and environment resource management (Devia et al., 2015).

Hydraulic-hydrologic flood models have been use intensively in every aspects of urban flood management. Lots of modeling techniques which can be one dimensional, two dimensional or coupling the two with many software tools are emerged. However, each models have its own limitation and uncertainties. To minimize these, detailed investigation on the available modeling approaches should be conducted (Teshome, 2020).

2.8.1 Urban Stormwater Networks Models

Several computer software's is currently available for urban stormwater drainage modelling. Since, the urban drainage system has hydrological & hydraulic attributes, it is better to use a model that has combined hydrological /hydraulics components to get a better representation of the flows and some of them are discuss as follows:

Table 2.2 Summarize urban stormwater drainage models: (Elliott & Trowsdale, 2007)

Model	Primary Intended use
MOUSE	Detailed simulation of urban drainage. Widespread use outside USA
MUSIC	Conceptual design for drainage design systems, with emphasis on treatment devise
P8-UCM	Estimation of urban stormwater polluted load
PURRS	Single site water use model originally for research but includes commercial users especially for rain tanks
StormTac	Management of lake catchment and conceptual design of stormwater treatment. Applied in Scandinavia
SWMM	Detailed model for planning and preliminary design. Widely used

2.8.1.1 SWMM Model

Stormwater runoff modeling techniques can be classified into two major categories; (1) unit hydrograph (UG) method and (2) kinematic wave (KW) approach.

SWMM is a dynamic hydrology-hydraulic water quality and quantity simulation model. It is use for single event or long-term (continuous) simulation of runoff quantity and quality from primarily urban areas. The runoff component operates on a collection of sub-catchment areas that receive precipitation and generate runoff and pollutant loads. The routing portion transports this runoff through a system of pipes, channels, storage/treatment devices, pumps, and regulators. It tracks the quantity and quality of runoff made within each sub-catchment. It tracks the flow rate, flow depth, and quality of water in each pipe and channel during a simulation period made up of multiple time steps. SWMM has been extend to model the hydrologic performance of specific types of low impact development (LID) controls (Simon, 2020). It conceptualizes a drainage system as a series of water and material flows between several major environmental compartments. These compartments include the atmosphere compartment, the land surface compartment, the groundwater compartment and the transport compartment. In general, the channel and pipe flow routings are govern by the Saint-Venant equations. In Brown et al. (2013) the Saint-Venant equations consist of mass Conservation equation (Equation 2.1) and momentum Conservation equation (Equation 2.2) for gradually varied, unsteady flow. In the transport compartment, SWMM solves the Saint-Venant equation using an explicit finite difference method and successive approximation.

$$\frac{\partial Q}{\partial x} + \frac{\partial A}{\partial t} = 0 \qquad 2.1$$

$$\frac{\partial h}{\partial x} + \frac{V}{g}\frac{\partial V}{\partial X} + \frac{1}{g}\frac{\partial V}{\partial t} = S_o - S_f \qquad 2.2$$

Where Q is discharge, A is area of flow cross section, V is velocity, h is depth of water, X is longitudinal distance, t denotes time, g is gravitational acceleration, S_o is channel slope term, and S_f is friction term.

The simulation time in individual channels and pipelines consists of multiple time steps. The results can be display as river basin maps, time series charts and tables and as statistical frequency analyses. The run-off process is based on sub-catchments with rainfalls with resulting surface runoff and its pollution. Furthermore, the runoff is conveyed into a system

of conduits, manholes and stormwater tanks, pumping stations, and treatment controls can also be included. The SWMM monitors the quantity and quality of runoff within each area. It also monitors the flow-rate, depth, and water quality in the individual pipe and channel sections during the simulation, which consists of several time steps (Hlustik, 2017).

SWMM is a distributed discrete time simulation model. It computes new values of its state variables over a sequence of time steps, where at each time step the system is subjected to a new set of external inputs. As its state variables are updated, other output variables of interest are computed and reported. This process is represented mathematically with the following general set of equations that are solved at each time step as the simulation proceeds:

$$X_t = f(X_{t-1}, I_t, P) \quad 2.3$$

$$Y_t = g(X_t, P) \quad 2.4$$

Where X_t is a vector of state variables at time t, Y_t is a vector of output variables at time t, I_t is a vector of input at time t, P is a vector of constant parameters, f is a vector-valued state transition function, and g is a vector-valued output transform function.

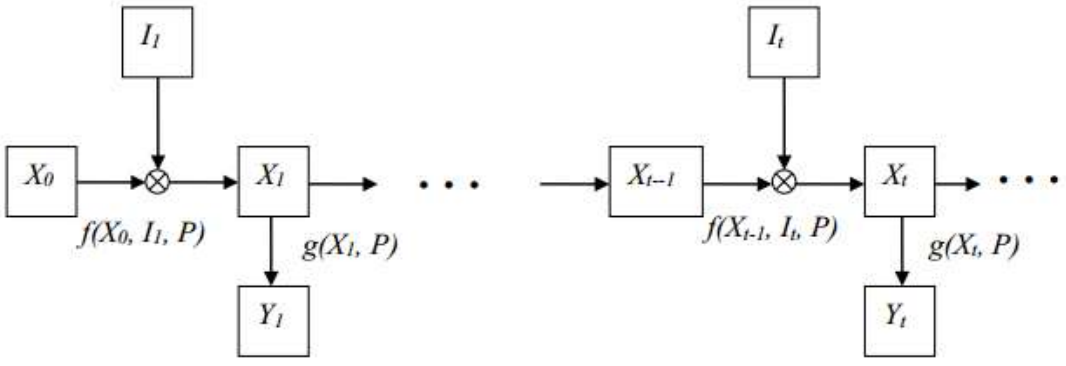

Figure 2.2 Block diagram of SWMM's state transition process

There are variables that make up the state vector *Xt*. This is a surprisingly small number given the comprehensive nature of SWMM. All other quantities can be computed from these variables, external inputs, and fixed input parameters (Rossman & Huber, 2016).

SWMM uses a nonlinear reservoir model to estimate surface runoff produced by rainfall over a sub-catchment. The model was first published by Chen and Shubinski (1971) and was included in the original release of SWMM. According to Rossman and Huber (2016) SWMM conceptualizes a sub-catchment as a rectangular surface that has a uniform slope *S* and a width *W* that drains to a single outlet channel as shown in Figure 2.3. Overland flow is generated by modeling the sub-catchment as a nonlinear reservoir, as sketched in Figure 2.4.

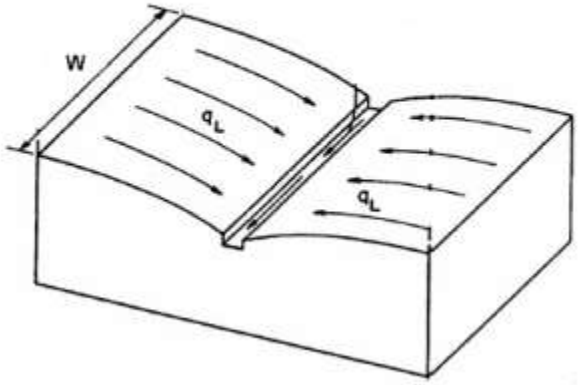

Figure 2.3: Idealized representation of a sub-catchment: (Rossman and Huber, 2016)

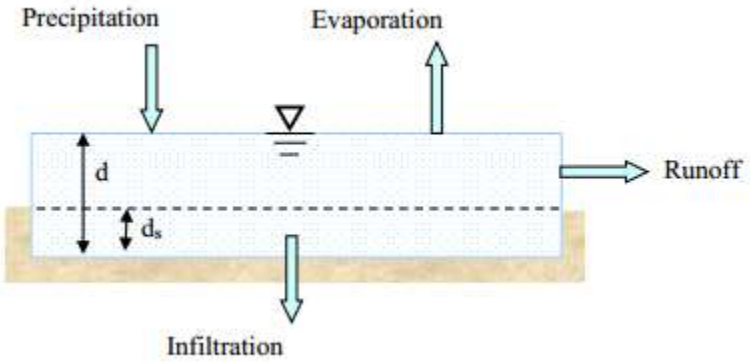

Figure 2.4: Nonlinear reservoir model of a sub-catchment

In this representation, the sub-catchment experiences inflow from precipitation (rainfall and snowmelt) and losses from evaporation and infiltration. The net excess ponds atop the

sub-catchment surface to a depth *d*. Ponded water above the depression storage depth d_s can become runoff outflow *q*. Depression storage accounts for initial rainfall abstractions such as surface ponding, interception by flat roofs and vegetation, and surface wetting.

From conservation of mass, the net change in depth *d* per unit of time *t* is simply the difference between inflow and outflow rates over the sub-catchment:

$$\frac{\partial d}{\partial t} = i - e - f - q \qquad 2.5$$

Where *i* is rate of rainfall + snowmelt (ft/s), *e* is surface evaporation rate (ft/s), *f* is infiltration rate (ft/s), and *q* is runoff rate (ft/s).

Note that the fluxes *i, e, f,* and *q* are expressed as flow rates per unit area (cfs/ft^2 = ft/s)

Assuming that flow across the sub-catchment's surface behaves as if it were uniform flow within a rectangular channel of width *W* (ft), height *d–ds*, and slope *S*, the Manning equation can be used to express the runoff's volumetric flow rate Q (cfs) as:

$$Q = \frac{1.49}{n} S^{1/2} R_x^{2/3} A_X \qquad 2.6$$

Here *n* is a surface roughness coefficient, *S* the apparent or average slope of the sub-catchment (ft/ft), A_x the area across the sub-catchment's width through which the runoff flows (ft^2), and R_x is the hydraulic radius associated with this area (ft).

By means of this model, the maximum flow, maximum velocity and maximum water level in each channel during simulation has been used to determine the hydraulic performance index in the entire network.

2.8.2 Culvert Hydraulic Models

Culvert hydraulic modeling conventions assume the flow through a culvert is steady and incompressible with constant density (Donahue & Howard, 2011). The cross sectional area of the culvert is assume not to change. One of the software products evaluated will allow changes in slope within a culvert, otherwise, the slope is assume constant. The analysis of culvert performance can be solved through a series of hand calculations based on simplifying assumptions. However, had calculations are tedious and prone to error, and as

a result it became desirable to automate the calculations required to solve culvert performance (Hotchkiss et al., 2008).

2.8.2.1 HY-8 Model

Hy-8 is a culvert hydraulic modeling tool developed by Philip Thompson and provided to the Federal highway Administration (FHWA), USA for distribution in early 1980s. Since the period the hydraulic model was developed, understanding of culvert hydraulics has increased significantly leading to development of more acceptable modeling techniques. Various organization and government departments have adopted the usage of the model in designing and analyzing culverts along roadway. The primary function of HY-8 is to compute headwater depths at the entrance of culverts (Hotchkiss et al., 2008).

HY-8 Culvert Analysis can be used to perform calculations for culvert analysis (including independent and multiple barrel sizing), hydrograph generation, hydrograph routing, roadway overtopping and outlet scour estimates. Given all of the appropriate data, HY-8 will compute the culvert hydraulics for circular, rectangular, elliptical, arch and custom culverts using both imperial and metric units. According to Hotchkiss et al. (2008) HY-8 produced the most accurate and consistent results.

2.9 Previously Study in Ethiopia

1. Hydraulic Performance Assessment of Stormwater Drainage Systems of Dejen Town Using Stormwater Management Model (SWMM), Ethiopia

This study was conducted to assess the current drainage performance of Dejen Town, to develop IDF curve, to estimate and predict flood amount, and to redesign drainage structures of the Town. Most of the existing drainage structures were inadequate to dispose runoff to the outfall area and most drainage structures in study area were poor. The output from rational method and stormwater management model (SWMM) also indicated that the discharge resulted from the sub-catchments was greater than the existing capacity. This implies in most of the canals, Junctions and outfalls the flood level was greater than the designed water level, and over-flooding occurs at drainage canals and the junctions. Construction of additional drainage structures with proper dimension especially for secondary roadsides with no drainage structures, design and construction of well-

connected structures, adopting the culture of clearing sediment and periodic repairing of drainage structures before total failure were the remedial measures to be taken to solve the problem (Tilahun, 2021).

2. Performance Assessment of Road Drainage Systems of Burayu Town, Oromia Region, Ethiopia

The objective of the study is to assess the Performance of Drainage Systems of Road at Burayu Town Administration. The study employed both primary and secondary instruments of data collection. The primary data collection instruments were observation (field visit), Interview, and photographs that show the existing drainage structure conditions and information that were gathered from the residents about the performance of the drainage structures during the rainy season. The secondary data sources were land cover map and geological map. Hydrological analysis was carried out by using Rational and SCS equations. Hydraulic parameters were determined from the design documents data during construction and from the construction sites by measuring the parameters where the structures are constructed by using Manning's equation and GIS was used for watershed delineation. The SCS method and rational method were used to calculate the hydrological analysis. This study suggests improving the integration of road and drainage structures, integrating solid waste management systems to prevent overflowing floods caused by blocked drains, maintaining the road stations properly, carefully cleaning the drainage structures, and taking appropriate steps to ensure that the road and drainage structures serve the stakeholders' needs in a sustainable manner (Bekele and Sahadeva, 2018).

3. Performance Assessment urban drainage system of Holeta town using stormwater management model (SWMM)

The general objective of the study was the Performance Assessment of Urban Drainage Systems of Holeta Town using the Stormwater Management Model (SWMM). The catchment that contributes runoff areas, weighted runoff coefficient was delineated using ArcGIS 10.3 tool. The Stormwater Management Model (SWMM 5.1) was applied to simulate the water level in the links and junctions by considering the current land use condition. The intensity duration frequency (IDF) curve was developed by using log-

Pearson Type III to analyze rainfall and the consequent peak runoff for different return periods using a rational method. The existing storm drainage systems of Holeta Town were: lack of well-connected drainage lines, solid and liquid wastes were directly disposed into the storm drainage system, which results in decreasing the efficiency of the system, unavailability of drainage systems at the proper place. The SWMM output indicates that in most of the junctions, the flood level was greater than the designed water level (Chali & Zewdie, 2020).

In my review, these studies have their own gaps in terms of hydrological analysis of rainfall data, and they don't have any way to show how they use the output of the SWMM model to decide whether or not the urban stormwater networks are hydraulically safe. In addition to that, most studies do not concern themselves with hydraulically based concepts; most of them are more management concerns. Therefore, in my study, I fill these knowledge gaps (making a recommended hydrological data analysis for developing a time series data IDF curve for the study area and making hydraulically performance analysis of urban stormwater networks of the study area by using PIV and PIF index) HY-8 modeling tools for evaluating the hydraulic performance of roadway culverts.

3 METHODOLOGY

3.1 Description of the Study Area

Woreta is a town in northwestern Amhara. This town is located in the Amhara Region's South Gondar Zone, east of Lake Tana, south of Addis Zemen, and north of Hamusit, with latitude and longitude coordinates of 11°55′N, 37°42′E and an elevation of 1828 meters above sea level, 625 kilometers from Addis Abeba and 55 kilometers from Bahirdar. It is the administrative center of Fogera woreda. The study area includes the existing built-up area of the town that is being developed for different urban land uses, about 548 ha. The town has four kebebles.

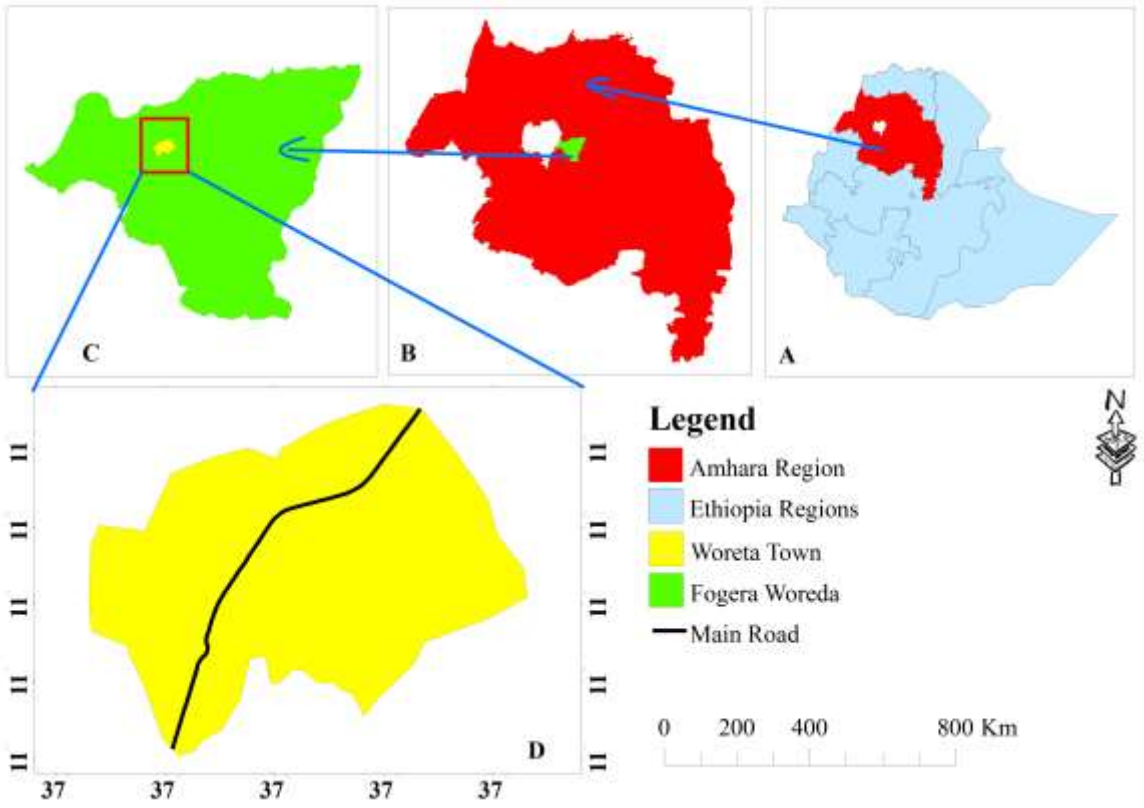

Figure 3.1Study area map A) Ethiopia Regions B) Amhara Region C) Fogera Woreda and D) Woreta Town

3.1.1 Topography

Woreta Town had a latitude and longitude of 11º55'N 37º42'E with an average elevation of 1775m – 1891m above sea level. The drainage of the town has outlets towards the Erza

river and the other one is the Gosho river. Based on Arc GIS analysis by using a 30m x 30m digital elevation model, the town topographic map is developed shown in Figure 3.2.

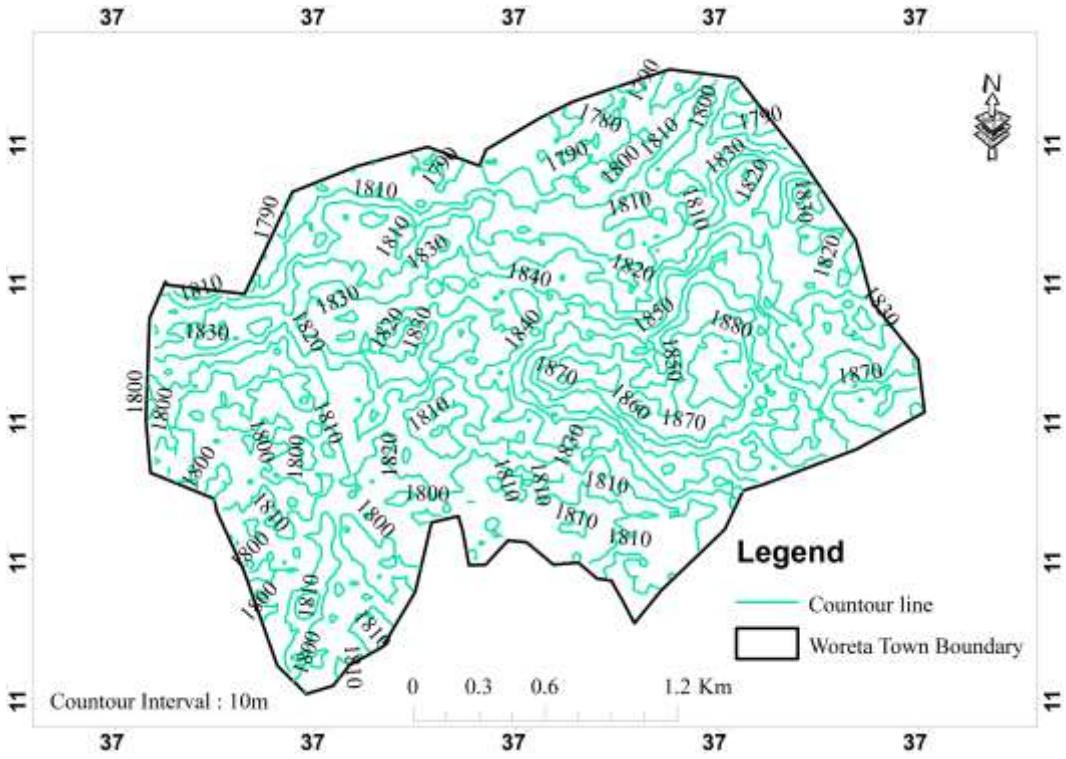

Figure 3.2 Topographic Map of the Woreta Town

3.1.2 Soil and Hydrogeology of the Study Area

Based on Arc GIS analysis by using Amhara Design and Supervision Works soil map, the study area has three types of soils (chromic Vertisols, Chromic Luvisols and Eutric Nitsols) and by using Africa Groundwater Atlas Country Hydrogeology Maps, Version 1.0, two types of hydrogeology aquifers. These are igneous volcano and unconsolidated sedimentary.

3.1.3 Climate of the Study Area

Woreta is found within Woina Dega zone. The metrological station is found in the town. According to Alelign et al. (2018) mean annual precipitation was 1225.8 mm with mean maximum and minimum temperatures of 27.9 and 12.6 °C. The major portion of the total annual rainfall is received between June and October.

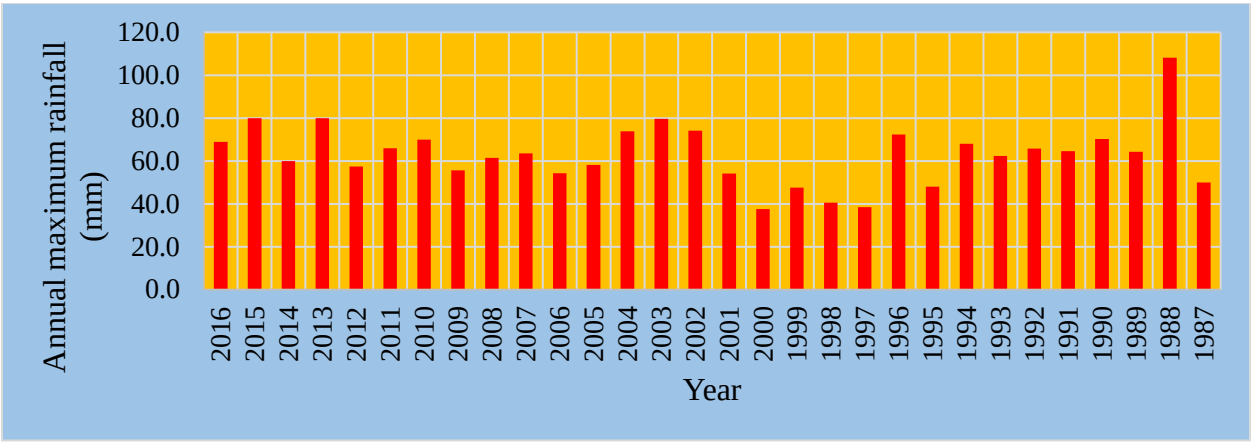

Figure 3.3 Annual maximum rainfall of study area

3.1.4 Land Use Land Cover

Because land use has a direct impact on flood amount, speed, and potential for damage, the study takes note of the catchment's land use and land cover. The land use and land cover of the study area was taken from ESRI land cover map 2020 with 10m resolution. The study area has a large area of built-up areas and croplands.

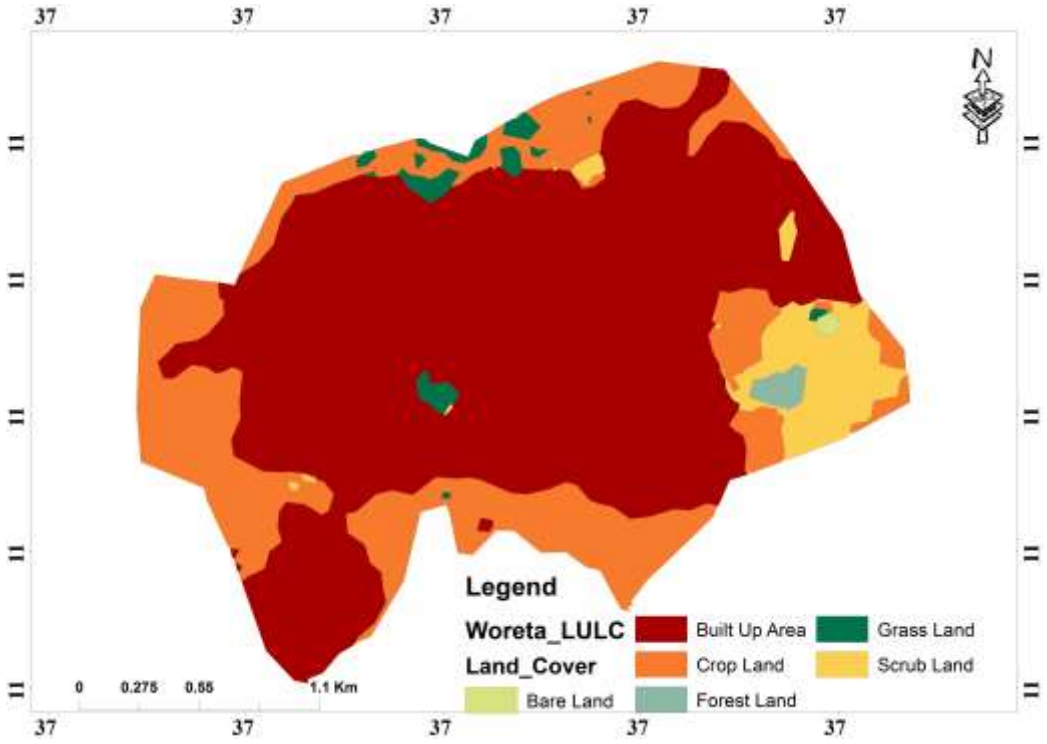

Figure 3.4 Land use land cover map of Woreta Town

3.2 Data Collection and Materials

This study involves the collection of both primary and secondary data and includes information from respective organizations.

3.2.1 Primary Data

Personal field observations and site investigations, as well as Google Earth data, are used to collect primary data using a base map and checklist.

- ✓ Site inspection: overall drainage system condition and scheduled camera
- ✓ Measure the drainage location and dimensions using GPS and TAPE material for the input of the SWMM model simulation.
- ✓ Measuring flow depth in selected drainage nodes for model calibration and validation. (See Table 3.3).
- ✓ Measure the roadway data, culvert data, tail water data, and culvert alignment with the roads for culvert analysis. (See Appendix A5).

Table 3.1 Existing culverts location and other details

Culvert No	Location/ community	Type	Size(mm)	Length across the road (m)	Latitude	Longitude
1	Arsema Megenteya	Circular Concrete	800	14.5	11.8940	37.6767
2	Muharba River	Box Concrete	9000 x 3000	13.8	11.8977	37.6807
3	Erza River	Box Concrete	15000 x 3500	17.25	11.9167	37.6919
4	Tishikena River	Box	1550 x 7420	14	11.9350	37.7075

Table 3.2 Detail of selected nodes that flow depth is measured

Number	Node Code	Depth (m)	Latitude	Longitude	Elevation
1	J13	1.05	11.9186	37.6926	1806.39
2	J37	0.9	11.919	37.6913	1807.29

Table 3.3 The average flow depth was recorded at the chosen outfalls after three hours.

Day	Rainfall Duration (min)	Average Flow depth (m)	
		J13	J29
7/31/2021	15	0.31	0.23
8/3/2021	30	0.50	0.43
8/8/2021	90	0.78	0.68
8/15/2021	30	0.46	0.42
8/31/2021	30	0.44	0.44
9/3/2021	15	0.35	0.23
9/12/2021	30	0.49	0.43
9/17/2021	15	0.36	0.21
9/18/2021	90	0.78	0.68
9/22/2021	75	0.77	0.65
6/19/2022	30	0.39	0.32
6/20/2022	30	0.51	0.41
6/24/2022	45	0.54	0.46
6/25/2022	45	0.71	0.64
6/28/2022	60	0.79	0.63
7/15/2022	45	0.6	0.49
7/31/2022	15	0.32	0.28

3.2.2 Secondary Data

Secondary data is collected through governmental offices, literature studies, and document analysis. Several printed books, journals, and manuals are used. In addition to that, the internet is the major tool to access government documents and different journals. The major collected secondary data includes:

Table 3.4 List of used secondary data's

No	Data Type	Data Sources	Purposes
1	Metrological data (1987-2016)	National Metrological Agency	To develop time series data
2	Land Cover Map (2020 land cover map)	Environment Systems Research Institute (ESRI) land cover	To determine the runoff coefficient of the study area and permeability and impermeability of the catchment.
3	Boundary map of the study area	Environment System Research Institute (ESRI) shape file	To catchment delineation and estimation of catchment characteristics
4	Digital Elevation Model	Advanced Space borne Thermal Emission and Reflection Radiometer (ASTER).	To make watershed and topographical map of the study area
5	Soil Map of the study area	Amhara Design and Supervision works Enterprise	To identify the catchment soil type and aquifers of the study area use as input for the model

3.2.3 Material Used

The following materials have been use to conduct this study:

- ✓ GPS (Geographic Positioning System) - To collect the coordinates and elevation data of different points at the outlet and junction of drainage structures and the inlet and outlet of the culverts.
- ✓ Tape meter: - To measure the existing urban stormwater drainage cross sections, road and natural water ways of the culvert

- ✓ Digital camera: - to snap pictures of the current stormwater drainage system and when drainage issues occur.

3.2.4 Software Package

This research is completely dependent on computer software and applications. The following is a list of the computer programs and software used in the research process:

Table 3.5 List of software packages

No	Software	Purpose
1	Arc GIS	For catchment delineation; dividing the catchment into sub-catchments and parameterizing the required elements for the models
2	Google earth	To verify watershed and sub-catchment discretization of the study area.
3	SWMM	To simulate the sub-catchment runoff and maximum channel flow rate, maximum velocity, and maximum water level of the channel.
4	HY-8	For culvert analysis and also to determine the flow regime and water surface profile in the culvert.
5	Microsoft Excel and Word	Large data manipulation, data analysis and manuscript writing.
6	Hydro-cad	To model and simulate and peak flow the catchments

3.3 Methods

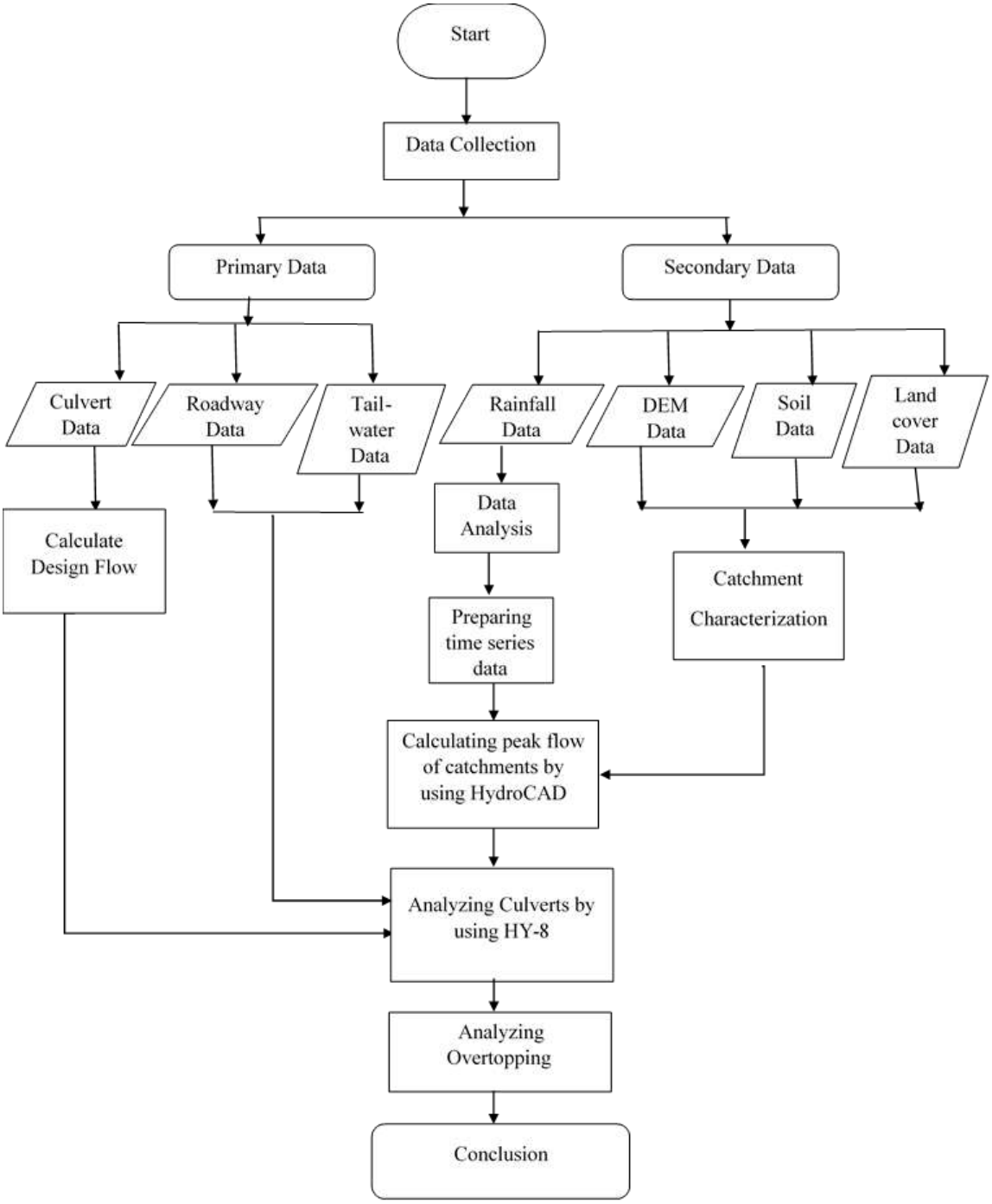

Figure 3.5 Workflow of evaluating HY-8 modeling tools of culverts.

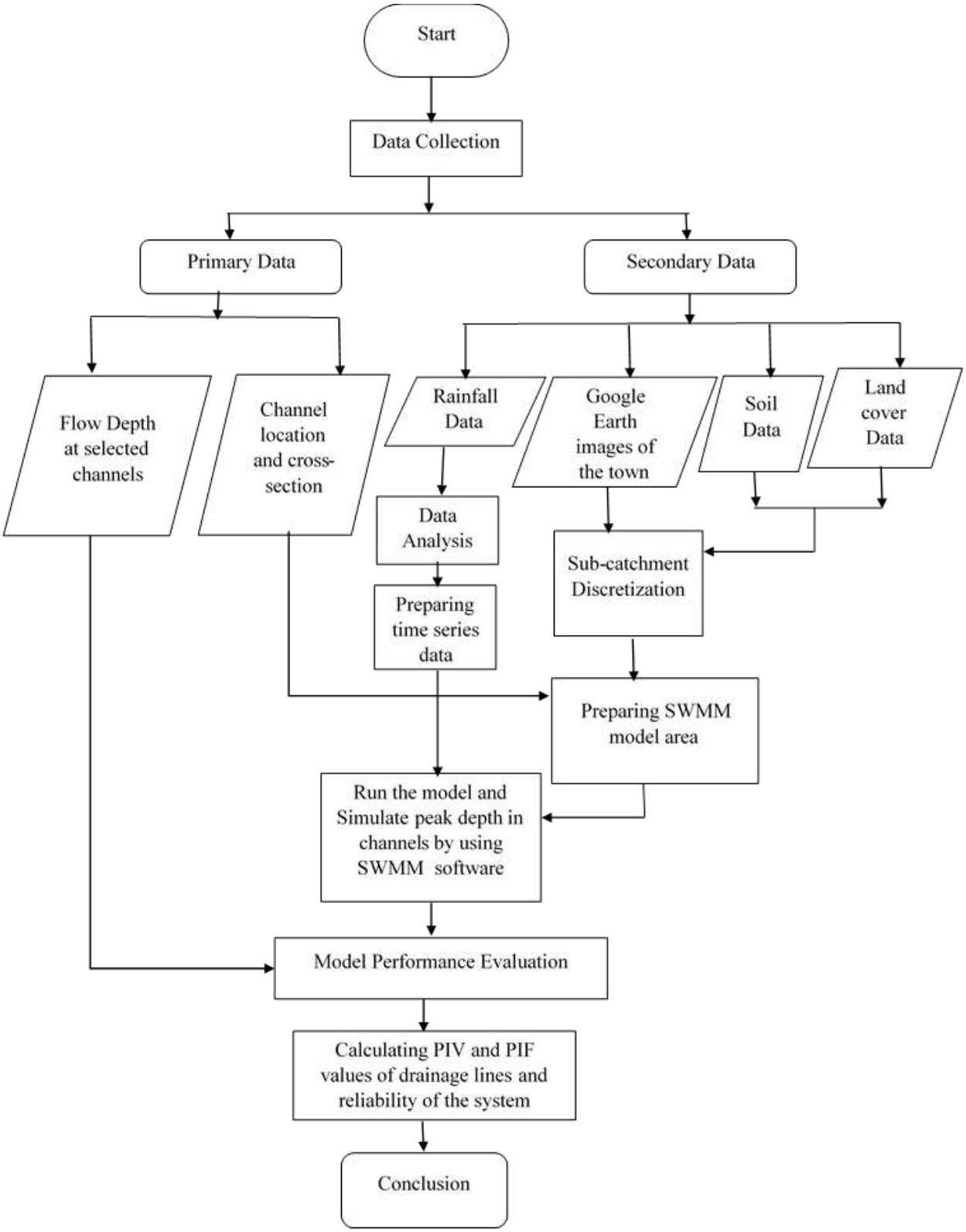

Figure 3.6 Workflow of evaluations of hydraulic performance index of storm drainages

3.3.1 Rainfall Data Analysis

Hydrological data is significantly used in engineering studies for the management and development of water resources. When utilized for frequency analysis or to simulate a hydrological system, these data should be steady, reliable, and uniform. The engineer requires a quick yet effective screening process to assess whether the data satisfies these requirements (Dahmen and Hall, 1989).

For this study, 30 years (1987–2016) of daily rainfall data of Woreta Town's neighboring metrological station were collected from the National Metrological Agency. Meanwhile, out of the total rainfall data, about 9.3% was not available. Additional data was collected from nearby metrological stations (Addis Zemen and Wanzaye) to fill in missing data gaps and to assess the consistency of rainfall data.

Table 3.6 Summary of Statistics for precipitation data and geographic position of selected rain gauge stations

Stations		Woreta	Wanzaye	Addis Zemen
Geographic Position	Latitude (N)	11.92	11.79	12.12
	Longitude (E)	37.7	37.68	37.77
	Elevation (m)	1819	1821	1940
Statistics of precipitation data	Minimum rainfall (mm)	0	0	0
	Maximum rainfall (mm)	118.6	134.2	87.8
	Standard deviation	9.53	9.78	11.26
	Data Collection Year	1987-2016	1987-2016	1987-2016
	Data Collection Period	30	30	30
	Amount of Missing data (%)	9.28	8.18	12.26

3.3.1.1 Filling Missing Data

Rainfall surrounds missing values, which are attributed to different reasons such as weather, instrumental failures, or human error in data entry. The estimation of the missing rainfall value becomes the first priority in the data preparation process. For this study, I used multiple imputation by using XLSTAT software. Because of a single imputation, the estimation of variability was ignored, which led to an underestimation of standard errors and confidence intervals. To overcome the underestimation problem, multiple imputation methods are used, where each missing value is estimated with a distribution of imputation reflecting uncertainty about the missing data. MI lead to the best estimation of missing values (Sattari et al., 2017).

Multiple imputation for missing data is an attractive method for handling missing data in multivariate analysis. The idea of multiple imputation for missing data was first proposed by Rubin (1977).

The following is the procedure for conducting the multiple imputation for missing data that was created by Rubin in 1987:

- ✓ The first step of multiple imputation for missing data is to impute the missing values by using an appropriate model which incorporates random variation.
- ✓ The second step of multiple imputation for missing data is to repeat the first step 3-5 times.
- ✓ The third step of multiple imputation for missing data is to perform the desired analysis on each data set by using standard, complete data methods.
- ✓ The fourth step of multiple imputation for missing data is to average the values of the parameter estimates across the missing value samples in order to obtain a single point estimate.
- ✓ The fifth step of multiple imputation for missing data is to calculate the standard errors by averaging the squared standard errors of the missing value estimates. After this, the researcher must calculate the variance of the missing value parameter

across the samples. Finally, the researcher must combine the two quantities in multiple imputation for missing data to calculate the standard errors.

3.3.1.2 Test absence of trend

A thorough analysis of rainfall trends is beneficial for rainfall forecasting, water resource development and management, designing water storage structures, irrigation practices and crop selection, drinking water supply, industrial development, and disaster management under current and future climatic conditions. (Patakamuri et al., 2020). To verify the absence of a trend, I use Spearman's rank-correlation method. It is simple and distribution-free, i.e., it does not require the assumption of an underlying statistical distribution. Another advantage is that its power is nearly uniform for linear and non-linear trends (WMO 1966). The method is based on the Spearman rank-correlation coefficient, Rsp, which is defined as:

$$R_{sp} = 1 - \frac{6 * \sum_{i=1}^{n} (D_i * D_i)}{n * (n * n - 1)} \quad 3.1$$

$$D_i = K_{xi} - K_{yi} \quad 3.2$$

Where n is total number of data, D is difference, i is the cronological order number, K_{xi} is the rank of variable x (random variable), and K_{yi} is the rank of variable y in there minimum to maximum order.

If there are ties, i.e. two or more ranked observations, y, with the same value, the convention is to take K_x as the average rank. test statistic:

$$t_t = R_{sp} \left[\frac{n-2}{1 - R_{sp} * R_{sp}} \right]^{0.5} \quad 3.3$$

Where t_t is t-distribution, and n-2 is v, degree of freedom.

Appendix C1 contains a table of the percentile points of the t-distribution for a significance level of 5 per cent (two-tailed). At a significance level of 5 percent (two-tailed), the two-sided critical region, U, of t_t, is bound by:

$$\{-\infty, t\{v, 2{,}5\%\}\} \text{ U } \{t\{v, 97.5\%\}, +\infty\}$$

The time series has no trend if:

$$t\{v, 2.5\%\} < t_t < t\{v, 97.5\%\}$$

If the time series does have the trend data cannot be used for frequency analaysis or modeling (Dahmen and Hall, 1989).

3.3.1.3 Tests for Stability of Variance and Mean

The F-Test for Stability of Variance

In addition to testing the time series for the absence of trend, one must test it for stability of variance and mean. The test for stability of variance is done first. There are two reasons for this sequence: Firstly,instability of the variance implies that the time series is not stationary and, thus, not suitable for further use; secondly, the test for stability of the mean is much simpler if one can use a pooled estimate of the variances of the two sub-sets. The test statistic is the ratio of the variances of two split, non-overlapping, sub-sets of the time series (Dahmen and Hall, 1989).

$$F_t = \frac{\sigma_1^2}{\sigma_2^2} = \frac{S_1^2}{S_2^2} \qquad 3.4$$

where S^2 is variance. Note that, to compute F_t it is irrelevant whether one uses the sample standard deviation, S, or the population standard deviation, σ. Formulae for computing the sample standard deviation, S, namely:

$$S = \left[\frac{\sum_{i=1}^{n}(X_i^2) - n * \bar{x}^2}{n-1}\right]^{0.5} \qquad 3.5$$

where x_i, is the observation, n is the total number of data in the sample, and $\bar{x}$ is the mean of the data.

The variance of the time series is stable, and one can use the sample standard deviation, s, as an estimate of the population standard deviation, σ , if

$$\{0, F\{v_1, v_2, 2.5\%\}\} \text{ U } \{F\{v_1, v_2, 97.5\%\}, +\infty\}$$

Or

$$F\{v_1, v_2, 2.5\%\} < F_t < F\{v_1, v_2, 97.5\%\}$$

Where, $v_1 = n_1-1$ is the number of degree of freedom for the numerator, $v_2 = n_2-1$ is the number of degree of freedom for the denominator, and n_1 and n_2 are the number of data in each sub-set (see Appendix C2) for F-distribution $F\{v_1,v_2,p\}$for the 5 per-cent of significance of (two-tailed).)

The t-Test for Stability of Mean

The t-test for stability of mean involves computing and then comparing the mean of two or three non-overlapping sub-sets of the time series (the same subsets from the F-test for stability of variance).

$$t_t = \frac{\bar{x}_1 - \bar{x}_2}{\left[\frac{(n_1-1)s_1^2 + (n_2-1)s_2^2}{n_1+n_2-2} * \left(\frac{1}{n_1}+\frac{1}{n_2}\right)\right]^{0.5}} \quad 3.6$$

Where n is the number of data in the sub-set, $\bar{x}$ the mean of sub-set, and s^2 its variance. The test static t_t is valied for small samoles with unknown variance. These variances can however differ only because of sampling variability if the t- test is applied in this form. The mean of the time series is consider stable if:

$$t\{v, 2.5\%\} < t_t < t\{v, 97.5\%\}$$

3.3.1.4 Tests for Relative Consistency and Homogeneity

A time series of hydrological data is relatively consistent if the periodic data are proportional to an appropriate simultaneous time series (Chang and Lee, 1974).

In other words, relative consistency means that the hydrological data at a certain observation station are generated by the same mechanism that generated similar (e.g. rainfall/rainfall) or related (e.g rainfall/runoff) data at other stations.

Recording of rain gage stations have undergone a significant change during the period of record inconsistency would arise in the rainfall data of the station. This inconsistency would be felt from the time the significant change took place. Some of the common causes for inconsistency of record are shifting of a rain gauge station to a new location, the neighborhood of the station undergoing a marked change, change in ecosystem due to calamities such forest fires, landslides and occurrence of observational error from a certain date. Testing for inconsistency of record is done by the double mass curve technique. It is

common practice to verify relative consistency with double-mass analysis. This technique is based on the principle that when each record data comes from the same parent population they are consistent. The procedure is that accumulated rainfall at the gauge station whose record is in doubt is plotted as ordinate versus the average concurrent accumulated average rainfall of nearby stations of rainfall data are available. A decide break in the slope of resulting plot in the precipitation regime of tested station. The precipitation values at tested station beyond the period of change of regime is correct by using the relation:

$$P_{cx} = P_x \frac{M_e}{M_a} \quad 3.7$$

Where P_{cx} is corrected precipitation at any time period t_1 at tested station, P_x is original recorded precipitation at time period t_1 at tested station, M_e is corrected slope of the double mass curve and M_a is original slope of the double mass curve.

3.3.1.5 Identification of Outliers

Outliers are part of the data, which are found significantly different from the trend of the whole data due to different reasons. It may be cause due to measuring equipment error, lack of curiosity induced by the data collectors' etc. It is important to identify those data and reject out of the total in order to reduce their negative impact that might cause deviation from the fact. Therefore, the following equations in logarithmic scale were use to identify outliers among the yearly maximum daily rainfall data.

$$Y_H = Y_{avg} + K_n * \delta_n - 1 \text{ , for higher outlier test}$$

$$Y_L = Y_{avg} - K_n * \delta_n - 1 \text{ , for lower outlier test}$$

Then

$$Higher\ outlier = 10^{YH} \quad 3.8$$

$$Lower\ outlier = 10^{YL} \quad 3.9$$

Where Y_H is higher outlier threshold in log unit, Y_L is lower outlier threshold in log unit, Y_{avg} is mean of logarithmic values, $\delta_n - 1$ is standard deviation of logarithmic values, K_n is values from the table by sample size

Mean, Standard deviation were computed using Microsoft excel software whereas K_n value is obtained from outlier test K_n table Appendix C3. Outliers were not found in the list of yearly maximum daily rain fall data ,after calculation is made using the formulae.

3.4 Development of IDF Curve for Woreta Town

Rainfall intensity, duration, and frequency IDF curves are graphs that show how much water falls in a catchment area over a specific period of time (Elsebaie, 2012). One of the first steps in many hydrologic design projects, such as urban drainage design, is determining the rainfall event or events to use.

Typically, the annual maximum series, which includes the highest values recorded each year, is used to determine the frequency of rainfall. In several parts of the world, there are widely used theoretical distribution functions that have been put to use.

The most common approach is to use a design storm or event that involves a relationship between rainfall intensity (or depth), duration, and the frequency or return period appropriate for the facility and site location (Chow, 1988). The curve is an important in put to design hydraulic structures including urban drainage. The curve is formulated for different probability distribution but in this study I use two extreme event probability distributions (Extreme value type I distribution [Gumbel] & Logarithmic Pearson Type-III distribution) which are the most commonly used for extreme event for this research purpose using thirty annual maximum rainfall data. The rainfall depths obtained from gauging station are of 24hr duration depth.

3.4.1 Preparation of Shorter Duration Rainfall

Design and analysis of drainage structures require rainfall intensity duration relationship of shorter duration. Because rainfall data of shorter duration is unavailable, appropriate IDF derivation for shorter duration is required. Ethiopian Road Authority (ERA) Drainage Design Manual of 2013 suggests the following equation for calculation of shorter duration rainfall from 24-hour duration rainfall.

$$R_{Rt} = \frac{t(b+24)^n}{24(b+t)^n} \qquad 3.10$$

The above equation is rearrange as

$$\frac{R_t}{R_{24}} = \frac{t(b+24)^n}{24(b+t)^n} \quad 3.11$$

$$R_t = \frac{t(b+24)^n}{24(b+t)^n} * R_{24} \quad 3.12$$

Where R_{24} is 24hr rainfall depth, R_t is Rainfall depth in a given duration t, and Coefficient; b=0.3 and n=0.78-1.09.

Then, the rainfall intensity is:

$$I_t = \frac{R_t}{t} \quad 3.13$$

$$I_t = \frac{R_{24} * (b+24)^n}{24(b+t)^n} \quad 3.14$$

Using b = 0.3 and n = 0.92 as suggested by ERA manual results are tabulated for rainfall durations 15, 30, 45… 180 minutes. The resulting table is seen Appendix D2.

3.4.2 Frequency Analysis Using Frequency Factors

In many hydraulic-engineering application such as those concerned with floods, the probability of occurrence of particular extreme event rainfall, e.g. a 24-h maximum rainfall, will be important (Xu et al., 2014). Such information is obtain by the frequency analysis of the point rainfall data**.** The magnitude of an extreme event is inversely related to its frequency of occurrence, very severe events occurring less frequently than more moderate events. The objective of frequency analysis of hydrologic data is to relate the magnitude of extreme events to their frequency of occurrence through the use of probability distributions. The hydrologic data analyzed are assumed to be independent and identically distributed, and the hydrologic system producing them (e.g., a storm rainfall system) is considered to be stochastic, space-independent, and time-independent (Gashaw et al., 2011). In order to satisfy the requirements of independence and identical distribution, the hydrologic data used should be carefully chosen. In reality, this is frequently accomplished by choosing the variable's annual maximum (Shahabi & Kermani, 2015). The purpose of frequency analysis of annual series is to obtain a relation between the magnitude of the event and its probability exceedance (Rossi et al., 1984). The probability analysis may be made either by empirical or by analytical method. A simple empirical technique is to arrange the given

annual extreme series in descending order of magnitude and to assign the order number m. the probability P of an event equaled to or exceeded is given by Weibull formula (Alam & Matin, 2005)

$$P = \left(\frac{m}{N+1}\right) \quad 3.15$$

The recurrence interval, T

$$T = \frac{1}{P} = \frac{N+1}{m} \quad 3.16$$

Where N is number of year of record and m is order number..

(Chow, 1988) proposed the frequency factor (Equation 3.17), and it is applicable to many probability distributions used in hydrologic frequency analysis. A probability distribution is a function representing the probability of occurrence of a random variable.. The magnitude X_T of a hydrologic event may be represent as the mean μ plus the departure ΔX_T of the variate from the mean.

$$X_T = \mu + K_T\sigma \quad 3.17$$

Which may be approximate by

$$X_T = \bar{x} + K_T s$$

The departure may be taken as equal to the product of standard deviation σ and a frequency factor K_T; that is $\Delta X_T = K_T\sigma$ the departure ΔX_T and the frequency factor K_T are function of return period and type of probability distribution to be used in the analysis.

In the event that the data variable analyzed is $Y = \log X$ then the same method is applied to the statistics fir the logarithms of the data, using

$$Y_T = \bar{y} + K_T S_Y \quad 3.18$$

And the required value is of X_T is found by taking the anti-log of Y_T. When local rainfall data are available, IDF curves can be develop using frequency analysis.

Extreme value type I distribution and Log Pearson Type III distribution which are commonly used for used extreme hydrological series (Singo et al., 2012).

Extreme value type I distribution

Extreme value type I distribution is applicable to the extreme hydrological events such as the minimum daily rainfall, rainfall intensity and flood peak flow. Storm rainfalls are most commonly modeled by the Extreme Value Type I distribution (Gumbel Method) (Chow, 1988).

For EVI, Chow (1988) derives the following expression for a frequency factor for Extreme value Type I distribution (Gumbel distribution)

$$K_T = -\frac{\sqrt{6}}{\pi}\left\{0.5772 + ln\left[ln\left(\frac{T}{T-1}\right)\right]\right\} \quad 3.19$$

Log Pearson Type III distribution

This distribution is suitable for both the annual non-extreme series and the extreme flood frequency analysis. The recommended technique for fitting a log Pearson Type III distribution to observe the annual peaks is to compute the base 10 logarithms of the rainfall at selected probability, P, by the following equation:

$$Log\ X_T = \bar{x} + K * S \quad 3.20$$

$$X_T = anti - log\ (log\ X_T) \quad 3.21$$

3.4.3 Testing the Goodness of Fit

The goodness of fit of a probability distribution can be tested by comparing the theoretical and sample values of the relative frequency or the cumulative frequency function. In the case of the relative frequency function, the χ^2 test is used.

The χ^2 test static χ_c^2 is given by

$$\chi_c^2 = \sum_{i=1}^{m} \frac{n[f_s(x_i) - p(x_i)]^2}{p(x_i)} \quad 3.22$$

Where m is the number of intervals. It may be noted that $nf_s(x_i) = n_i$, the observed number of occurrence in interval i , and $np(x_i)$ is the corresponding expected number of occurrence in interval i ; so the calculation of (Equation 3.21) is a matter of squaring the difference between the observed and expected numbers of occurrence divided by expected number of occurrence in interval and summing the result overall interval. To describe the χ^2 test, the χ^2 probability distribution must be define. The χ^2 distribution function is tabulated in many statistics texts.

$$Z = \frac{X - \bar{x}}{\sigma} \tag{3.23}$$

$$B = \frac{1}{2}[1 + 0.196854|Z| + 0.115194\,|Z|^2 + 0.000344|Z|^3 + 0.019527|Z|^4]^{-4} \tag{3.24}$$

Where $|Z|$the absolute value of Z and the standard normal distribution is has

$$\mathrm{F(z)} = \mathrm{B} \qquad \text{for z} < 0$$

$$\mathrm{F(z)} = 1 - \mathrm{B} \ \text{ for z} \geq 0$$

In the χ^2 test, $v = m - p - 1$, where, *m* is the number of intervals as before, and *p* is the number of parameters used in fitting the proposed distribution. A confidence level is choose for the test; it is often express as $1 - \alpha$, where α is termed the significance level. A typical value for the confidence level is 95 percent.

3.5 Determining Peak Flow

In the design of practically all hydraulic structures, the peak flow that can be express with in an assigned frequency (says 1 in 100 years) is of primary importance to adequately proportion the structure to accommodate its effect (Kundzewicz et al., 1999). The design of bridges, culverts waterways, and spillways for dams and estimation of scour at a hydraulic structure are some examples where peak flood values are required (Bagatur et al., 2016).

In hydrologic systems, there is a lot of modeling of rainfall-runoff. Stormwater management modeling software and HydroCAD 10.10.2c were used to simulate the hydrologic processes at the study site. Terdiman (2019) claims that city engineers and developers frequently use this program. The peak flow rate and volume of the runoff are calculated by HydroCAD using the Natural Resources Conservation Service (NRCS) Technical Release 20 (TR-20) runoff technique procedure. The Curve Number (CN) value is a key input parameter for HydroCAD's TR-20 algorithm, which it uses to calculate the peak flood magnitude.

3.5.1 SCS Method

The main competitor of the Rational Method is the Soil Conservation District (SCS) Method. Like the Rational Method, the SCS Method makes use of a runoff coefficient. In this case it is called the runoff curve number (CN) and it is determined by the land cover and underlying soil type. Unlike the rational method, however, there is not a linear relationship between the curve number and the resulting runoff. Rather, this method uses the curve number to translate a rainfall depth into depth of direct runoff using the following equation:

$$Q = \frac{(P - 0.2S)^2}{(P + 0.8S)} \qquad 3.25$$

Where Q is the direct runoff in millimeter, P is the rainfall in millimeter, S is the potential maximum retention after runoff begins, in millimeter, and is related to the Runoff Curve Number (CN), as follows:

$$S = \frac{1000}{CN} - 10 \qquad 3.26$$

According to Chow (1988) for designing and analyzing roadway culverts, a 25-yr return period rainfall intensity is used to determine design discharge.

The concept of first abstraction is one that the SCS employs (Ia). Initial abstraction is the total amount of water lost to receiving waterways downstream prior to runoff. It includes surface water trapped in depressions, surface water trapped on vegetation, evaporation, and transpiration (sometimes counted together and known as evapotranspiration).

Although the SCS Method is widely applicable, it does have some limitations. One of these is that it does not realistically model the runoff in cases when the CN values are very low (below about CN=40), especially when the rainfall amount is small. If this is the case, the Rational Method should be used to estimate the runoff (Lapides et al., 2021).

3.6 Culvert Hydraulic Analysis

The chief aim of this task was to determine the opening sizes of the drainage structures from the rate of flood runoff (discharge) and the volume of runoff that will pass through the drainage structures. This method deploys the hydraulic characteristics of the stream influencing the maximum discharge, such as velocity of flow, slope of the stream, cross sectional area of the stream and shape and roughness of the stream. This method will be

used for major streams to compute the design flood levels at crossing sites after the design discharges have been estimated by the hydrological methods of either the Rational or SCS Methods .Cross-Sections of the crossing sites are being determined by the survey.

3.6.1 Model Input Parameters of HY-8

The application of the Hy-8 tool for hydraulic analysis of culverts involves the collection of a range of data which serves as input data before the running of the model. These data defined the culvert barrels and the surrounding site conditions at each of the analyzed crossings. A crossing is defined as the location where a channel crosses a roadway, floodplain, or another embankment. HY-8 allows for the definition and modeling of up to six culverts at each crossing. Data requirements include discharge data, tail water data, roadway and culvert data. The Discharged data's are obtain from the hydrological analysis of the watershed using the rational formula.

- ✓ Tail water data which includes the channel type, slope and the channels invert elevation were all obtained on the field through observation and direct measurement. The tail water data are use to define the water surface profile downstream of the channel crossing.
- ✓ Information on the Roadway data which include the crest length and crest elevation of the road and surface condition of the road (paved or gravel) were collect by measurement and direct observation at each of the culvert location.
- ✓ Culvert Data were acquire by measuring the span or diameter of the selected culverts and diameter of the pipe culvert. In addition, the shape of the culverts were record and use as input file at the culvert data section.

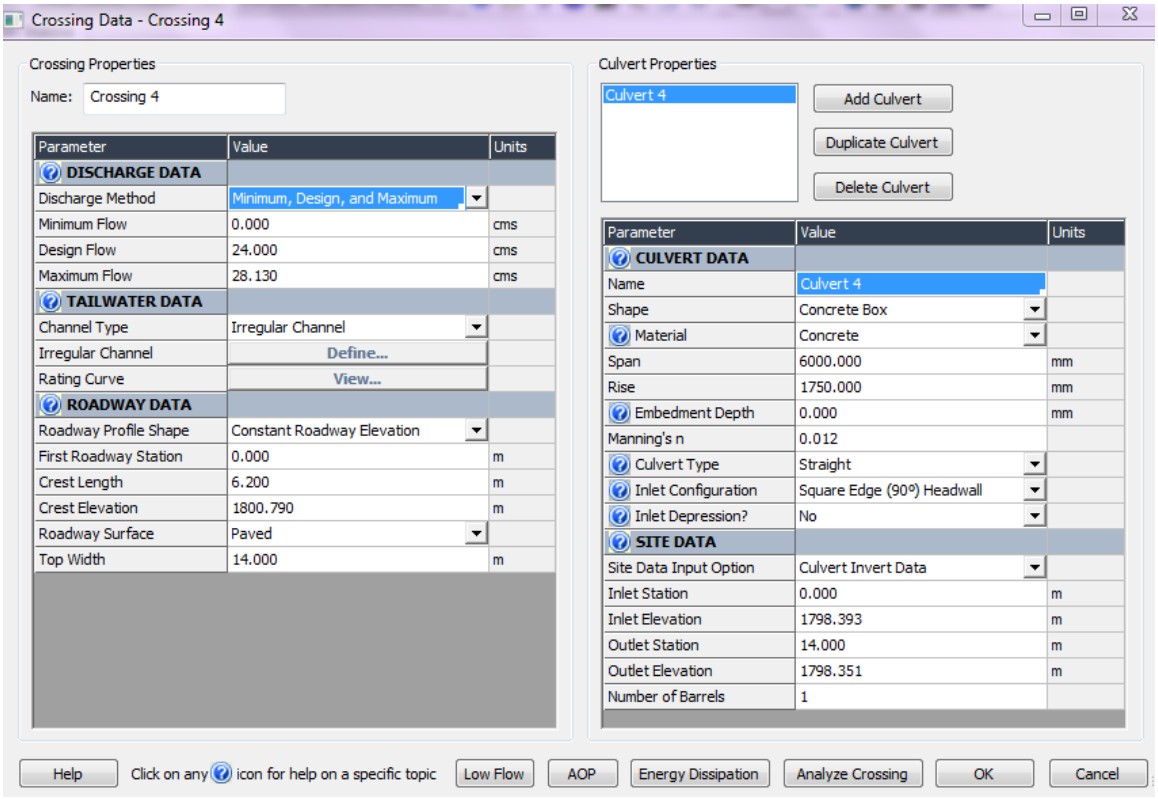

Figure 3.7 Typical culvert crossing data window in HY-8 modelling tool

3.6.2 Model Run and Analysis

All the parameters necessary to define crossing and culvert information's are done using the culvert data window. This is follow by the hydraulic analysis of the culvert including the balancing inflow through multiple culverts and over the roadway. The analysis of the culverts involves the necessary hydraulic calculation after which the overtopping table will be generate and display. At this stage, it's possible to view the water surface profiles as well as a customized table made up of any parameters reckoned during the analysis. In the case of overtopping of culverts after analysis, the culvert can be re-analyze after adding the size of the hydraulic culvert or by adding the number of barrels until the design flow is completely accommodated.

3.6.3 Water Surface Profile of Analyzed Culverts

HY- 8 tool is use to plot the water profile using the direct step method in each direction and the sequent depth associated with each of the steps. However, a hydraulic jump occurs and the length of the jump is calculate from that position, if the sequent depth associated

with the forward profile matches the depth along the backward profile through the culvert. Once a profile is select, the stoner may then plot and view the profile.

3.7 Stormwater Modelling

3.7.1 Sub-catchment Discretization

The study areas will require some level of discretization into multiple sub-catchments in order to properly characterize the spatial variability in overland drainage pathways, surface properties, and connections into drainage pipes and channels. Discretization begins with the identification of drainage boundaries (drainage divides) using a topographic map, the location of major sewer inlets using a sewer system map, and the selection of channel/pipes to be simulated "downstream" in the model (Rossman and Huber, 2016). The study area discretization is done by using both Google Earth and ArcGIS and the collected location data of both drainage lines during site observation by using GPS As sketched in Figure 3.8

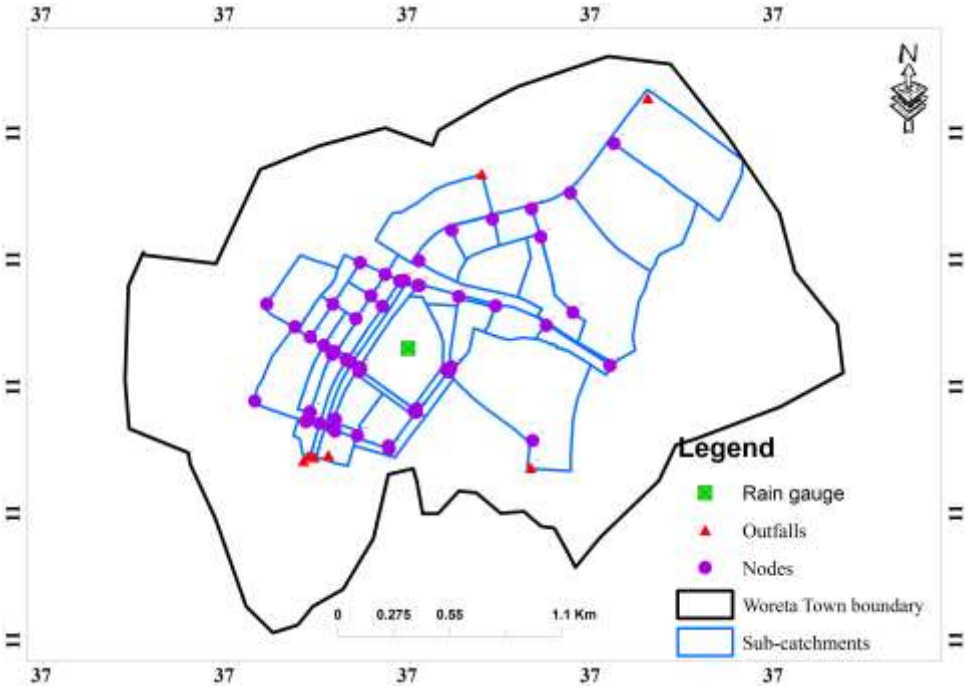

Figure 3.8: Discretized sub-catchments of the study area

3.7.2 Model Parameterization

SWMM requires three major parameters categories for runoff quantity modelling including the physical catchment characteristics, rainfall and infiltration data. The physical catchment data required for runoff modeling include catchment area, percentage of

impervious area, catchment width, average slope, surface depression storage and surface roughness (Rossman and Huber, 2016). Sub-catchment outflow is a function of the coefficient of α, and excess in ponded depth above depression storage.

$$\alpha = \frac{1.49 W S^{1/2}}{An} \qquad 3.27$$

Note that the relative area *A*, width *W*, slope *S*, and roughness *n* are combined into the single parameter α. Equivalent changes in computed runoff may be caused by appropriate alteration of any of these parameters. Note also that the width and slope are the same for both the pervious and impervious subareas. Manning's roughness and relative area are the only parameters available to the modeler to characterize the relative contributions of pervious and impervious areas to the outlet hydrograph.

A. Sub-catchment Area

In principle, the catchment and sub-catchment areas can be defined by constructing drainage divides on topographic maps. In this study, the area of each sub-catchment was calculated by using ArcGIS.

B. Percent of Imperviousness

The percent imperviousness of a sub-catchment is another parameter that can, in principle, be measured accurately from aerial photos or land use maps (Rossman and Huber, 2016). Percent impervious surface area has emerged as a key factor to explain and generally predict the degree of impact severity to streams and watersheds (Bauer, Loffelholz, and Wilson, 2007). One approach to estimating impervious area across large areas with multiple land uses is to associate a percent impervious area with each category of land use. Then, by knowing the percentage of each land use within a sub-catchment, one can calculate its percentage impervious area. According to David, Butler, and John (2004), the percentage imperviousness represents the degree of urban development of the catchment and is defined as:

$$PIMP = \frac{A_i}{A} * 100 \qquad 3.28$$

Where A_i is impervious (roofs and paved areas) area (ha), and A is total catchment area (ha).

C. Sub-catchment width (W)

If overland flow is visualized as running down-slope off an idealized, rectangular catchment, then the width of the subcatchment is the physical width of overland flow. This may be seen for the idealized catchment shown once again in Figure 2.3 (Idealized representation of a sub-catchment) in which the lateral flow per unit width, q_l, is computed and multiplied by the width to obtain the total inflow into the channel (Rossman and Huber, 2016).

Because real sub-catchments will not be rectangular with properties of symmetry and uniformity, it is necessary to adopt other procedures to obtain the width for more general cases. According to Rossman and Huber (2016), A good estimate for the width can be obtained by determining the average maximum length of overland flow and dividing the area by this length.

D. Manning's Roughness Coefficient (n)

Values of Manning's roughness coefficient, *n*, are not as well known for overland flow as for channel flow because of the considerable variability in landscape features, transitions between laminar and turbulent flow, very small flow depths, etc. Most studies indicate that for a given surface cover, *n* varies inversely in proportion to depth, discharge or Reynold's number (Rossman and Huber, 2016).

E. Depression Storage

Depression (retention) storage (depth d_s in Figure 2.4) is a volume that must be filled prior to the occurrence of runoff on both pervious and impervious areas (Zhang & Guo, 2014). It represents a loss or "initial abstraction" caused by such phenomena as surface ponding, surface wetting, interception and evaporation (Rossman and Huber, 2016).

According to Butler et al. (2018) depression storage for impervious areas (Dstor Imperv = 0.12–0.31) and pervious areas (Dstor Perv = 0.49–1.22) were estimated using

Equation *3.29*, which applies a coefficient depending on the surface type and ground slope.

$$d = \frac{k}{\sqrt{S}} \qquad 3.29$$

Where d is depression storage (mm), *k* is a coefficient depending on the surface type (0.07 for impervious surfaces and 0.28 for pervious surfaces) and *s* is the ground slope.

The study area summary of sub-catchments parameters (see Appendix A6), conduits property (see Appendix A7), and nodes property (see Appendix A8).

3.7.3 Parameter Sensitivity

Sensitivity analysis was used to identify key parameters and the parameter precision required for calibration (Niyonkuru et al., 2018). The sensitivity analysis was carried out by varying the value of a particular input parameter while holding the other parameters constant during the simulation. Sensitivity of surface runoff volume and peak flow estimates to key surface runoff parameters is list in **Error! Reference source not found.**

Previous studies using EPA SWMM have found that runoff flow depth is more sensitive to Width-K and N-Imperv and Dstore-Imperv have negative coefficients (Vorobevskii et al., 2020).

Table 3.7 Sensitivity of runoff volume and peak flow to surface runoff parameters (Rossman and Huber, 2016)

Parameter	Typical effect on hydrograph	Effect of increase on runoff volume	Effects of increase on runoff peak
Area	Significant	Increase	Increase
Imperviousness	Significant	Increase	Increase
Width	Affect shape	Decrease	Increase
Slope	Affect shape	Decrease	Increase
Roughness	Affect shape	Increase	Decrease
Depression storage	Moderate	Decrease	Decrease

3.7.4 SWMM Calibration and Validation

The calibration of the hydrological model typically employs two main techniques: continuous and (multi)-event matching. Since the study investigates modeling storm events and overloading of SWSS, calibration with short heavy rain events instead of long time series with dry weather or regular stormwater flow provides more accurate results (Senarath et al., 2000). The model can be calibrated using a variety of methodologies and performance metrics depending on the availability of observation data (Moriasi et al., 2015). In general, there are many parameters available for validation in the SWMM: sub-catchment runoff, node/pipe water depth, pipe node inlet/outlet discharge and node flooding consistent model performance over a set time period. This was accomplished by keeping the values of the model's input parameters within the preset ranges. The model was calibrate and verified by the link/channel flow of selected channels that flow depth was measured. These measured flow depth at the selected node is converted into observed flow the channel by using equation 3.30

$$Q_o = \frac{A}{n} * R^{2/3} * S^{1/2} \qquad 3.30$$

Where, Q_o is Observed flow (m^3/sec), A is area of the channel (m^2), n is roughness of the channel, R is hydraulic radius of the channel, and S is slope of the channel.

3.7.5 Performance of SWMM

The evaluation of hydrologic model behavior and performance is commonly made and reported through comparisons of simulated and observed variables. Frequently, comparisons are made between simulated and measured link flow at the channel outlet. Efficiency criteria are commonly used by hydrologists to provide an objective assessment of the "closeness" of the simulated behavior to the observed measurements (Krause et al., 2005). While there are a few efficiency criteria used for this study such as:

A. Coefficient of determination (R^2)

The coefficient of determination R^2 is defined as the squared value of the coefficient of correlation according to Bravais Pearson. It is calculated as:

$$R^2 = \left(\frac{\sum_{i=1}^{n}(O_i - \bar{O})(P_i - \bar{P})}{\sqrt{\sum_{i=1}^{n}(O_i - \bar{O})^2}\sqrt{\sum_{i=1}^{n}(P_i - \bar{P})^2}} \right)^2 \quad 3.31$$

With O observed and P predicted values. The range of R^2 lies between 0 and 1which describes how much of the observed dispersion is explained by the prediction. A value of zero means no correlation at all whereas a value of 1 means that the dispersion of the prediction is equal to that of the observation.

B. Index of agreement (d)

The index of agreement *d* was proposed by Willmot (1981) to overcome the insensitivity of *E* and *r*2 to differences in the observed and predicted means and variances. The index of agreement represents the ratio of the mean square error and the potential error Willmott (1981) and is defined as:

$$d = 1 - \frac{\sum_{i=1}^{n}(O_i - P_i)^2}{\sum_{i=1}^{n}(|P_i - \bar{O}_i| + |O_i - \bar{O}|)^2} \quad 3.32$$

The range of d is similar to that of R^2 and lies between 0 (no correlation) and 1 (perfect fit).

C. Nash-Sutcliffe Efficiency (NSE)

The efficiency NSE proposed by Nash and Sutcliffe (1970) is defined as one minus the sum of the absolute squared differences between the predicted and observed values normalized by the variance of the observed values during the period under investigation (Krause et al., 2005). It is calculated as in:

$$NSE = 1 - \frac{\sum_{i=1}^{n}(O_i - P_i)^2}{\sum_{i=1}^{n}(O_i - \bar{O})^2} \quad 3.33$$

The range NSE lies between 1 and -∞. An eicency of 1 (NSE=1) corresponding to perfect match of modelled to observed data. An efficiency of lower than zero indicates that the mean value of the observed time series would have been a better predictor than the model.

3.7.6 Urban Drainage System Performance

The freeboard of a channel is the vertical distance from the top of the channel to the water surface at the design condition. To calculate the freeboard performance index according to the simulation, maximum flow rate for each channel was calculated. As maximum flow rate varies in each channel, a specific penalty curve for each channel is obtained. The PIV_i and PIF_i penalty curve for each channels or for the channels that has equal amount of maximum flow is developed to determine PIV_i and PIF_i of each channel by using the height of the difference between channel depth and simulated maximum water head of the chancel. The Vol_i is also calculate by multiplying maximum channel water volume by the time of peak.

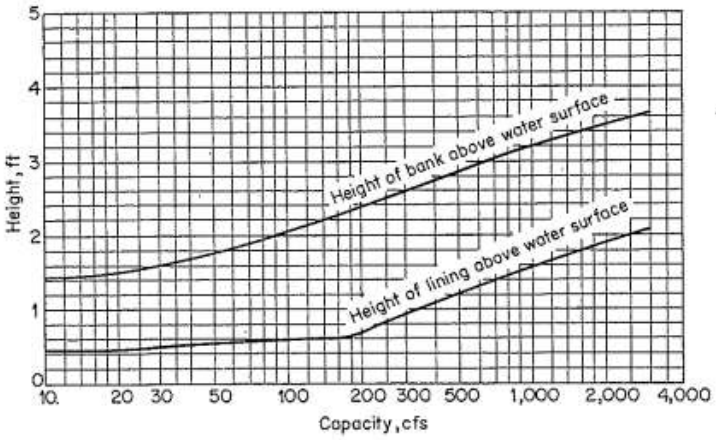

Figure 3.9 Recommended freeboard and height of bank of lined channel (U.S. Bureau of reclamation)

Due to Tabesh et al. (2016), the velocity should never exceed 6 meters per second in a channel. Maximum values for channels with different covers are shown in Table 3.8.

Table 3.8 Maximum allowable velocity for different channel cover (Tabesh et al., 2016)

Material	Maximum Velocity(m/s)
Clay	4.5-5.5
Cementite	3.5-4.5
Stone and cement	3.0-4.0

In this study, the cover of channels is stone and cement. Therefore, the maximum suggested velocity is 4 meters per second. According to what has been mentioned, the hydraulic performance for velocities greater than 6 meters per second is not acceptable and its PIV is assumed 0.25. Because of the fact that the channel is performing with a flow velocity of 6 meters per second, the performance index was determined to be 0.25, noting that this value cannot be zero and the system performance index ought to be under 0.5. The maximum performance with PIV equal to 1 is achieved when the velocity is less than 4 meters per second. Then velocity penalty curve is obtained.

After calculating the velocity and freeboard performance indices, network reliability could be determine. To calculating the network reliability, weighted average can be use.

A weighting function is apply to summarize the channel performance index as follows:

$$PIV_t = \frac{\sum_1^N PIV_i * Vol_i}{\sum_1^N Vol_i} \quad 3.34$$

$$PIF_t = \frac{\sum_1^N PIF_i * Vol_i}{\sum_1^N Vol_i} \quad 3.35$$

Where, PIF_t and PIV_t are the freeboard and the velocity performance indices in the entire network, respectively, PIV_i and PIF_i are the velocity and the freeboard performance indices in channel i, respectively, Vol_i is the maximum volume of water flowing inside the channel during the simulation and N is the number of channels (Tabesh et al., 2016).

The goal of this paper is to prevent flooding in the urban areas for this reason the weight of freeboard performance index is taken as 0.6 and the weight of velocity performance index is taken as 0.4 (Tabesh et al., 2016). Reliability is calculate by equation 3.36.

$$Rel_t = 0.6\ PIF_t + 0.4\ PIV_t \quad 3.36$$

4 RESULT AND DISSCUSION

4.1 Current Condition of Drainage Facilities

From field surveys and field observations, the community's current status of the drainage system has been investigated. Closed and open drainage lines with rectangular shapes are existing drainage facilities in Woreta Town. Closed drainage lines are found only along main roads, while open drainage channels are found along sub-mains and local roads. Due to this investigation, I have seen many storm drainages with problems. These are flooding in the case of minimum free board and sedimentation in cases where the channel flow velocity is less than the permissible velocity. Also overtopping of floods in the road in case of inadequacy of culverts openings and sedimentations. As shown in the figure below culvert 3 has sedimentation problem the two openings are closed.

Figure 4.1 Observed existing conditions of some storm drainages and culverts in the study area

4.2 Rainfall Data Analysis

4.2.1 Filling Missing Data

The missing values of the rainfall data are filled in, and then the maximum annual rainfall data of the three stations is described in Appendix A1. Due to this result, the maximum and minimum average maximum depth of rainfall of Woreta metrological station is 108.2mm in 1988 and 48mm in 1995 respectively.

4.2.2 Test for Absence of Trend

The trend analysis of rainfall data of metrological stations used in this study is done by using Spearman's rank-correlation method.

Table 4.1 Summary of trend analysis results of rainfall data's of metrological stations

Metrological Stations	t_t	t (V,2.5%)	t (V,97.5%)	Remarks
Woreta	-2.04	0.635	2.04	no trend
Wanzaye	-2.04	0.651	2.04	no trend
Addis zemen	-2.04	-1.01	2.04	no trend

As the table shows above, t (V, 2.5%) of all stations are between t_t and t (V, 97.5%). Therefore, there is no trend in the rainfall data of the three metrological stations.

4.2.3 Tests for Stability of Variance and Mean

Test for variance stability analysis of these metrological stations are done by F- test.

Table 4.2 Summary of test stability of variance

Metrological Stations	F_t	F (V_1,V_2,2.5%)	F (V_1,V_2,97.5%)	Remarks
Woreta	0.925	0.36	2.73	stable
Wanzaye	0.502	0.36	2.73	stable
Addis zemen	0.927	0.36	2.73	stable

According to the table above, F (V1, V2, 2.5%) of all stations are located between Ft and F (V1, V2,97.5%). Therefore, the variance of these rainfall data for the three metrological stations is stable.

Test of mean stability analysis of these metrological stations are done by t- test.

Table 4.3 Summary of test stability of mean

Metrological Stations	t_t	t(V,2.5%)	t(V,97.5%)	remarks
Woreta	-2.12	-0.237	2.12	stable
Wanzaye	-2.12	-0.748	2.12	stable
Addis zemen	-2.12	-0.486	2.12	stable

As the table shown above, t (V,2.5%) of all stations are between t_t and t (V,97.5%). Therefore, the mean of the rainfall data of the three metrological stations is stable.

As shown in the above tables, there was no trend, and the variance and mean were stable. Therefore, the time series is stationary in the sense used for this data screening, and there is no immediate objection to using the data to develop an intensity duration frequency curve.

4.2.4 Tests for Relative Consistency and Homogeneity

A double mass curve was used to check the relative consistency and homogeneity of hydrological data at Woreta station by comparing it with other stations (Wanzaye station and Addis Zemen station) in the area, and that can be used to adjust inconsistency in precipitation data. Figure 4.2 shows the results before making a correction. In addition, Figure 4.3 shows the cumulative annual rainfall of Woreta station versus the average accumulative annual rainfall of neighboring stations. The ratio between the variables is fixed by the correction factor of 0.737. Multiplying the values of each year that the curve in the graph occurred. Then the corrected annual maximum rainfall data is shown in Appendix A2.

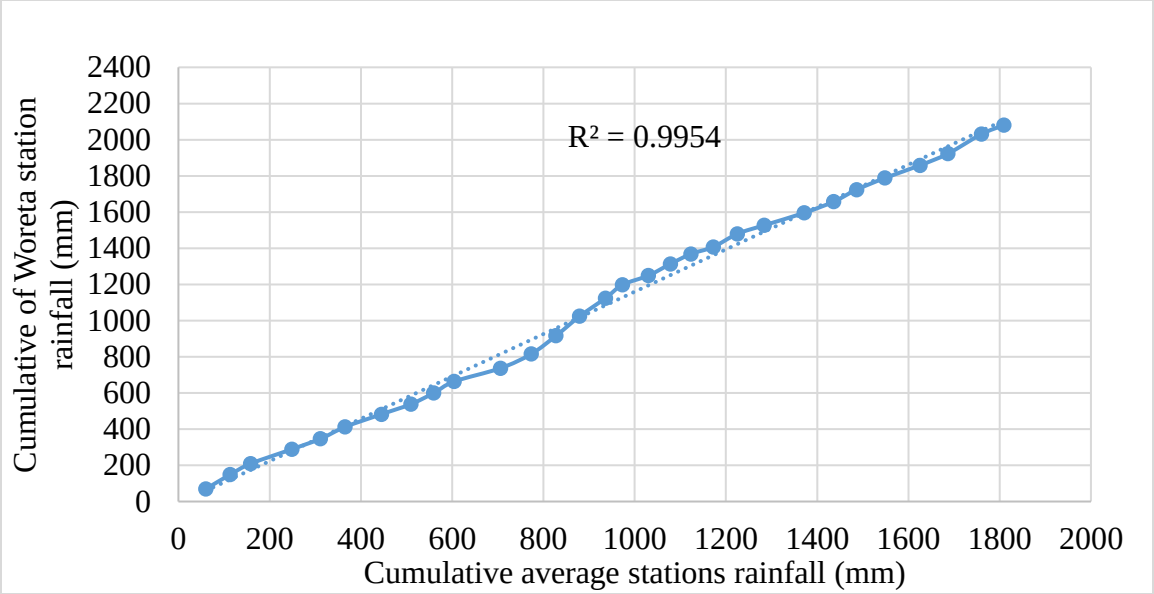

Figure 4.2 Double mass curve before correcting inconsistency of Woreta rainfall station.

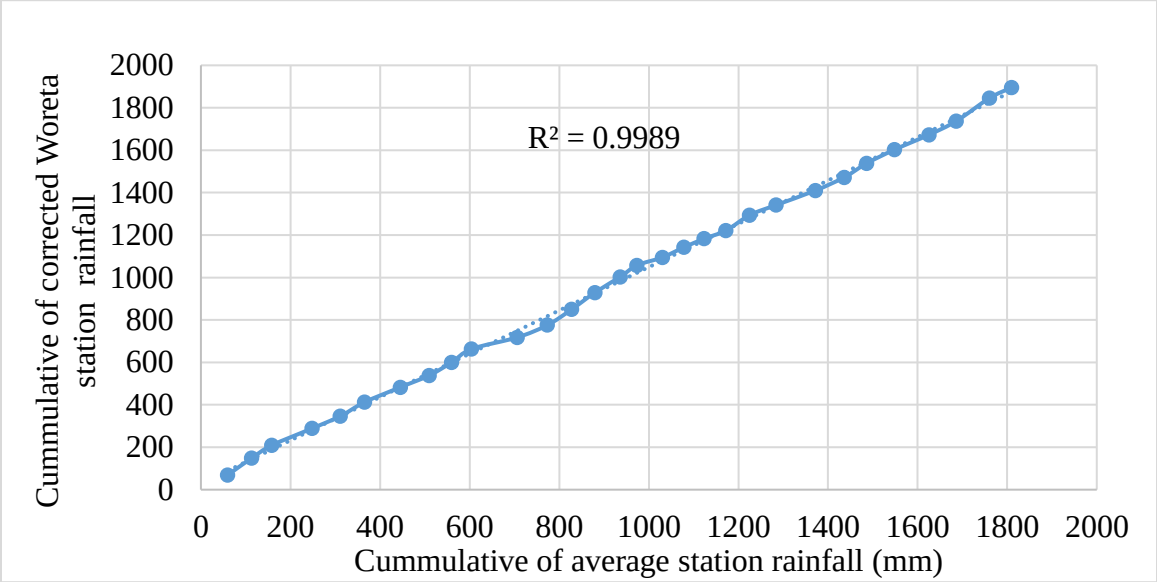

Figure 4.3 Double mass curve after corrected inconsistency of Woreta rainfall station.

4.2.5 Testing Outlier

Outlier's area the data points that depart from the trend of remaining data as shown at calculated the Skewness coefficient is greater than +0.4 our data therefore this data is check for higher outlier.

Higher outlier test

From table sample size for N (30year) rainfall data, Kn=2.563 (from Appendix C3).

$$Y_H = 2.047$$

$$\text{antilog}\,(Y_H) = 10^{Y_H} \Rightarrow 10^{2.047} = 111.4$$

The higher recorded daily maximum rainfall is 108.2mm in the 1988, which lower than boundary value of higher outliers. Hence, there are no higher outlier's data recorded the result of statistical analysis is Appendix A2

4.3 Intensity Duration Frequency Curve

Reliable estimations of the intensity of the rainfall are required for appropriate hydrologic studies. Estimates of rainfall intensities for various durations and recurrence intervals are included in the IDF relationship. So, the shortest time rainfall depth for the study area is determined (see Appendix E2). Then IDF curve develop to obtain the depth and intensity of 15-minute interval that used input for SWMM and HydroCAD to get good simulated peak flow..

Two common frequency analysis techniques were used to develop the relationship between rainfall intensity, storm duration, and return periods from rainfall data for the regions under study. Rainfall intensity of these two distribution functions are:

Table 4.4 Rainfall intensity developed by Gumbel distribution

Duration (hr)	Return period (yr)					
	2	5	10	25	50	100
0.25	89.2	107.9	120.3	136.0	147.7	159.2
0.5	62.7	75.9	84.6	95.6	103.8	112.0
0.75	48.6	58.8	65.5	74.1	80.4	86.7
1	39.7	48.1	53.6	60.6	65.8	70.9
1.25	33.7	40.8	45.4	51.4	55.8	60.1
1.5	29.3	35.4	39.5	44.6	48.4	52.2
1.75	25.9	31.3	34.9	39.5	42.9	46.2
2	23.2	28.1	31.4	35.4	38.5	41.5
2.25	21.1	25.5	28.5	32.2	34.9	37.7
2.5	19.3	23.4	26.1	29.5	32.0	34.5
2.75	17.8	21.6	24.0	27.2	29.5	31.8
3	16.5	20.0	22.3	25.2	27.4	29.5

Table 4.5 Rainfall intensity developed by Log-Person type III distribution

Duration (hr)	Return period (yr)					
	2	5	10	25	50	100
0.25	85.5	105.0	118.5	136.2	149.9	164.0
0.5	60.1	73.8	83.3	95.8	105.4	115.3
0.75	46.5	57.2	64.5	74.2	81.6	89.3
1	38.1	46.8	52.8	60.7	66.8	73.0
1.25	32.3	39.6	44.7	51.4	56.6	61.9
1.5	28.0	34.4	38.9	44.7	49.2	53.8
1.75	24.8	30.5	34.4	39.5	43.5	47.6
2	22.3	27.4	30.9	35.5	39.0	42.7
2.25	20.2	24.8	28.0	32.2	35.4	38.8
2.5	18.5	22.7	25.7	29.5	32.5	35.5
2.75	17.1	21.0	23.7	27.2	29.9	32.8
3	15.9	19.5	22.0	25.3	27.8	30.4

Chi square method was employed to test the fitness of the yearly maximum rainfall data (1987- 2016) records with respect to both Gumbel's and Log Pearson type III probability distribution methods. Details of the test of data is in Appendix A4. As the table shows critical values at α=0.05 (i.e 7.8147) in both distributions is greater than statistics of them

1.0106 for Log-Person and 2.2957 for Gumbel distribution but the statistics values of Log-Person type III is much less than Gumbel. Therefore, I select Log-Person type III probability distribution to develop intensity duration frequency curve of the town.

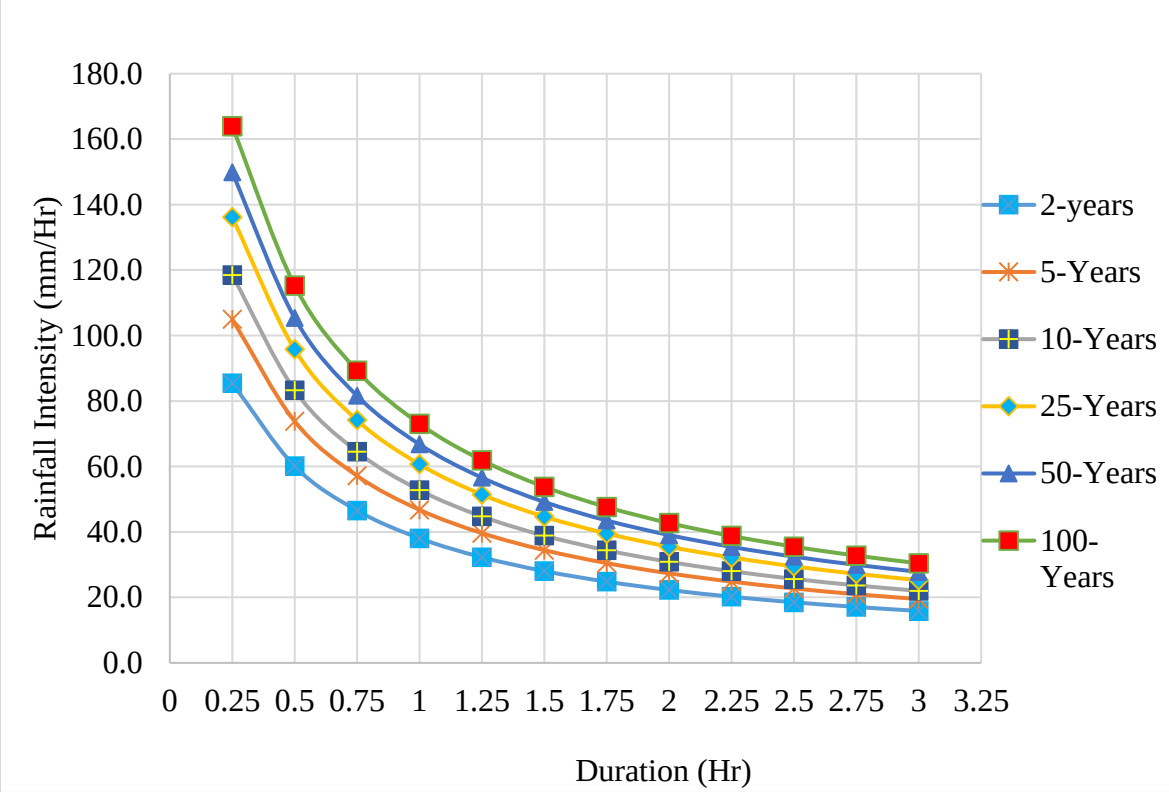

Table 4.6 Intensity duration frequency curve of Woreta Town

4.4 Hydrological Analysis

4.4.1 Design Flow of Culverts

The design discharge of each culverts is calculated by Manning's roughness method by using the collected cross-sectional and location data's of culverts in Appendix A2. The manning roughness values of each culverts is get from Appendix C4 by using there lining types. The calculated design discharge of culverts is:

Table 4.7 Calculated design flows of culverts

No	Name	Area (m^2)	Manning coefficient	Velocity (m/s)	Design Discharge (m^3/s)
1	Culvert 1	0.5	0.031	0.663	1.33
2	Culvert 2	24.3	0.012	3.253	79.05
3	Culvert 3	31.5	0.012	3.074	96.84
4	Culvert 4	10.5	0.015	2.679	28.13

At culvert 3 there was 4 openings but the two openings are closed by silt therefore for this study I use the cross section area of only two openings. If these silted openings are cleaned the cross sectional area of the culvert is increased into 52.5 m^2 and also the velocity is increased into 3.327 m/sec and the design flow of this culvert is 174.7 m^3/sec.

4.4.2 Peak Flows of Catchments of Culverts

The peak flows of the catchments of each culvert are determined by using Hydro-Cad software in SCS TR-20 by 25-yrs. The software input data is calculated by using ArcGIS by making watershed analysis calculating the slope, areas, and length of longest flow path and by land use analysis calculating the land cover to determine the curve number of each catchments. These are:

Table 4.8 Catchment characteristics of culverts

No	Name	Time Concentration (hr)	Area (ha)	Average Run-off Curve No	Average Run-off Coefficient
1	Culvert 1	0.5	964.8	84	0.4
2	Culvert 2	0.5	347.9	84	0.4
3	Culvert 3	1	4096	82	0.4
4	Culvert 4	0.5	1013.4	79	0.38

Then the detail of peak flow of each culverts catchments is:

Table 4.9 The peak flow of all culverts catchment

No	Name	Peak Flow (m^3/sec)
1	Culvert 1	37.0
2	Culvert 2	13.3
3	Culvert 3	134.9
4	Culvert 4	24.0

According to calculated peak flows of catchments of culverts, these are listed in Table 4.9. The peak flow of the rational method in all catchments is much higher than the peak flow of SCR TR-20. Then for this study, I used SCR TR-20 peak runoff because of all catchments having an area of greater than 50 ha. For designing and analysis of roadway culverts, a 25-yr return period discharge is used. Therefore, for this study, I used the peak discharge of a 25-year return period. The details of the model outputs of this peak flow calculation are (see Appendix B1)

4.4.3 Sub-catchments Runoff

The surface runoff of sub-catchments of each drainage line is calculated by using SWMM by considering the infiltration of it. As I described before, SWMM is a distributed model that allows a study area to be subdivided into any number of irregularly shaped sub-catchment areas to best capture the effect that spatial variability in topography, drainage pathways, land cover, and soil characteristics has on runoff generation. Generation of runoff is therefore computed on a per sub-catchment basis. It was done by using Equation 2.6. The infiltration is also calculated by using the curve number method. In addition, % of zero imperviousness of roof is taken 100% and for asphalt roads 50%. For the detail of simulated sub-catchments runoff, (see Appendix D1). For simulation, 3-hour precipitations with return periods of 5 years were used by reffering the table in appendix C5

4.4.4 Calibration and Validation

All models, from simple lumped to complicated distributed physically based models, need to be calibrated because it is challenging to determine values of model parameters from field data. The model was calibrated and validated for 2 years (2021 and 2022). The length of data used for calibration and validation of the model was 10 days of

average flow depth in C21 and C36 in 2021 and verified for 7 days in the year 2022. The calibration is done by trial and error by using or changing sensitive parameters of the model (by adjusting the measured and calculated physical parameters of modeled sub-catchments and drainage channels). After making some trials by changing the senisetive paramers (N pervious and N impervious) by using 0.6 for N-pervious and 0.03 for N-impervious the model performance is in all efficiency criterias is more acceptable. Then the model performance is:

Table 4.10 The second trial's model calibration performance value.

Link Code	R^2	d	NSE
C21	0.96	0.95	0.78
C36	0.99	0.97	0.97

Therefore the model performances of the second trial of is the highest, in this case for this study the N-pervious and N-impervious values of the developed model is 0.6 and 0.03 respectively. The observed and simulated channel flow depth of both channels used for calibration of the model are set in Table 4.11.

Table 4.11 Summary of observed and simulated data during calibration and validation of the SWMM

Day	Observed average channel flow depth (m)		Simulated average channel flow depth (m)	
	C21	C36	C21	C36
7/31/2021	0.31	0.23	0.21	0.28
8/3/2021	0.50	0.43	0.44	0.44
8/8/2021	0.78	0.68	0.74	0.69
8/15/2021	0.46	0.42	0.44	0.44
8/31/2021	0.44	0.44	0.44	0.44
9/3/2021	0.35	0.23	0.21	0.28
9/12/2021	0.49	0.43	0.44	0.44
9/17/2021	0.36	0.21	0.21	0.28
9/18/2021	0.78	0.68	0.74	0.69
9/22/2021	0.77	0.65	0.69	0.65
6/19/2022	0.43	0.32	0.44	0.44
6/20/2022	0.51	0.41	0.44	0.44
6/24/2022	0.54	0.68	0.52	0.58
6/25/2022	0.60	0.42	0.52	0.58
6/28/2022	0.79	0.63	0.63	0.59
7/15/2022	0.60	0.50	0.52	0.58
7/31/2022	0.28	0.23	0.21	0.26

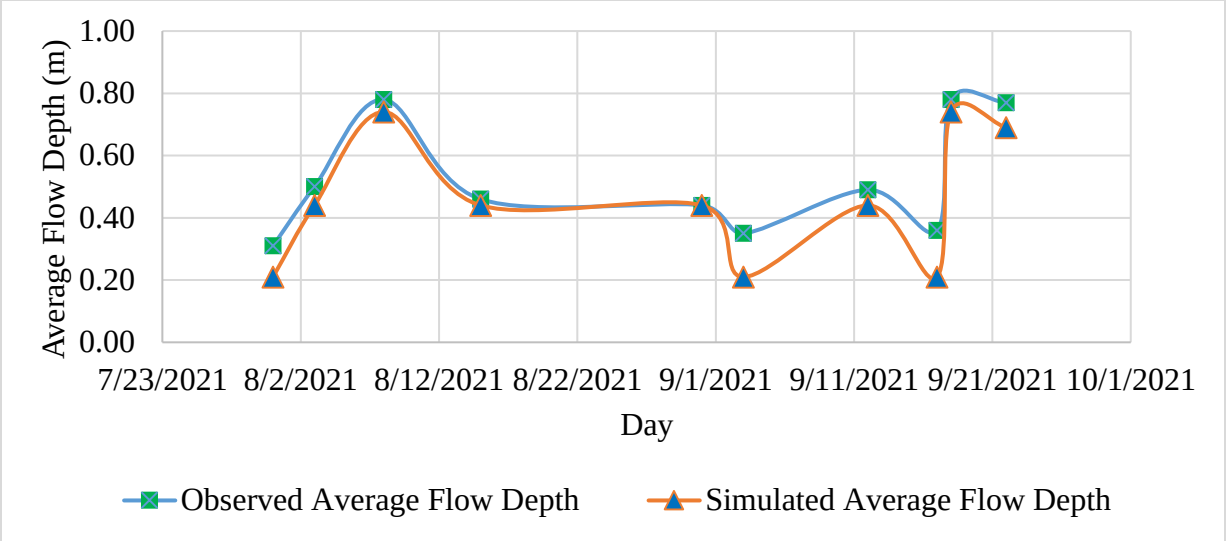

Figure 4.4 Calibration results of average observed and simulated flow depth of link C21

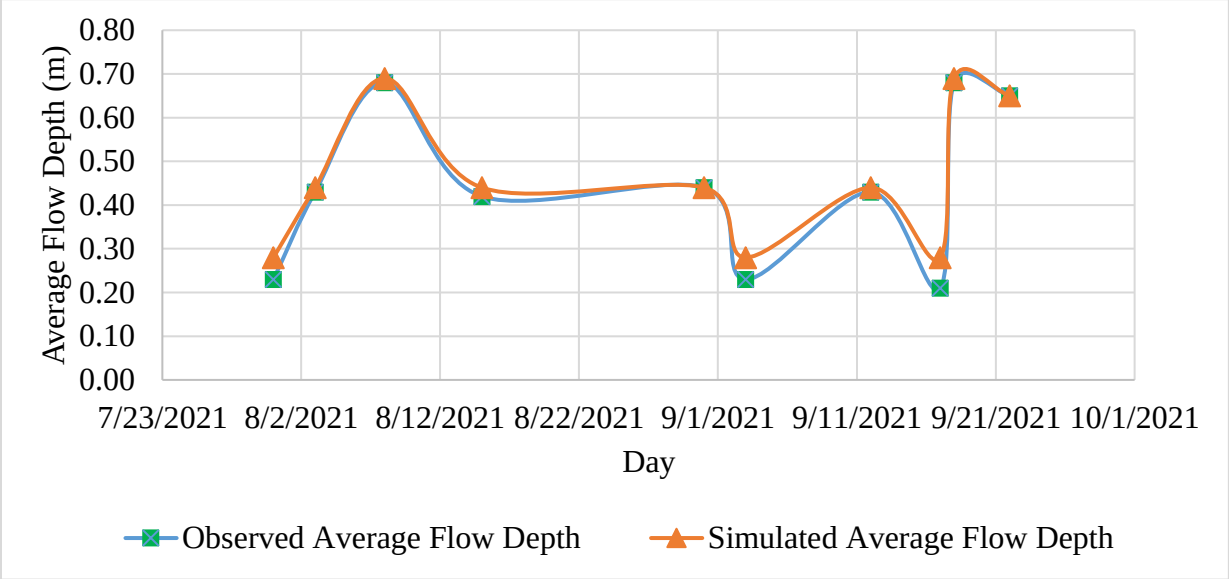

Figure 4.5 Calibration results of average observed and simulated flow depth of link C36

Results of model validation performance is:

Table 4.12 Results of model validation performance

Link Code	R^2	NSE	d
C21	0.9	0.68	0.91
C36	0.7	0.63	0.88

As the result shows, the observed and simulated link flow depth are more correlated. Therefore, the outputs of this model are used for further study.

4.5 HY-8 Model Outputs

Overtopping will happen as indicated below if the headwater elevation is higher than the road elevation. The program determines the discharge for each culvert and for the road that will result in the same headwater height when overtopping has occurred. The model-analyzed outcome, as displayed in the table in the Appendix B2-B5 for each culverts, indicates that: Because the discharge begins flowing over the road at a headwater elevation of 1809.55 m and 1810.88 m, respectively, at culverts 1 and 3, overtopping occurs there. However, culvert 2 and 4 peak discharge headwater elevation is less than the roadway elevation (i.e in culvert 2, 1809.35 m < 1809.65 m; in culvert 4, 1800.69 m < 1800.790 m) therefore overtopping is does not occur.

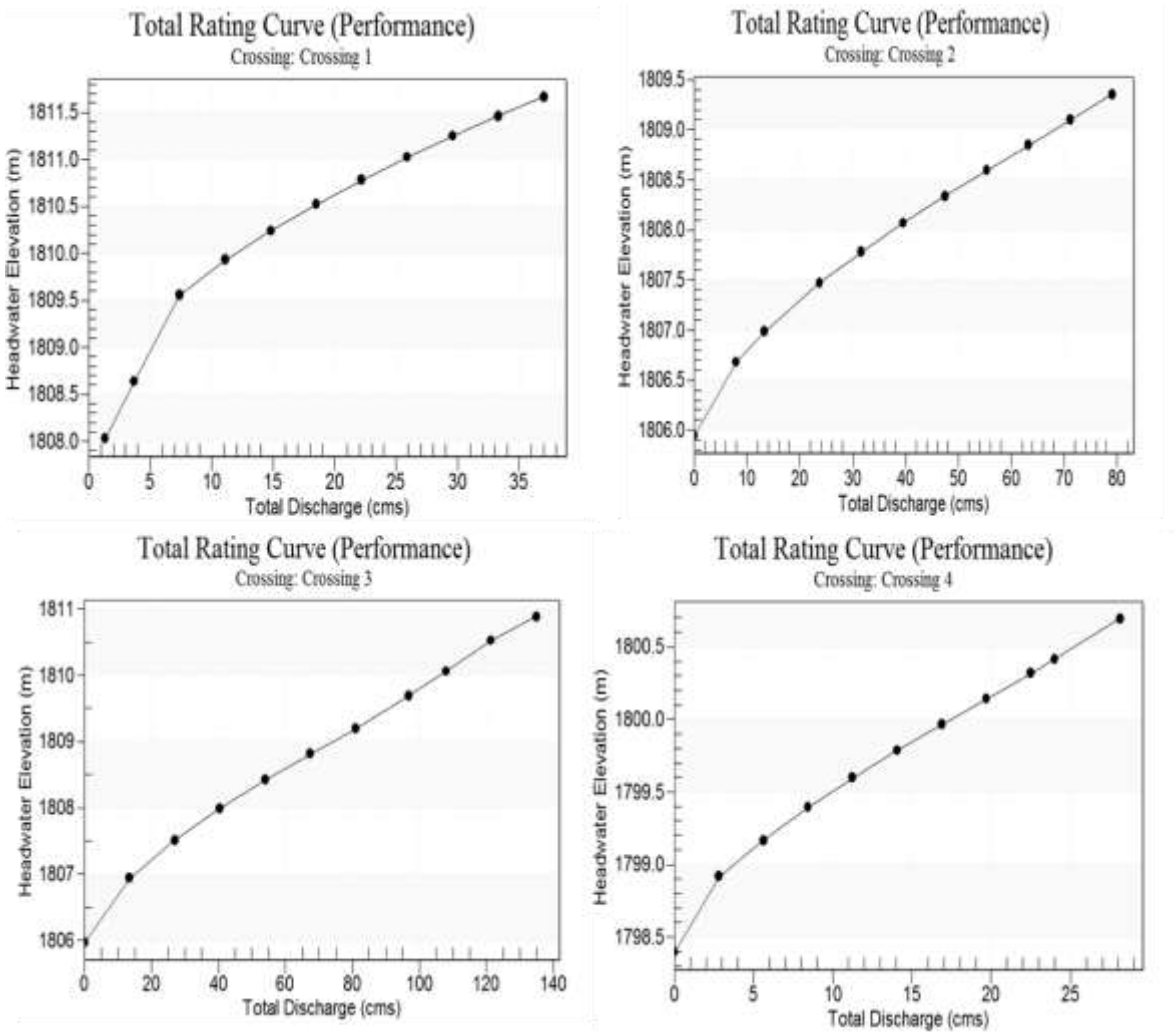

Figure 4.6 Rating curve of each crossings.

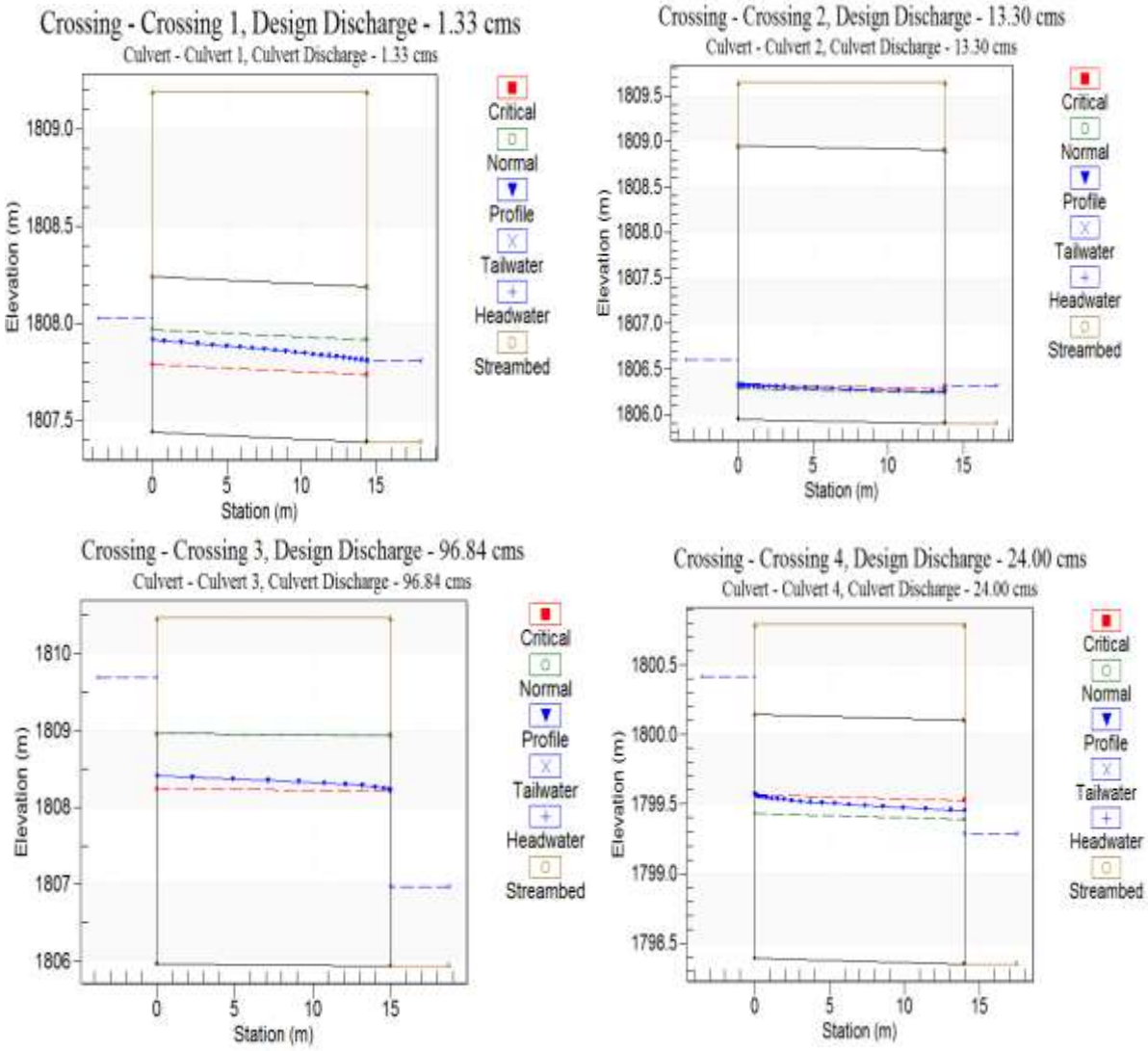

Figure 4.7 Water surface profiles of crossings

4.6 SWMM Outputs

For this study, I used time series data or the precipitation depth per unit time from the developed IDF curves of town. With a return period of 5 years and a 3 hour rainfall duration to analyze the existing drainage structures. In addition, the modeled area was classified into two to show all drainage components in the working area of the model. The results of each are shown below:

4.6.1 Link Flow

The simulated model has many outputs (sub-catchments runoff, node depth, node flooding, outfall loading, link flow, and conduit surcharges) with tabulated, time series profile plots, and graphs. But for the aim of this study I was used only link flow outputs that containes maximum flow rate, maximum velocity and maximum water level of each channel.

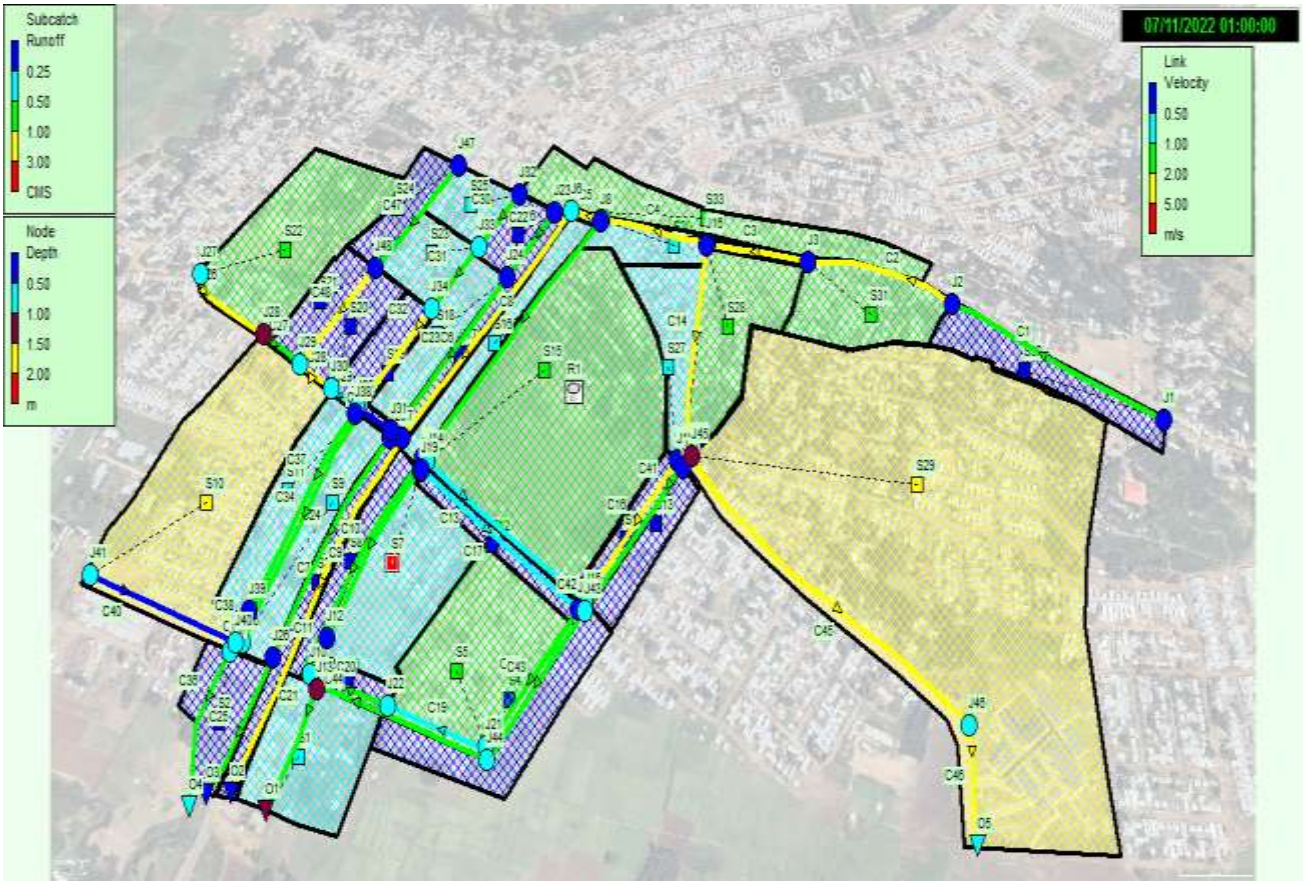

Figure 4.8 Map of model area one simulated results

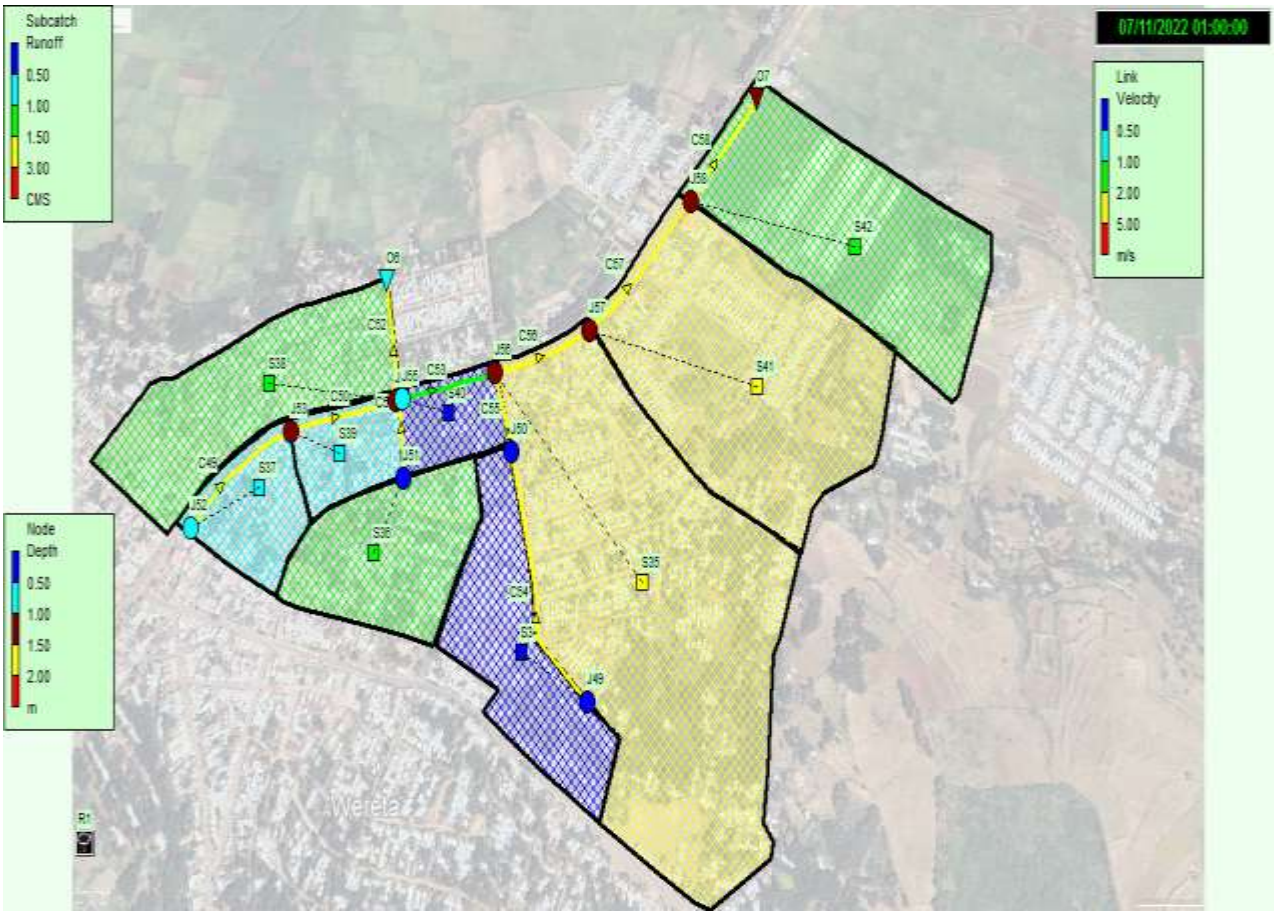

Figure 4.9 Map of model area two simulated results

4.7 Performance Index of Freeboard

The simulated outputs of all links are attached in the Appendix C1. Due to these outputs in the case of maximum flow C55 has the highest maximum flow (3.378 m3/sec), and C40 has the lowest maximum flow (0.142 m^3/sec). For this study, the penalty curve of freeboard of the channels used to determine the channel freeboard performance index is developed in groups of channels that have the same maximum flow rate. This means that they have the same recommended freeboard because it is determined by the channel maximum flow rate.

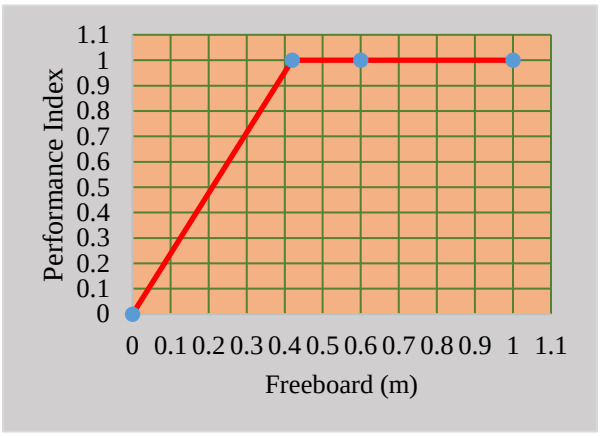

a)

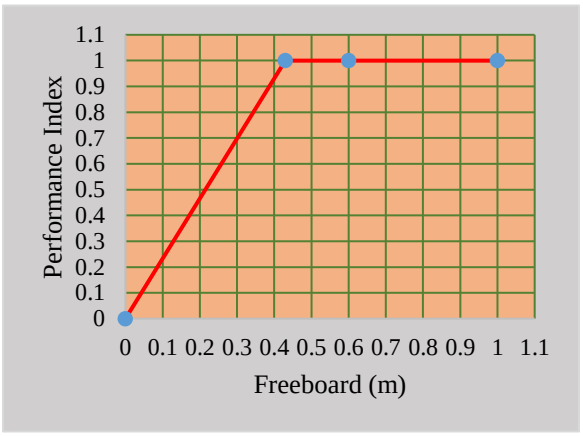

b)

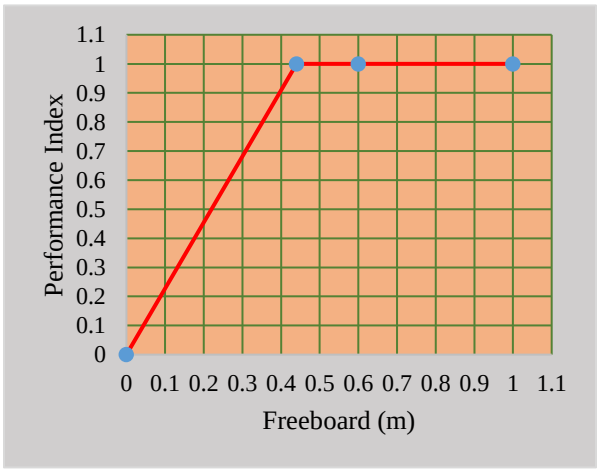

c)

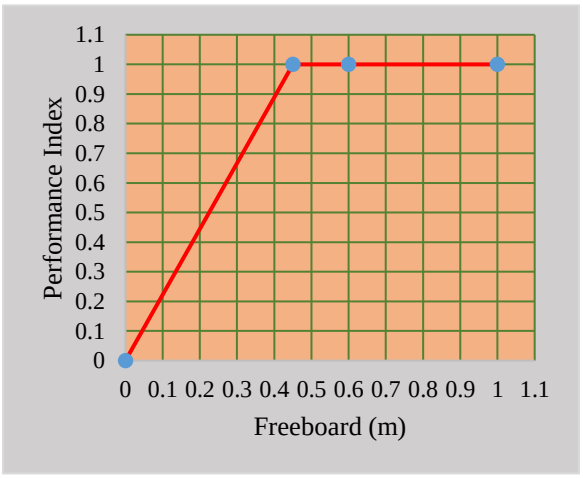

d)

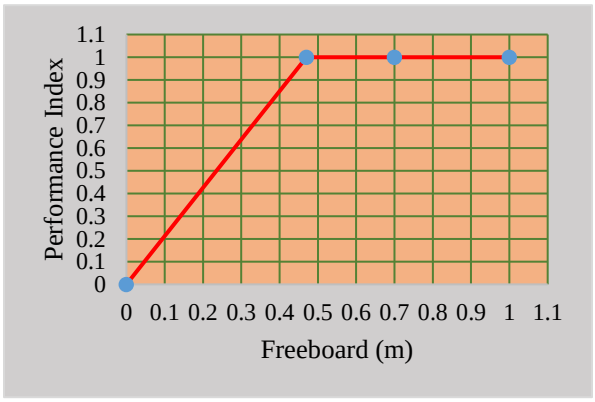
Performance Index
1.1
1
0.9
0.8
0.7
0.6
0.5
0.4
0.3
0.2
0.1
0
0 0.1 0.2 0.3 0.4 0.5 0.6 0.7 0.8 0.9 1 1.1
Freeboard (m)

e)

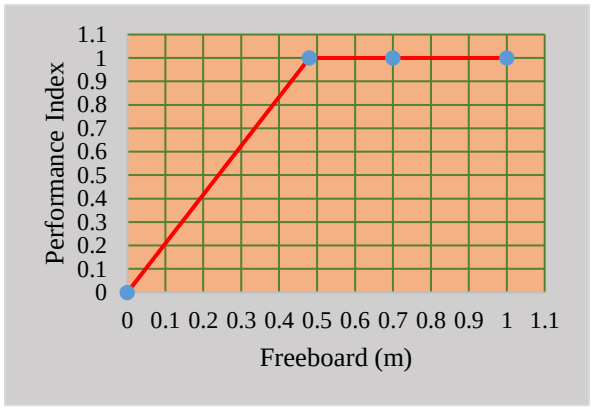
Performance Index
1.1
1
0.9
0.8
0.7
0.6
0.5
0.4
0.3
0.2
0.1
0
0 0.1 0.2 0.3 0.4 0.5 0.6 0.7 0.8 0.9 1 1.1
Freeboard (m)

f)

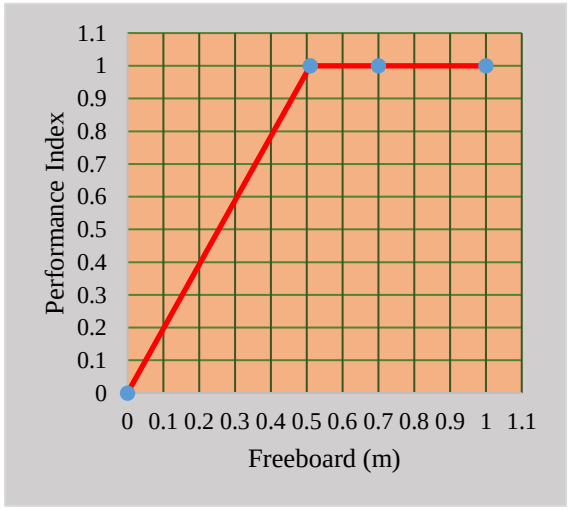
Performance Index
1.1
1
0.9
0.8
0.7
0.6
0.5
0.4
0.3
0.2
0.1
0
0 0.1 0.2 0.3 0.4 0.5 0.6 0.7 0.8 0.9 1 1.1
Freeboard (m)

g)

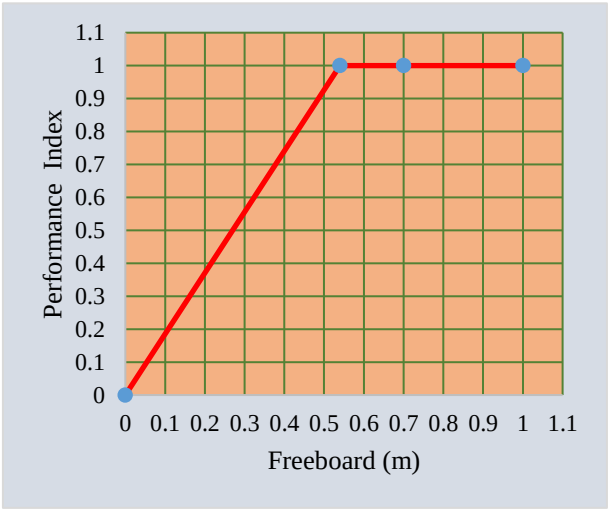
Performance Index
1.1
1
0.9
0.8
0.7
0.6
0.5
0.4
0.3
0.2
0.1
0
0 0.1 0.2 0.3 0.4 0.5 0.6 0.7 0.8 0.9 1 1.1
Freeboard (m)

h)

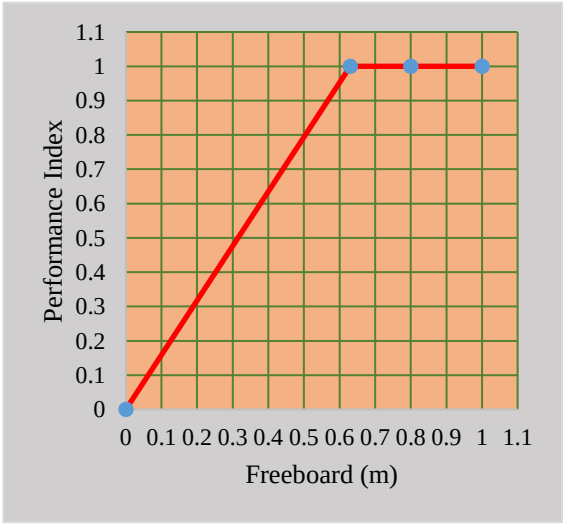
Performance Index
1.1
1
0.9
0.8
0.7
0.6
0.5
0.4
0.3
0.2
0.1
0
0 0.1 0.2 0.3 0.4 0.5 0.6 0.7 0.8 0.9 1 1.1
Freeboard (m)

i)

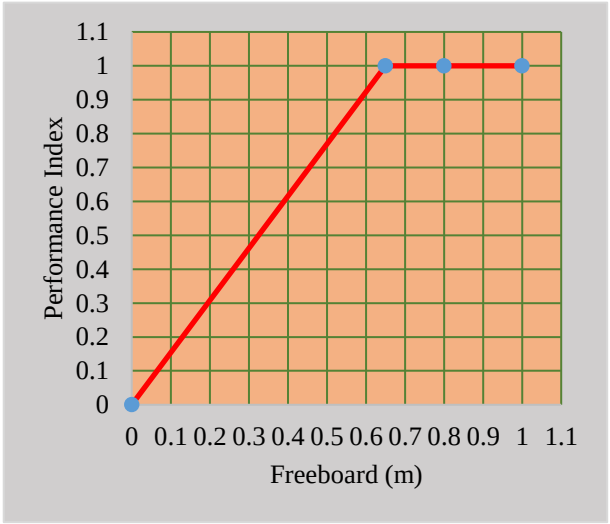
Performance Index
1.1
1
0.9
0.8
0.7
0.6
0.5
0.4
0.3
0.2
0.1
0
0 0.1 0.2 0.3 0.4 0.5 0.6 0.7 0.8 0.9 1 1.1
Freeboard (m)

j)

Figure 4.10 Developed penalty curve of channel freeboards for different maximum flow rates.

Where: a) For 0.42 m^3/sec, b) for 0.43 m^3/sec, c) for 0.44 m^3/sec, d) for 0.45 m^3/sec, e) for 0.47 m^3/sec, f) for 0.48 m^3/sec g) for 0.51 m^3/sec h) for 0.54 m^3/sec i) for 0.63 m^3/sec j) for 0.65 m^3/sec

Therefore there are channels that has poor performance index of free board or channel there PIF is zero. These are C5, C13, C14, C21, C29, C31, C33, C34, C35, C39, C49, C51, C56, and C57. Based on each individual value, the entire system PIF is 50.19%.

4.8 Performance Index of Velocity

Due to the simulated outputs of link flow maximum velocity, C51 has the highest maximum velocity (4.41 m/sec), and C39 has the lowest maximum velocity (0.39 m/sec). The details simulated maximum velocity of all drainage channels are listed in Appendix B7.

The developed penalty curve of velocity of the channels used for this study that is used for estimation of the velocity performance index of each channel is:

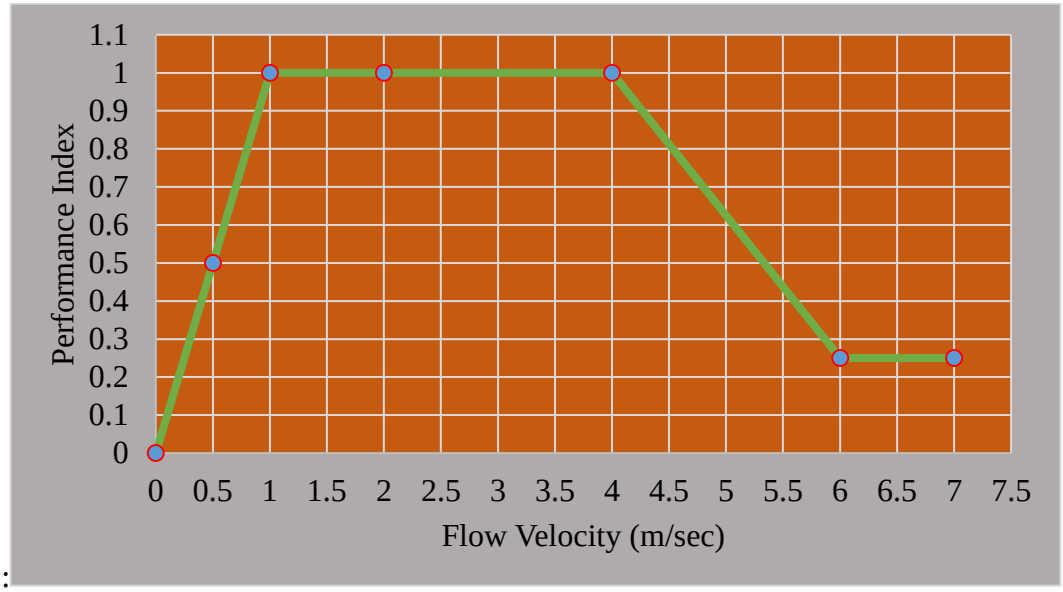

:

Figure 4.11 Developed penalty curve of channel velocity

By using this penalty curve the velocity performance index of each channels is determined these results are set in Appendix C2. From this result most of the channels has high velocity

performance except C39 based on. This channel has low PIV value (0.38). As I showed in Figure 4.1 that because of this low velocity, there is the occurrence of siltation of mud and storage of water. The PIV of the entire system is 98.12%.

4.9 Weighted System Reliability

After calculating the velocity and freeboard performance index of each channel, the reliability of the entire drainage network was calculated. Therefore, the reliability of the entire drainage system is 69.36%. This means these structures have acceptable performance.

5 CONCLUSION AND RECOMMENDATION

5.1 Conclusion

Understanding of the urban region's hydrology, topography, and land cover serve as the foundation for urban drainage infrastructure planning and maintenance. These structures must be well designed because they are constructed with the highest budgets. Urban drainage problems are a factor in flooding, road erosion, soil degradation, sedimentation, and water logging. Most of these issues are concentrated in numerous Ethiopian towns. Controlling these drainage issues requires research on the hydraulic performance of urban drainage infrastructure.

The study evaluated and modeled urban storm drainage system performance in Woreta Town by using SWMM to get maximum channel flow rate, maximum velocity, and maximum channel water level, and the HY-8 model to analyze overtopping of culverts. SWMM was used to model the hydraulic and hydrologic performance of drainage. The model result was compared with the observed flow depth for 17 days in both 2021 and 2022 at two chosen outfalls using the calibration and validation. 10 days of flow depth in 2021 will be used for calibration, and 7 days of flow depth in 2022 will be used for validation. Using these reported depths, the manning equation is then used to determine the observed flow rate for each channel. This allows for a comparison of the simulated and observed flow rates in certain channels. By using this channel flow rate, the performance of SWMM was evaluated. And the model has higher performance.

Using the software SWMM, the hydraulic conditions were simulated to obtain network hydraulic parameters such as maximum velocity, maximum flow rate, and maximum water level in the channel. By means of two penalty curves defined in this paper, system performance was divided into three sub-categories: maximum performance, acceptable performance, and unacceptable performance. The entire network performance was calculated by applying a weighting function to each of the system components. The suggested method was tested on the Woreta Town stormwater collection network. For simulation, 3-hour precipitations with return periods of 5 years were used. As expected, because of the insufficient channel height, there were many problems with the freeboard performance index, but the velocity performance index of the storm drainage system has

maximum performance. The hydraulic performance index gives a better understanding to decision makers and also helps to improve network management.

In this study, analyses from the overtopping of four culverts are evaluated by evaluating HY-8 modeling tools. From the HY-8 modeling tool results, two culverts (culvert 1 and culvert 3) have overtopping problems because of the inadequacy of their cross-sections. The other two culverts (culvert 2 and culvert 4) have no overtopping problems.

In addition, some of the study area storm drainage networks have poor freeboard performance (unacceptable performance). These are C5, C13, C14, C21, C29, C31, C33, C34, C35, C39, C49, C51, C56, and C57. And most of the study area's storm drainage networks have high velocity performance, except for C39.

The overall storm drainage system reliability of the study area is 69.36%. This shows the system has good hydraulic performance. These hydraulic performance indexes give a better understanding to decision makers and also help to improve network management.

5.2 Recommendation

Based on the findings and evaluations of this study the following points could be taken as recommendations and suggestions for further designing and construction of drainage structures.

The drainage structures should be designed with reliable hydrological data and hydraulic analysis. The hydrological analysis should be done at a required level by considering the land use land cover, the soil, and the rainfall intensity of the town.

The stormwater drainages that have an unacceptable freeboard performance index must be redesigned and the height of the channel increased. Overtopping occurs on culvert 1 and 3. Culvert 1 should be redesigned but culvert 3, as shown opening is closed by silted soil. This must be removed to stop overtopping of flow over the road.

For the other researchers in this study area I recommend to study the position and the location of roadway culverts of the study areas.

REFFERENCES

Ababa, A., & Chen, J. (2020). Flooding Problems and Surface Water Drainage Conditions in Assosa.

Abhijit, P. (2011). Effects of Bad Drainage on Roads. Environmental Research, 1(1), 1–8.

Adisu, M., & Hailemikael, M. (2017). An Approach to Drainage System Sustainability in Wolaita Soddo Town: A Case Study from Southern Ethiopia. International Journal of Waste Resources, 07(02), 2–5. https://doi.org/10.4172/2252-5211.1000271

Agarwal, S., & Kumar, S. (2019). Applicability of SWMM for semi urban catchment flood modeling using extreme rainfall events. International Journal of Recent Technology and Engineering, 8(2), 245–251. https://doi.org/10.35940/ijrte.A3169.078219

Alam, M. J. B., & Matin, A. (2005). Study of plotting position formulae for Surma basin in Bangladesh. Journal of Civil Engineering (IEB), 33(1), 9–17.

Alamdari, N., & Hogue, T. S. (2022). Assessing the effects of climate change on urban watersheds: a review and call for future research. Environmental Reviews, 30(1), 61–71. https://doi.org/10.1139/ER-2021-0003

Alelign, A., Tekeste, Z., & Petros, B. (2018). Prevalence of malaria in Woreta town, Amhara region, Northwest Ethiopia over eight years. BMC Public Health, 18(1), 1–6. https://doi.org/10.1186/S12889-018-5913-8/FIGURES/3

Ali, A. M. (2020). Manual RC Box Culvert Analysis and Designing. International Journal of Innovative Science and Research Technology, 5(8), 91–115. https://doi.org/10.38124/ijisrt20aug018

Alves, B., Angnuureng, D. B., Morand, P., & Almar, R. (2020). A review on coastal erosion and flooding risks and best management practices in West Africa: what has been done and should be done. Journal of Coastal Conservation, 24(3). https://doi.org/10.1007/S11852-020-00755-7

Angelakis, A. N., Zaccaria, D., Krasilnikoff, J., Salgot, M., Bazza, M., Roccaro, P., Jimenez, B., Kumar, A., Yinghua, W., Baba, A., Harrison, J. A., Garduno-Jimenez,

A., & Fereres, E. (2020). Irrigation of world agricultural lands: Evolution through the Millennia. In Water (Switzerland) (Vol. 12, Issue 5). MDPI AG. https://doi.org/10.3390/W12051285

Arden, S., & Jawitz, J. W. (2019). The evolution of urban water systems: societal needs, institutional complexities, and resource costs. Urban Water Journal, 16(2), 92–102. https://doi.org/10.1080/1573062X.2019.1634109

Azari, B., & Tabesh, M. (2022). Urban storm water drainage system optimization using a sustainability index and LID/BMPs. Sustainable Cities and Society, 76. https://doi.org/10.1016/j.scs.2021.103500

Bagatur, T., Management, F. O.-J. of F. R., & 2018, undefined. (2016). Development of predictive model for flood routing using genetic expression programming. Wiley Online Library, 11, S444–S454. https://doi.org/10.1111/jfr3.12232

Bajracharya, A. R., Rai, R. R., & Rana, S. (2016). Effects of Urbanization on Storm Water Run-off : A Case Study of Kathmandu Metropolitan City, Nepal. Journal of the Institute of Engineering, 11(1), 36–49. https://doi.org/10.3126/jie.v11i1.14694

Balkham, M., Haskoning, R., Fosbeary, C., Kitchen, A., & Rickard, C. (2010). Culvert design and operation guide. In Culvert Design and Operation Guide (Vol. 1, Issue 1). http://www.ihsti.com/tempimg/4a6c788-CIS888614800302323.pdf

Batty, M. (2018). Digital twins. Environment and Planning B: Urban Analytics and City Science, 45(5), 817–820. https://doi.org/10.1177/2399808318796416

Bauer, M. E., Loffelholz, B. C., & Wilson, B. (2007). Estimating and mapping impervious surface area by regression analysis of landsat imagery. In Remote Sensing of Impervious Surfaces (pp. 3–19). CRC Press. https://doi.org/10.1201/9781420043754.pt1

Bekele, M., & Sahadeva, K. N. (2018). Performance Assessment of Road Drainage Systems of Burayu Town , Oromia Region, Ethiopia. International Journal of Research in Engineering & Management, 2(2), 40–55.

Boguniewicz-Zabłocka, J., & Capodaglio, A. G. (2020). Analysis of alternatives for sustainable stormwater management in small developments of Polish urban catchments. Sustainability (Switzerland), 12(23), 1–20. https://doi.org/10.3390/su122310189

Brown, S. A., Schall, J. D., Morris, J. L., Doherty, C. L., Stein, S. M., & Warner, J. C. (2013). Urban Drainage Design Manual. Hydraulic Engineering Circular, 22(22), 478.

Brunen, B., Daguet, C., & Jaeger, J. A. G. (2020). What attributes are relevant for drainage culverts to serve as efficient road crossing structures for mammals? Journal of Environmental Management, 268. https://doi.org/10.1016/j.jenvman.2020.110423

Burian, S. J., & Edwards, F. G. (2002). Historical perspectives of urban drainage. Global Solutions for Urban Drainage, 1–16. https://doi.org/10.1061/40644(2002)284

Butler, D., Digman, C., Makropoulos, C., & Davies, J. (2018). Urban drainage. CRC Press. https://www.taylorfrancis.com/books/mono/10.1201/9781351174305/urban-drainage-david-butler-christopher-digman-christos-makropoulos-john-davies

Chali, W. E., & Zewdie, M. (2020). Performance Assessment of Urban Drainage Systems of Holeta Town Using Stormwater Management Model (Swmm). 11(4).

Chang, M., & Lee, R. (1974). Objective double-mass analysis. Water Resources Research, 10(6), 1123–1126. https://doi.org/10.1029/WR010I006P01123

Chow, V. Te. (2007). Open-channel hydraulics. McGraw-Hill.

Chow, V. T. D. R. M. L. W. M. (1988). Applied Hydrology. McGraw-Hill, Inc.

Dagnachew, 2011. (2011). Road and urban storm water drainage network integration in Addis Ababa: Addis Ketema Sub-city. Journal of Engineering and Technology Research, 3(7), 217–225. http://www.academicjournals.org/JETR

Dahmen, E. R., & Hall, M. J. (1989). Screening of Hydrological Data: Tests for Stationarity and Relative Consistency. International Institute for Land Reclamation and Improvement/ILRI, 58.

David, Butler and John, W. D. (2004). Urban Drainage (second edi). Taylor & Francis e-Library,.

Devia, G. K., Ganasri, B. P., & Dwarakish, G. S. (2015a). A Review on Hydrological Models. Aquatic Procedia, 4, 1001–1007. https://doi.org/10.1016/j.aqpro.2015.02.126

Devia, G. K., Ganasri, B. P., & Dwarakish, G. S. (2015b). A Review on Hydrological Models. Aquatic Procedia, 4(Icwrcoe), 1001–1007. https://doi.org/10.1016/j.aqpro.2015.02.126

Donahue, J. P., & Howard, A. F. (2011). Hydraulic design of culverts on forest roads. 17(12), 1545–1551. https://doi.org/10.1139/X87-237

Elsebaie, I. H. (2012). Developing rainfall intensity – duration – frequency relationship for two regions in Saudi Arabia. 1932, 131–140. https://doi.org/10.1016/j.jksues.2011.06.001

Erena, S. H., Worku, H., & De Paola, F. (2018). Flood hazard mapping using FLO-2D and local management strategies of Dire Dawa city, Ethiopia. Journal of Hydrology: Regional Studies, 19, 224–239. https://doi.org/10.1016/j.ejrh.2018.09.005

Ethiopian Roads Authority. (2013). Drainage Design manual-2013.

Ferrer, A. L. C., Thomé, A. M. T., & Scavarda, A. J. (2018). Sustainable urban infrastructure: A review. Resources, Conservation and Recycling, 128, 360–372. https://doi.org/10.1016/J.RESCONREC.2016.07.017

Gashaw, W., basin, D. L.-N. river, & 2011, undefined. (2011). Flood hazard and risk assessment using GIS and remote sensing in Fogera Woreda, Northwest Ethiopia. Springer, 179–206. https://doi.org/10.1007/978-94-007-0689-7_9

Gichuhi, G., & Gitahi, S. (2021). Sustainable Urban Drainage Practices and Their Effects on Aquifer Recharge. African Handbook of Climate Change Adaptation, 809–827. https://doi.org/10.1007/978-3-030-45106-6_67

Gupta, A. K., & Nair, S. S. (2011). Urban floods in Bangalore and Chennai: Risk management challenges and lessons for sustainable urban ecology. Current Science, 100(11), 1638–1645.

Hanumanthanaik, D., & Gowda, B. G. (2022). A STUDY ON THE SEASONAL TREND OF PHYSICOCHEMICAL PARAMETERS OF MINOR-RAYA CANAL WATER OF TUNGABHADRA DAM HOSPET, KARNATAKA, INDIA. Journal of Advanced Scientific Research, 13(07), 99–113. https://doi.org/10.55218/jasr.2022137112

Haslbeck, J. M. B., Ryan, O., Robinaugh, D. J., Waldorp, L. J., & Borsboom, D. (2021). Modeling Psychopathology: From Data Models to Formal Theories. Psychological Methods. https://doi.org/10.1037/MET0000303

Hlustik, P. (2017). Practical assessment of the SWMM programme. IOP Conference Series: Earth and Environmental Science, 92(1). https://doi.org/10.1088/1755-1315/92/1/012018

Hoang, L., & Fenner, R. A. (2016). System interactions of stormwater management using sustainable urban drainage systems and green infrastructure. Urban Water Journal, 13(7), 739–758. https://doi.org/10.1080/1573062X.2015.1036083

Hotchkiss, R. H., Thiele, E. A., James Nelson, E., & Thompson, P. L. (2008). Culvert Hydraulics comparison of current computer models and recommended improvements. Transportation Research Record, 2060, 141–149. https://doi.org/10.3141/2060-16

Jacobson, C. R. (2011). Identification and quantification of the hydrological impacts of imperviousness in urban catchments: A review. In Journal of Environmental Management (Vol. 92, Issue 6, pp. 1438–1448). https://doi.org/10.1016/j.jenvman.2011.01.018

Jaeger, R., Tondera, K., Pather, S., Porter, M., Jacobs, C., & Tindale, N. (2019). Flow control in culverts: A performance comparison between inlet and outlet control. Water (Switzerland), 11(7). https://doi.org/10.3390/w11071408

Jayasooriya, V. M., Ng, A. W. M., Muthukumaran, S., & Perera, C. B. J. (2020). Optimization of green infrastructure practices in industrial areas for runoff management: A review on issues, challenges and opportunities. In Water (Switzerland) (Vol. 12, Issue 4). MDPI AG. https://doi.org/10.3390/W12041024

Karimpour, S., & Gohari, S. (2020). An experimental study on the effects of debris accumulation at the culvert inlet on downstream scour. Journal of Rehabilitation in Civil Engineering, 8(2), 184–199. https://doi.org/10.22075/JRCE.2020.18210.1348

Kim, H. M., Miao, J., & Phelps, N. A. (2020). International urban development leadership. In Exporting Urban Korea? (pp. 131–145). Routledge. https://doi.org/10.4324/9781003047599-10

Krause, P., Boyle, D. P., & Bäse, F. (2005). Comparison of different efficiency criteria for hydrological model assessment. Advances in Geosciences, 5, 89–97. https://doi.org/10.5194/adgeo-5-89-2005

Kundzewicz, Z., Journal, K. T.-H. S., & 1999, undefined. (1999). Flood protection and management: quo vadimus? Taylor & Francis, 44(3), 417–432. https://doi.org/10.1080/02626669909492237

Lapides, D. A., Sytsma, A., & Thompson, S. (2021). Implications of Distinct Methodological Interpretations and Runoff Coefficient Usage for Rational Method Predictions. Journal of the American Water Resources Association, 57(6), 859–874. https://doi.org/10.1111/1752-1688.12949

Le, H. T. T., Nguyen, C. Van, & Le, D.-H. (2022). Numerical study of sediment scour at meander flume outlet of boxed culvert diversion work. PLOS ONE, 17(9), e0275347. https://doi.org/10.1371/JOURNAL.PONE.0275347

Lombardi, R., & Davis, M. A. L. (2022). Incorporating alluvial hydrogeomorphic complexities into paleoflood hydrology, magnitude estimation and flood frequency analysis, Tennessee River, Alabama. Journal of Hydrology, 612. https://doi.org/10.1016/j.jhydrol.2022.128085

Loudyi, D., Hasnaoui, M. D., & Fekri, A. (2022). Flood Risk Management Practices in Morocco: Facts and Challenges (pp. 35–94). https://doi.org/10.1007/978-981-16-2904-4_2

Lourenço, I. B., Guimarães, L. F., Alves, M. B., & Miguez, M. G. (2020). Land as a sustainable resource in city planning: The use of open spaces and drainage systems to structure environmental and urban needs. Journal of Cleaner Production, 276. https://doi.org/10.1016/j.jclepro.2020.123096

Marijnissen, R. J. C., Kok, M., Kroeze, C., & van Loon-Steensma, J. M. (2021). Flood risk reduction by parallel flood defences – Case-study of a coastal multifunctional flood protection zone. Coastal Engineering, 167. https://doi.org/10.1016/j.coastaleng.2021.103903

Mays, L. W. (2001). Stormwater Collection Systems Design Handbook. McGraw-Hill Professional Publishing.

Moriasi, D. N., Gitau, M. W., Pai, N., & Daggupati, P. (2015). Hydrologic and water quality models: Performance measures and evaluation criteria. Transactions of the ASABE, 58(6), 1763–1785. https://doi.org/10.13031/trans.58.10715

Mukherjee, D. (2014). Highway Surface Drainage System & Problems of Water Logging In Road Section. 44–51.

Muste, M., & Xu, H. (2022). Multi-pronged approach for monitoring sedimentation processes at multi-barrel culverts. Journal of Hydrology, 610. https://doi.org/10.1016/j.jhydrol.2022.127840

Nagappa, V., Gedamu, B. H., Engineering, W. R., Yigzaw, H. A., Eshete, A. S., & Engineering, W. R. (2020). HYDROLOGICAL ANALYSIS FOR THE DESIGN. 11(11), 136–148.

Naserisafavi, N., Yaghoubi, E., & Sharma, A. K. (2022). Alternative water supply systems to achieve the net zero water use goal in high-density mixed-use buildings. Sustainable Cities and Society, 76. https://doi.org/10.1016/j.scs.2021.103414

Niyonkuru, P., Sang, J. K., Nyadawa, M. O., & Munyaneza, O. (2018). Calibration and validation of EPA SWMM for stormwater runoff modelling in Nyabugogo catchment , Rwanda. Journal of Sustainable Research in Engineering, 4(4), 152–159.

O'Flaherty, C. A. (2020). Surface drainage for roads. Highways, 201–225. https://doi.org/10.1201/9781482269291-15

Parkinson, J., & Mark, O. (2015). Urban Stormwater Management in Developing Countries. Water Intelligence Online, 5(0), 9781780402574–9781780402574. https://doi.org/10.2166/9781780402574

Patakamuri, S. K., Muthiah, K., & Sridhar, V. (2020). Long-Term homogeneity, trend, and change-point analysis of rainfall in the arid district of ananthapuramu, Andhra Pradesh State, India. Water (Switzerland), 12(1). https://doi.org/10.3390/w12010211

Ponnurangam, G. T. P. (2019). The Effect of Poor Surface Drainage Structure on Pavement Performance - A Case Study. International Journal of Science and Research (IJSR), 8(2), 443–449. https://www.ijsr.net/archive/v8i2/ART20195002.pdf

Qin, Y., Huang, Z., Yu, Z., Liu, Z., & Wang, L. (2019). A Novel Buffer Tank to Attenuate the Peak Flow of Runoff. Civil Engineering Journal, 5(12), 2525–2534. https://doi.org/10.28991/cej-2019-03091430

Rangari, V. A., & Sai Prashanth, S. (2018). Simulation of Urban Drainage System Using a Storm Water Management Model (SWMM). Asian Journal of Engineering and Applied Technology, 7(1), 7–10. https://doi.org/10.51983/ajeat-2018.7.1.872

Ribas, A., Olcina, J., & Sauri, D. (2020). More exposed but also more vulnerable? Climate change, high intensity precipitation events and flooding in Mediterranean Spain. Disaster Prevention and Management: An International Journal, 29(3), 229–248. https://doi.org/10.1108/DPM-05-2019-0149/FULL/HTML

Rossi, F., Fiorentino, M., & Versace, P. (1984). Two-Component Extreme Value Distribution for Flood Frequency Analysis. Water Resources Research, 20(7), 847–856. https://doi.org/10.1029/WR020I007P00847

Rossman, L. A., & Huber, W. C. (2016). Storm Water Management Model Reference Manual Volume I – Hydrology. U.S. Environmental Protection Agency, I(January), 231. www2.epa.gov/water-research

Sangal, S. K., & Bonema, S. R. (1994). A Methodology for Calibrating SWMM Models. Journal of Water Management Modeling, 176–200. https://doi.org/10.14796/JWMM.Rl76-24

Saraswat, C., Kumar, P., & Mishra, B. K. (2016). Assessment of stormwater runoff management practices and governance under climate change and urbanization: An analysis of Bangkok, Hanoi and Tokyo. In Environmental Science and Policy (Vol. 64, pp. 101–117). Elsevier Ltd. https://doi.org/10.1016/j.envsci.2016.06.018

Sattari, M. T., Rezazadeh-Joudi, A., & Kusiak, A. (2017). Assessment of different methods for estimation of missing data in precipitation studies. Hydrology Research, 48(4), 1032–1044. https://doi.org/10.2166/nh.2016.364

Schäfer, B. (2019). Achieving Sustainable Urban Drainage through Multifunctionality. https://www.diva-portal.org/smash/get/diva2:1348442/FULLTEXT01.pdf

Senarath, S., Ogden, F., … C. D.-W. R., & 2000, undefined. (2000). On the calibration and verification of two-dimensional, distributed, Hortonian, continuous watershed models. Wiley Online Library, 36(6), 1495–1510. https://doi.org/10.1029/2000WR900039

Shaaban, K. (2022). Challenges and Lessons Learned from Building a New Road Drainage System in a Developing Country. 2022 Intermountain Engineering, Technology and Computing, IETC 2022. https://doi.org/10.1109/IETC54973.2022.9796861

Shahabi, S., & Kermani, R. H. (2015). Flood frequency analysis using density function of wavelet (Case study: Polroud River). In Journal of Applied Research in Water and Wastewater (Vol. 3, Issue 1).

Shimabuku, M., Diringer, S., & Cooley, H. (2018). Stormwater Capture in California: Innovative Policies and Funding Opportunities (Issue June). Pacific Institute.

http://pacinst.org/wp-content/uploads/2018/06/Pacific-Institute-Stormwater-Capture-in-California.pdf

Silveira, A. L. L. (2002). Problems of modern urban drainage in developing countries. Water Science and Technology, 45(7), 31–40. https://doi.org/10.2166/WST.2002.0114

Simon, M. (2020). An Introduction to the Storm Water Management Model (SWMM). July.

Singo, L. R., Kundu, P. M., Odiyo, J. O., Mathivha, F. I., & Nkuna, T. R. (2012). Flood frequency analysis of annual maximum stream flows for Luvuvhu River Catchment, Limpopo Province, South Africa. 16th SANCIAHS Hydrology Symposium, March 2016, 1–3.

Sobieraj, J., Bryx, M., & Metelski, D. (2022). Stormwater Management in the City of Warsaw: A Review and Evaluation of Technical Solutions and Strategies to Improve the Capacity of the Combined Sewer System. In Water (Switzerland) (Vol. 14, Issue 13). MDPI. https://doi.org/10.3390/w14132109

Spitzhüttl, F., Goizet, F., Unger, T., & Biesse, F. (2020). The real impact of full hydroplaning on driving safety. Accident Analysis and Prevention, 138. https://doi.org/10.1016/j.aap.2020.105458

Starnes, A. L., Morris, I., Wilson, C. M. D., Cook, W., Richardson, C. P., Trujillo, D., Howell, T., Cortes, D. D., Dugas, D., & Jauregui, D. (2022). Collaborative Framework to Create a Culvert Asset Management System for NMDOT. International Conference on Transportation and Development 2022: Application of Emerging Technologies - Selected Papers from the Proceedings of the International Conference on Transportation and Development 2022, 6, 34–45. https://doi.org/10.1061/9780784484364.004

Šuvalija, S., Hadžić, E., & Milišić, H. (2021). Urban Stormwater Management – New Challenges. Lecture Notes in Networks and Systems, 233, 1046–1054. https://doi.org/10.1007/978-3-030-75275-0_115

Tabesh, M., Azari, B., & Rezaei, H. R. (2016). Hydraulic Performance Assessment of Stormwater Networks. November.

Taka, G. N., Huong, T. T., Shah, I. H., & Park, H. S. (2020). Determinants of energy-based CO2 emissions in Ethiopia: A decomposition analysis from 1990 to 2017. Sustainability (Switzerland), 12(10). https://doi.org/10.3390/su12104175

Terdiman, M. (2019). Environmental challenges. In The Palgrave Handbook of the Hashemite Kingdom of Jordan (pp. 135–150). Palgrave Macmillan. https://doi.org/10.1007/978-981-13-9166-8_8

Teshome, M. (2020). A review of recent studies on urban stormwater drainage system for urban flood management. Preprints, 100(October), 295. https://doi.org/10.20944/preprints202010.0295.v1

Tilahun, B. Z. (2021). Hydraulic Performance Assessment of Storm Water Drainage Systems of Dejen Town Using Storm Water Management Model (SWMM), Ethiopia. 9(9), 1358–1383.

Tingsanchali, T. (2012). Urban flood disaster management. Procedia Engineering, 32, 25–37. https://doi.org/10.1016/j.proeng.2012.01.1233

Tsihrintzis, V. A., & Hamid, R. (1998). Runoff quality prediction from small urban catchments using SWMM. Hydrological Processes, 12(2), 311–329. https://doi.org/10.1002/(SICI)1099-1085(199802)12:2<311::AID-HYP579>3.0.CO;2-R

Turner, S., Horton, A. A., Rose, N. L., & Hall, C. (2019). A temporal sediment record of microplastics in an urban lake, London, UK. Journal of Paleolimnology, 61(4), 449–462. https://doi.org/10.1007/S10933-019-00071-7

Uppala, P., & Dey, S. (2021). Design of Potential Rainwater Harvesting Structures for Environmental Adoption Measures in India. Polytechnica, 4(2), 59–80. https://doi.org/10.1007/S41050-021-00035-9

Valipour, M., Krasilnikof, J., Yannopoulos, S., Kumar, R., Deng, J., Roccaro, P., Mays,

L., Grismer, M. E., & Angelakis, A. N. (2020). The evolution of agricultural drainage from the earliest times to the present. In Sustainability (Switzerland) (Vol. 12, Issue 1). MDPI. https://doi.org/10.3390/SU12010416

Vorobevskii, I., Janabi, F. Al, Schneebeck, F., Bellera, J., & Krebs, P. (2020). Urban floods: Linking the overloading of a storm water sewer system to precipitation parameters. Hydrology, 7(2), 1–23. https://doi.org/10.3390/hydrology7020035

Wali, E., Phil-Eze, P. O., Wizor, C. H., Abdullahi, M., Afolabi, O. O., Eze, I. C., & Bosco-Abiahu, L. C. (2021). Flood Vulnerability Assessment on Selected Communities in Ikwerre Local Government Area of Rivers State, Nigeria, Using Remote Sensing and GIS Techniques. Journal of Geography, Environment and Earth Science International, 46–57. https://doi.org/10.9734/jgeesi/2021/v25i930308

Walsh, C. J., Leonard, A. W., Ladson, A. R., & Fletcher, T. D. (2004). Urban Stormwater and the Ecology of Streams. CRC for Freshwater Ecology and CRC for Catchment Hydrology. http://www.urbanstreams.unimelb.edu.au/Docs/urban_stormwater_streamecology.pdf

Willmott, C. J. (1981). On the validation of models. Physical Geography, 2(2), 184–194. https://doi.org/10.1080/02723646.1981.10642213

Xu, K., Ma, C., Lian, J., & Bin, L. (2014). Joint probability analysis of extreme precipitation and storm tide in a coastal city under changing environment. PLoS ONE, 9(10). https://doi.org/10.1371/JOURNAL.PONE.0109341

Yan, Y., Lidberg, W., Tenenbaum, D. E., & Pilesjö, P. (2020). The accuracy of drainage network delineation as a function of environmental factors: A case study in Central and Northern Sweden. Hydrological Processes, 34(26), 5489–5504. https://doi.org/10.1002/HYP.13963

Yazdanfar, Z., & Sharma, A. (2015). Urban drainage system planning and design - Challenges with climate change and urbanization: A review. Water Science and Technology, 72(2), 165–179. https://doi.org/10.2166/wst.2015.207

Zhang, S., & Guo, Y. (2014). Stormwater Capture Efficiency of Bioretention Systems. Water Resources Management, 28(1), 149–168. https://doi.org/10.1007/S11269-013-0477-Y

APPENDIX

Appendix A1 A photo showing some of the flooding issues in the area of study

Appendix A2 Maximum annually rainfall depth of selected metrological stations

YEAR	Maximum annual rainfall (mm)		
	Woreta	Wanzaye	Addis Zemen
1987	50	53	45.3
1988	108.2	94.9	53
1989	64.3	51.4	70.5
1990	70.2	94.8	59
1991	64.6	62.2	62.19
1992	65.8	48.7	51.36
1993	62.4	83	46.5
1994	68	91	83.5
1995	48	79	39.5
1996	72.4	57.5	48.2
1997	38.5	54.7	42.5
1998	55	57.7	32.4
1999	64.5	54.8	42
2000	51	66.6	46.5
2001	73.5	47.9	27
2002	100.6	60	53.2
2003	108	30.7	73.3
2004	100.2	59.7	48.4
2005	79	78.5	57
2006	73.7	134.2	69
2007	63.5	54.2	35
2008	61.5	56.7	43.6
2009	55.6	86.8	42
2010	70	99	60
2011	66	60	48.4
2012	57.5	77.6	48
2013	80	92.7	87.8
2014	60	56	33.7
2015	80	68.6	38.5
2016	68.9	68.9	50.61

Appendix A3 Statistical description of maximum annual rainfall

year	Woreta Maximum Annuall Rainfall Depth (mm)	Y=log X
2016	68.9	1.838
2015	80.0	1.903
2014	60.0	1.778
2013	80.0	1.903
2012	57.5	1.760
2011	66.0	1.820
2010	70.0	1.845
2009	55.6	1.745
2008	61.5	1.789
2007	63.5	1.803
2006	54.3	1.735
2005	58.2	1.765
2004	73.8	1.868
2003	79.6	1.901
2002	74.1	1.870
2001	54.2	1.734
2000	37.6	1.575
1999	47.5	1.677
1998	40.5	1.608
1997	38.5	1.585
1996	72.4	1.860
1995	48.0	1.681
1994	68.0	1.833
1993	62.4	1.795

Statistical description of normal values (X)	
Mean	63.17770961
Standard Error	2.640193334
Median	63.9
Mode	80
Standard Deviation	14.46093445
Sample Variance	209.1186252
Kurtosis	2.100756674
Skewness	0.663496268
Range	70.61460566
Minimum	37.58539434
Maximum	108.2
Sum	1895.331288
Count	30

Statistical description of Log value (Y)	
Mean	1.79
Standard Error	0.018316754
Median	1.805492349
Mode	1.903089987
Standard Deviation	0.10
Sample Variance	0.010065104
Kurtosis	0.656799454

1992	65.8	1.818	Skewness	-0.269351672
1991	64.6	1.810	Range	0.45920815
1990	70.2	1.846	Minimum	1.575019111
1989	64.3	1.808	Maximum	2.034227261
1988	108.2	2.034	Sum	53.68672607
1987	50.0	1.699	Count	30

Appendix A4 Summary of goodness of fit test of probability distributions in chi-square test by EasyFit

EasyFit - Evaluation Version

Log-Pearson 3 [#39]					
Chi-Squared					
Deg. of freedom Statistic P-Value Rank	3 1.0106 0.79868 34				
α	0.2	0.1	0.05	0.02	0.01
Critical Value	4.6416	6.2514	7.8147	9.8374	11.345
Reject?	No	No	No	No	No
Gumbel Max [#25]					
Chi-Squared					
Deg. of freedom Statistic P-Value Rank	3 2.2957 0.51335 42				
α	0.2	0.1	0.05	0.02	0.01
Critical Value	4.6416	6.2514	7.8147	9.8374	11.345
Reject?	No	No	No	No	No

Appendix A5 Measured data of the roadway, culvert data, tail water data and culvert alignment with the roads for culvert analysis

LIST OF DATAS	CULVERT DATA LISTS			
TAIL WATER DATA				
Channel Type	Irregular	Irregular	Irregular	Irregular
Bottom Width				
Channel Length				
Inlet Elevation				
Outlet Elevation				
ROADWAY DATA				
Road Profile Shape	Constant Roadway Elevation	Constant Roadway Elevation	Constant Roadway Elevation	Constant Roadway Elevation
First Roadway Station	0 + 00	0 + 00	0+00	0+00
Crest Length (m)	4.3	9.2	9	6.2
Crest Elevation	1809.191	1809.645	1810.460	1800.793
Roadway Surface	Paved	Paved	Paved	Paved
Top Width	14.4	13.8	15	14
CULVERT DATA				
Name	Culvert 1	Culvert 2	Culvert 3	Culvert 4
Shape of Culvert	Circular	Concert Box	Concert Box	Concert Box
Material of Culvert	Corrugated Steel	Concrete	Concrete	Concrete
Diameter (mm)	800			
Span (mm)		9000	15000	3000
Rise(mm)		3000	3500	1750
Embedment Depth		0	0	0
Culvert Type	Straight	Straight	Straight	Straight
Inlet Configuration	Square edge with headwall	Square edge with headwall	1:1 Bevel (45º flare) Wing wall	Square edge with headwall
Inlet Depression	No	No	No	No
SITE DATA				
Site Data Input option	Culvert Invert Data	Culvert Invert Data	Culvert Invert Data	Culvert Invert Data
Inlet Station	0+00	0+00	0+00	0+00

Inlet Elevation	1807.441	1805.945	1805.960	1798.393
Outlet Station	0+ 14.40	0+13.80	0+15	0+14
Outlet elevation	1807.389	1805.902	1805.940	1798.351
Number of Barrels	4	2	4	2

Appendix A6 Summary of sub-catchments parameters

Sub-catchments code	Area (ha)	Width (m)	Slope (%)	% of Imperv	N-Imperv	N-Perv	Dstore Imperv	Dstore Perv
S-1	2.37	159.5	6.71	16.4	0.03	0.6	0.18	0.73
S-2	1.32	103.3	8.46	21.4	0.03	0.6	0.2	0.81
S-3	1.47	30	8.99	56.5	0.03	0.6	0.21	0.84
S-4	1.82	42.8	7.49	24.5	0.03	0.6	0.19	0.77
S-5	4.11	194.9	9.89	41.9	0.03	0.6	0.22	0.88
S-6	0.49	35.6	6.72	35.8	0.03	0.6	0.18	0.73
S-7	3.62	144.7	8.96	31.3	0.03	0.6	0.21	0.84
S-8	1.05	32.5	7.19	39.5	0.03	0.6	0.19	0.75
S-9	2.27	330.9	8.92	26.7	0.03	0.6	0.21	0.84
S-10	8.24	265.5	9.78	43	0.03	0.6	0.22	0.88
S-11	1.96	330.5	7.08	45.2	0.03	0.6	0.19	0.75
S-12	0.91	342.5	5.63	44.7	0.03	0.6	0.17	0.66
S-13	1.01	42.6	7.73	49.1	0.03	0.6	0.19	0.78
S-14	0.86	34.8	4.74	28.6	0.03	0.6	0.15	0.61
S-15	13.18	345.1	11.63	11.5	0.03	0.6	0.24	0.95
S-16	1.91	39.2	7.66	82	0.03	0.6	0.19	0.77
S-17	1.51	31.6	9.65	52.8	0.03	0.6	0.22	0.87
S-18	2.11	86	9.99	44.6	0.03	0.6	0.22	0.88
S-19	1.51	99.3	11.92	41.3	0.03	0.6	0.24	0.97
S-20	1.5	74.8	11.87	33.5	0.03	0.6	0.24	0.96
S-21	1.46	76	11.83	39.4	0.03	0.6	0.24	0.96
S-22	6.7	256.1	11.26	25.7	0.03	0.6	0.23	0.94
S-23	1.76	133.1	10.5	44.8	0.03	0.6	0.23	0.91
S-24	1.66	70.1	9.69	23.2	0.03	0.6	0.22	0.87
S-25	1.6	133.7	9.13	43.9	0.03	0.6	0.21	0.85
S-26	1.1	76.5	8.41	61.3	0.03	0.6	0.2	0.81
S-27	2.17	122.8	7.66	43.3	0.03	0.6	0.19	0.77

S-28	3.72	188.3	14.75	40.1	0.03	0.6	0.27	1.08
S-29	26.94	614.2	15.76	24.4	0.03	0.6	0.28	1.11
S-30	1.8	333.3	6.81	67.8	0.03	0.6	0.18	0.73
S-31	3.44	267.9	14.77	40.6	0.03	0.6	0.27	1.08
S-32	2.26	66.1	8.75	33.1	0.03	0.6	0.21	0.83
S-33	5.36	79.8	7.95	54.7	0.03	0.6	0.2	0.79
S-34	6.26	154.6	11.25	34.8	0.03	0.6	0.23	0.94
S-35	25.42	363.2	15.33	32.7	0.03	0.6	0.27	1.1
S-36	6.63	371.4	11.58	35.2	0.03	0.6	0.24	0.95
S-37	3.77	178	11.23	50.1	0.03	0.6	0.23	0.94
S-38	10.92	284.8	10.89	51.7	0.03	0.6	0.23	0.92
S-39	3.17	191.1	10.88	56	0.03	0.6	0.23	0.92
S-40	2.98	198.2	11.06	28.3	0.03	0.6	0.23	0.93
S-41	21.16	382.1	14.64	25	0.03	0.6	0.27	1.07
S-42	19.51	312.7	14.71	16.6	0.03	0.6	0.27	1.07

Appendix A7 Summary of conduits property

Conduits Code	Conduit type	Inlet node	Outlet node	Length(m)	Depth (m)	Width (m)	Roughness
C1	Open/ Rectangular/Masonry	J1	J2	365	0.55	0.6	0.025
C2	Open/ Rectangular/Masonry	J2	J3	268	0.85	0.6	0.025
C3	Open/ Rectangular/Masonry	J3	J4	186.9	0.9	0.6	0.025
C4	Open/ Rectangular/Masonry	J4	J5	194.7	0.7	1	0.025
C5	Open/ Rectangular/Masonry	J5	J6	77	0.5	0.5	0.025
C6	Closed/ Rectangular/Masonry	J6	J7	479	1.2	0.95	0.025
C7	Open/ Rectangular/Masonry	J7	O2	501	1.2	1.3	0.025
C8	Open/ Rectangular/Masonry	J8	J9	493.2	0.9	0.65	0.025
C9	Closed/ Rectangular/Masonry	J9	J10	334.6	0.9	0.65	0.025

C10	Open/ Rectangular/Masonry	J11	J12	261.2	0.8	0.7	0.025
C11	Open/ Rectangular/Masonry	J12	J10	45	0.8	0.7	0.025
C12	Open/ Rectangular/Masonry	J10	J13	26.7	0.9	0.9	0.025
C13	Open/ Rectangular/Masonry	J14	J15	334.6	0.8	0.5	0.025
C14	Open/ Rectangular/Masonry	J16	J17	375.8	0.85	0.7	0.025
C15	Open/ Rectangular/Masonry	J17	J18	25	0.9	1	0.025
C16	Open/ Rectangular/Masonry	J18	J15	239.5	0.9	0.8	0.025
C17	Open/ Rectangular/Masonry	J19	J20	333	0.7	0.6	0.025
C18	Open/ Rectangular/Masonry	J20	J21	209	0.9	0.75	0.025
C19	Open/ Rectangular/Masonry	J21	J22	158.4	1.05	1.05	0.025
C20	Open/ Rectangular/Masonry	J22	J13	114.6	1.1	1.1	0.025
C21	Open/ Rectangular/Masonry	J13	O1	122	1.05	1	0.025
C22	Closed/ Rectangular/Masonry	J23	J24	77	0.55	0.95	0.025
C23	Closed/ Rectangular/Masonry	J24	J25	405.1	0.55	0.95	0.025
C24	Open/ Rectangular/Masonry	J25	J26	338	1.2	0.95	0.025
C25	Open/ Rectangular/Masonry	J26	O3	168.3	1.2	1	0.025
C26	Open/ Rectangular/Masonry	J27	J28	186	1.1	0.6	0.025
C27	Open/ Rectangular/Masonry	J28	J29	88.7	0.9	0.6	0.025
C28	Open/ Rectangular/Masonry	J29	J30	77	0.9	0.6	0.025

C29	Open/ Rectangular/Masonry	J30	J35	58	0.9	0.6	0.025
C30	Open/ Rectangular/Masonry	J32	J33	124	0.7	0.4	0.025
C31	Open/ Rectangular/Masonry	J33	J34	135	0.7	0.4	0.025
C32	Open/ Rectangular/Masonry	J34	J35	191	0.7	0.4	0.025
C33	Open/ Rectangular/Masonry	J31	J35	71.3	0.7	0.4	0.025
C34	Open/ Rectangular/Masonry	J35	J36	358.4	0.8	0.7	0.025
C35	Open/ Rectangular/Masonry	J36	J37	17.7	0.9	0.7	0.025
C36	Open/ Rectangular/Masonry	J37	O4	198	0.9	0.8	0.025
C37	Open/ Rectangular/Masonry	J38	J39	302.6	0.8	0.7	0.025
C38	Open/ Rectangular/Masonry	J39	J40	51.6	0.8	0.7	0.025
C39	Open/ Rectangular/Masonry	J40	J37	12.8	0.8	0.7	0.025
C40	Open/ Rectangular/Masonry	J41	J40	268.7	0.9	0.8	0.025
C41	Open/ Rectangular/Masonry	J42	J43	254.6	0.95	0.65	0.025
C42	Open/ Rectangular/Masonry	J15	J43	16.9	1.15	1.15	0.025
C43	Open/ Rectangular/Masonry	J43	J44	222	1.15	1.15	0.025
C44	Open/ Rectangular/Masonry	J44	J13	275.3	1.2	1.2	0.025
C45	Open/ Rectangular/Masonry	J45	J46	537.2	1.15	1.2	0.025
C46	Open/ Rectangular/Masonry	J46	O7	133.2	1.2	1.2	0.025
C47	Open/ Rectangular/Masonry	J47	J48	162	0.85	0.7	0.025

C48	Open/ Rectangular/Masonry	J48	J29	273.1	0.85	0.7	0.025
C49	Closed/ Rectangular/Masonry	J52	J53	220.7	1	0.4	0.025
C50	Open/ Rectangular/Masonry	J53	J54	205.6	1.1	0.4	0.025
C51	Open/ Rectangular/Masonry	J51	J54	136	0.9	0.75	0.025
C52	Open/ Rectangular/Masonry	J54	O5	231.3	1.1	1.1	0.025
C53	Open/ Rectangular/Masonry	J55	J56	196.5	1	0.4	0.025
C54	Open/ Rectangular/Masonry	J49	J50	504.9	0.8	0.7	0.025
C55	Open/ Rectangular/Masonry	J50	J56	145.9	0.95	0.7	0.025
C56	Open/ Rectangular/Masonry	J56	J57	185	1.2	0.9	0.025
C57	Open/ Rectangular/Masonry	J57	J58	314.3	1.15	1.1	0.025
C58	Open/ Rectangular/Masonry	J58	O6	277.5	1.15	1.2	0.025

Appendix A8 Summary of nodes property

Node Code	Node Type	Latitude (degree)	Longitude (degree)	Elevation (m)	Depth (m)
J1	Junction	11.921485	37.70475	1875.928	0.55
J2	Junction	11.923266	37.701931	1868.368	0.85
J3	Junction	11.924132	37.699684	1848.875	0.9
J4	Junction	11.92454	37.69805	1838.186	0.7
J5	Junction	11.925032	37.696309	1828.836	0.5
J6	Junction	11.925251	37.695643	1825.524	1.2
J7	Junction	11.921638	37.693237	1812.881	1.2
J8	Junction	11.925034	37.696227	1828.345	0.9

J9	Junction	11.921395	37.693629	1813.009	0.9
J10	Junction	11.918733	37.692421	1806.476	0.9
J11	Junction	11.921223	37.69361	1812.802	0.8
J12	Junction	11.919115	37.692563	1806.947	0.8
J13	Junction	11.918583	37.692555	1806.394	1.05
J14	Junction	11.921349	37.693695	1812.538	0.8
J15	Junction	11.919564	37.69616	1811.031	1.15
J16	Junction	11.92454	37.69805	1838.186	0.8
J17	Junction	11.921416	37.697692	1824.464	0.9
J18	Junction	11.921292	37.697494	1821.28	0.9
J19	Junction	11.921237	37.693611	1812.818	0.7
J20	Junction	11.91946	37.696064	1810.515	0.9
J21	Junction	11.91793	37.694926	1808.486	1.05
J22	Junction	11.918383	37.693543	1808.208	1.1
J23	Junction	11.925233	37.695426	1824.944	0.55
J24	Junction	11.924111	37.694661	1821.447	0.55
J25	Junction	11.92171	37.693069	1812.753	1.2
J26	Junction	11.918926	37.691871	1807.033	1.2
J27	Junction	11.924212	37.689528	1820.239	1.1
J28	Junction	11.9232	37.690788	1815.349	0.9
J29	Junction	11.922755	37.691465	1814.904	0.9
J30	Junction	11.922382	37.69206	1813.571	0.9
J31	Junction	11.921759	37.693062	1813.823	0.7
J32	Junction	11.925517	37.694779	1825.229	0.7
J33	Junction	11.92458	37.694156	1823.018	0.7
J34	Junction	11.923561	37.693481	1819.365	0.7
J35	Junction	11.922115	37.692516	1813.087	0.8
J36	Junction	11.919079	37.691403	1807.654	0.9
J37	Junction	11.918997	37.691263	1807.292	0.9
J38	Junction	11.921982	37.692424	1812.646	0.8

J39	Junction	11.91943	37.691438	1808.864	0.8
J40	Junction	11.919096	37.691324	1807.711	0.8
J41	Junction	11.919911	37.689	1807.853	0.9
J42	Junction	11.921196	37.697611	1821.787	0.95
J43	Junction	11.919411	37.696156	1810.542	1.15
J44	Junction	11.917796	37.694952	1808.628	1.2
J45	Junction	11.921386	37.697703	1824.34	1.15
J46	Junction	11.918161	37.701321	1817.467	1.2
J47	Junction	11.926045	37.693668	1828.298	0.85
J48	Junction	11.924211	37.692457	1825.912	0.85
J49	Junction	11.923832	37.703106	1856.569	0.8
J50	Junction	11.927185	37.701683	1819.464	0.95
J51	Junction	11.926786	37.699842	1825.942	0.9
J52	Junction	11.926133	37.696276	1827.167	1
J53	Junction	11.92748	37.697731	1820.167	1.1
J54	Junction	11.927971	37.699536	1813.841	1.1
J55	Junction	11.928012	37.699633	1813.303	1
J56	Junction	11.928426	37.701276	1809.904	1.2
J57	Junction	11.929133	37.702992	1804.216	1.15
J58	Junction	11.931326	37.704929	1800.155	1.15
O1	Outfall	11.917513	37.692258	1806.41	1.05
O2	Outfall	11.917442	37.691637	1805.169	1.2
O3	Outfall	11.917482	37.691372	1804.703	1.2
O4	Outfall	11.917274	37.691155	1805.033	0.9
O5	Outfall	11.929972	37.699065	1800.049	1.1
O6	Outfall	11.933332	37.706426	1797.714	1.15
O7	Outfall	11.916969	37.701238	1813.202	1.2

Appendix B1 Peak flow hydrograph of the catchment of culverts

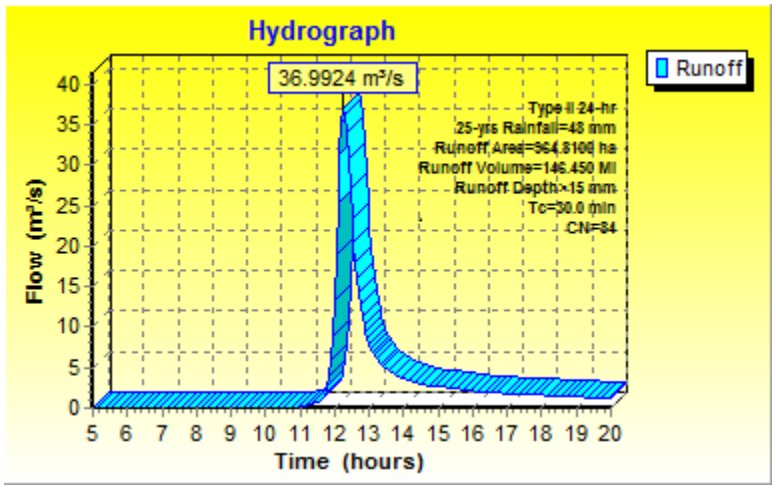

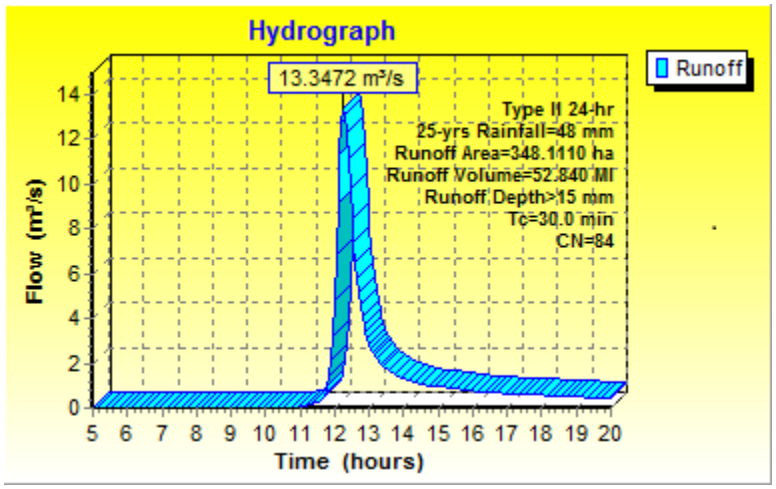

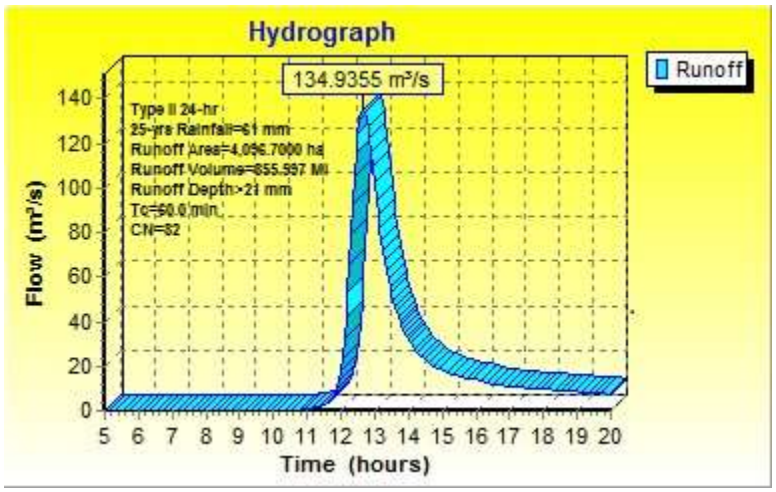

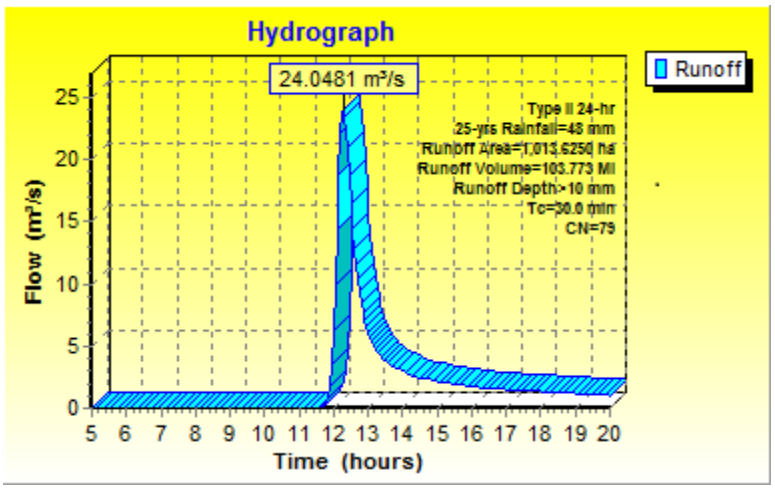

Appendix B2 Summary of flow at crossing on culvert 1

Headwater Elevation (m)	Total Discharge (cms)	Culvert 1 Discharge (cms)	Roadway Discharge (cms)	Iterations
1808.03	1.33	1.33	0.00	1
1808.64	3.70	3.70	0.00	1
1809.55	7.40	5.82	1.58	6
1809.93	11.10	6.53	4.57	4
1810.24	14.80	7.05	7.75	3
1810.52	18.50	7.42	11.08	3
1810.78	22.20	7.73	14.47	3
1811.02	25.90	8.02	17.88	3
1811.25	29.60	8.28	21.32	3
1811.46	33.30	8.51	24.79	3
1811.66	37.00	8.73	28.27	3
1809.19	5.06	5.06	0.00	Overtopping

Appendix B3 Summary of flow at crossing on culvert 2

Headwater Elevation (m)	Total Discharge (cms)	Culvert 2 Discharge (cms)	Roadway Discharge (cms)	Iterations
1805.94	0.00	0.00	0.00	1
1806.68	7.90	7.90	0.00	1
1806.98	13.30	13.30	0.00	1
1807.47	23.71	23.71	0.00	1
1807.78	31.62	31.62	0.00	1
1808.07	39.52	39.52	0.00	1
1808.34	47.43	47.43	0.00	1
1808.59	55.34	55.34	0.00	1
1808.84	63.24	63.24	0.00	1
1809.10	71.14	71.14	0.00	1
1809.35	79.05	79.05	0.00	1
1809.65	87.74	87.74	0.00	Overtopping

Appendix B4 Summary of flow at crossing on culvert 3

Headwater Elevation (m)	Total Discharge (cms)	Culvert 3 Discharge (cms)	Roadway Discharge (cms)	Iterations
1805.96	0.00	0.00	0.00	1
1806.94	13.49	13.49	0.00	1
1807.51	26.98	26.98	0.00	1
1807.99	40.47	40.47	0.00	1
1808.42	53.96	53.96	0.00	1
1808.81	67.45	67.45	0.00	1
1809.19	80.94	80.94	0.00	1

1809.69	96.84	96.84	0.00	1
1810.06	107.92	107.92	0.00	1
1810.52	121.41	121.18	0.23	5
1810.88	134.90	130.77	4.13	4
1810.46	119.48	119.48	0.00	Overtopping

Appendix B5 Summary of flow at crossing on culvert 4

Headwater Elevation (m)	Total Discharge (cms)	Culvert 4 Discharge (cms)	Roadway Discharge (cms)	Iterations
1798.39	0.00	0.00	0.00	1
1798.92	2.81	2.81	0.00	1
1799.16	5.63	5.63	0.00	1
1799.39	8.44	8.44	0.00	1
1799.60	11.25	11.25	0.00	1
1799.79	14.07	14.07	0.00	1
1799.97	16.88	16.88	0.00	1
1800.14	19.69	19.69	0.00	1
1800.32	22.50	22.50	0.00	1
1800.41	24.00	24.00	0.00	1
1800.69	28.13	28.13	0.00	1
1800.79	29.47	29.47	0.00	Overtopping

Appendix B6 Summary of freeboard performance index of channels

Link / Channel	Maximum volume of the channel (Voli)	Freeboard performance Index (PIF_i)	PIF_i*Vol_i
C1	445.4	1.0	445.4
C2	471.2	1.0	471.2
C3	2392.9	1.0	2392.9
C4	2389.9	0.9	2198.7
C5	1056.7	0.0	0.0
C6	6388.1	1.0	6388.1
C7	7021.8	1.0	7021.8
C8	1142.4	1.0	1142.4
C9	1659.1	1.0	1659.1
C10	1982.0	0.9	1843.2
C11	1982.0	1.0	1982.0
C12	2753.1	0.8	2257.5
C13	897.1	0.0	0.0
C14	2020.0	0.0	0.0
C15	2020.0	1.0	2020.0
C16	3526.7	0.7	2609.8
C17	432.0	0.8	354.2
C18	472.6	1.0	472.6
C19	2653.5	0.7	1777.8
C20	2950.0	1.0	2950.0
C21	4619.2	0.0	0.0
C22	552.0	1.0	552.0
C23	1727.5	0.7	1140.2
C24	1780.4	1.0	1780.4
C25	1836.9	1.0	1836.9
C26	3557.4	1.0	3557.4

C27	1698.0	0.0	0.0
C28	3841.2	0.3	1152.4
C29	945.0	0.0	0.0
C30	789.5	0.6	481.6
C31	1567.0	0.0	15.7
C32	1822.9	0.1	200.5
C33	2776.1	0.0	0.0
C34	4290.0	0.0	0.0
C35	2286.9	0.0	0.0
C36	1009.6	1.0	1009.6
C37	1031.0	1.0	1031.0
C38	1840.3	0.9	1674.7
C39	607.0	0.0	0.0
C40	562.3	1.0	562.3
C41	4868.6	1.0	4868.6
C42	5573.1	0.8	4625.7
C43	6483.2	0.8	5445.9
C44	15061.1	0.1	2108.6
C45	15247.1	0.7	10977.9
C46	868.6	1.0	868.6
C47	1599.8	1.0	1599.8
C48	1975.0	0.6	1086.2
C49	2097.9	0.0	0.0
C50	3740.4	1.0	3740.4
C51	14688.0	0.0	0.0
C52	1694.6	0.7	1186.2
C53	3814.3	1.0	3814.3
C54	3839.5	1.0	3839.5
C55	18443.9	0.1	2397.7
C56	7856.6	0.0	0.0

C57	6681.6	0.0	0.0

Appendix B7 Summary of Velocity performance index of channels

Link / Channel	Maximum Velocity (m/sec)	Velocity performance Index (PIV)	Maximum volume of the channel (Voli)	PIVi*Voli
C1	1.56	1	445.4	445.44
C2	2.42	1	471.2	471.24
C3	3.02	1	2392.9	2392.92
C4	2.79	1	2389.9	2389.86
C5	2.52	1	1056.7	1056.72
C6	2.55	1	6388.1	6388.08
C7	2.15	1	7021.8	7021.8
C8	1.97	1	1142.4	1142.4
C9	1.77	1	1659.1	1659.12
C10	1.38	1	1982.0	1981.98
C11	1.84	1	1982.0	1981.98
C12	0.99	0.9	2753.1	2477.79
C13	0.89	0.8	897.1	717.696
C14	2.36	1	2020.0	2019.96
C15	3.43	1	2020.0	2019.96
C16	2.85	1	3526.7	3526.74
C17	0.97	0.97	432.0	419.04
C18	1.07	1	472.6	472.56
C19	0.81	0.8	2653.5	2122.8
C20	1.87	1	2950.0	2949.96
C21	1.75	1	4619.2	4619.16
C22	1.78	1	552.0	552
C23	1.82	1	1727.5	1727.52

C24	1.68	1	1780.4	1780.38
C25	1.55	1	1836.9	1836.9
C26	2.2	1	3557.4	3557.4
C27	1.05	1	1698.0	1698
C28	2.1	1	3841.2	3841.2
C29	0.83	0.85	945.0	803.25
C30	1.43	1	789.5	789.48
C31	1.91	1	1567.0	1567.02
C32	2.07	1	1822.9	1822.86
C33	1.93	1	2776.08	2776.08
C34	2.28	1	4290	4290
C35	1.51	1	2286.9	2286.9
C36	1.42	1	1009.56	1009.56
C37	1.76	1	1031.04	1031.04
C38	2.34	1	1840.32	1840.32
C39	0.39	0.38	606.96	230.6448
C40	1.71	1	562.32	562.32
C41	2.41	1	4868.64	4868.64
C42	1.74	1	5573.1	5573.1
C43	1.74	1	6483.24	6483.24
C44	2.4	1	15061.14	15061.14
C45	3.44	1	15247.08	15247.08
C46	1.26	1	868.56	868.56
C47	2.25	1	1599.84	1599.84
C48	2.09	1	1974.96	1974.96
C49	2.16	1	2097.9	2097.9
C50	3.86	1	3740.4	3740.4
C51	4.41	0.85	14688	12484.8
C52	1.54	1	1694.58	1694.58
C53	3.39	1	3814.26	3814.26

C54	2.71	1	3839.52	3839.52
C55	3.3	1	18443.88	18443.88
C56	2.35	1	7856.64	7856.64
C57	2.02	1	6681.6	6681.6

Appendix C1: Percentile point of the t- Distribution

Percentile Points of the t-Distribution t{v,p for the 5-Per-Cent Level of Significance (Two-Tailed)

$p = P(t <= t_p)$:		0.025	0.975
v:	4	−2.78	2.78
	5	−2.57	2.57
	6	−2.54	2.54
	7	−2.36	2.36
	8	−2.31	2.31
	9	−2.26	2.26
	10	−2.23	2.23
	11	−2.20	2.20
	12	−2.18	2.18
	14	−2.14	2.14
	16	−2.12	2.12
	18	−2.10	2.10
	20	−2.09	2.09
	24	−2.06	2.06
	30	−2.04	2.04
	40	−2.02	2.02
	60	−2.00	2.00
	100	−1.98	1.98
	160	−1.97	1.97
	∞	−1.96	1.96

Note: It is customary to take the next higher v-value if the required number of degrees of freedom is not listed in a table. It is evident that this practice will produce a more severe test.

Appendix C2: Percentile point of F-Distribution

Percentile Points of the F-Distribution $F\{\upsilon_1,\upsilon_2,p\}$ for the 5-Per-Cent Level of Significance (Two-Tailed)

p = P(F < = F_p)		v_1: 4	5	6	7	8	9	10	11	12	14	16
0.025	v_2: 5	.107	.140	.169								
0.975		7.39	7.15	6.98								
0.025	6		.143	.172	.195							
0.975			5.99	5.82	5.70							
0.025	7			.176	.200	.221						
0.975				5.12	4.99	4.90						
0.025	8				.204	.226	.244					
0.975					4.53	4.43	4.36					
0.025	9					.230	.248	.265				
0.975						4.10	4.03	3.96				
0.025	10						.252	.269	.284			
0.975							3.78	3.72	3.66			
0.025	11							.273	.288	.301		
0.975								3.53	3.47	3.43		
0.025	12								.292	.305	.328	
0.975									3.32	3.28	3.21	
0.025	14									.312	.336	.355
0.975										3.05	2.98	2.92

Continued

p = P(F <= F_p)		v_1:14	16	18	20	24	30	40	60	100	160	∞
0.025	v_2:16	.342	.362	.379								
0.975		2.82	2.76	2.71								
0.025	18		.368	.385	.400							
0.975			2.64	2.60	2.56							
0.025	20			.391	.406	.430						
0.975				2.50	2.46	2.41						
0.025	24				.415	.441	.468					
0.975					2.33	2.27	2.21					
0.025	30					.453	.482	.515				
0.975						2.14	2.07	2.01				
0.025	40						.498	.533	.573			
0.975							1.94	1.88	1.80			
0.025	60							.555	.600	.642		
0.975								1.74	1.67	1.60		
0.025	100								.625	.674	.706	
0.975									1.56	1.48	1.44	
0.025	160									.696	.733	
0.975										1.42	1.36	
0.025	∞											1.00
0.975												1.00

Appendix C3: Kn values of different sample size

Outlier test K_n values

Sample size *n*	K_n	Sample size *n*	K_n	Sample size *n*	K_n	Sample size *n*	K_n
10	2.036	24	2.467	38	2.661	60	2.837
11	2.088	25	2.486	39	2.671	65	2.866
12	2.134	26	2.502	40	2.682	70	2.893
13	2.175	27	2.519	41	2.692	75	2.917
14	2.213	28	2.534	42	2.700	80	2.940
15	2.247	29	2.549	43	2.710	85	2.961
16	2.279	30	2.563	44	2.719	90	2.981
17	2.309	31	2.577	45	2.727	95	3.000
18	2.335	32	2.591	46	2.736	100	3.017
19	2.361	33	2.604	47	2.744	110	3.049
20	2.385	34	2.616	48	2.753	120	3.078
21	2.408	35	2.628	49	2.760	130	3.104
22	2.429	36	2.639	50	2.768	140	3.129
23	2.448	37	2.650	55	2.804		

Source: U.S. Water Resources Council, 1981. This table contains one-sided 10-percent significance level K_n values for the normal distribution.

Appendix C4: Manning roughness values of different types of linings

Type of lining	condition	n
Glazed coating of enamel Timber	In perfect order	0.010
	(a) Plane boards carefully laid	0.014
	(b) Plane Boards inferior workmanship or aged,	0.016
	(c) None-plane boards carefully laid	0.016
	(d) Non-plane boards inferior workmanship or aged	0.018
Masonry	(a) Neat cement plaster	0.013
	(b) Sand and cement plaster	0.015
	(c) Concrete, Steel troweled	0.014
	(d) Concrete, Wood troweled	0.015
	(e) Brick in good condition	0.015
	(f) Brick in rough condition	0.017
	(g) Masonry in bad condition	0.020
Stone work	(a) Smooth, dressed ashlar	0.015
	(b) Rubble set in cement	0.017
	(c) Fine, well packed gravel	0.020
Earth	(a) Regular surface in good condition	0.020
	(b) In ordinary condition	0.025
	(c) With Stones and weeds	0.030
	(d) In poor condition	0.035
	(e) Partially obstructed with debris or weeds	0.050
Steel	(a) Welded	0.013
	(b) Riveted	0.017
	(c) Slightly tuberculated	0.020
	(d) Cement Mortar lined	0.011
Cast Iron & Ductile Iron	(a) Unlined	0.013
	(b) cement mortar lined	0.011
Asbestos Cement		0.012
Plastic (Smooth)		0.011

Appendix C5 Return periods of different hydraulic structures

Generalized design criteria for water-control structures

Type of structure	Return period (years)	ELV
Highway culverts		
Low traffic	5–10	–
Intermediate traffic	10–25	–
High traffic	50–100	–
Highway bridges		
Secondary system	10–50	–
Primary system	50–100	–
Farm drainage		
Culverts	5–50	–
Ditches	5–50	–
Urban drainage		
Storm sewers in small cities	2–25	–
Storm sewers in large cities	25–50	–
Airfields		
Low traffic	5–10	–
Intermediate traffic	10–25	–
High traffic	50–100	–
Levees		
On farms	2–50	–
Around cities	50–200	–
Dams with no likelihood of loss of life (low hazard)		
Small dams	50–100	–
Intermediate dams	100 +	–
Large dams	–	50–100%
Dams with probable loss of life (significant hazard)		
Small dams	100 +	50%
Intermediate dams	–	50–100%
Large dams	–	100%
Dams with high likelihood of considerable loss of life (high hazard)		
Small dams	–	50–100%
Intermediate dams	–	100%
Large dams	–	100%

Appendix D1 Sub-catchments calculated runoff by SWMM

Sub-catchment	Total Precipitation (mm)	Total Infiltration (mm)	Impervious Runoff (mm)	Pervious Runoff (mm)	Total Runoff (mm)	Total Runoff (10^6*ltr)	Peak Runoff (m^3/sec)	Runoff Coefficient
S1	120.8	15.61	19.81	83.52	83.52	1.98	0.28	0.691
S2	120.8	14.68	25.85	89.01	89.01	1.17	0.17	0.737
S3	120.8	8.12	65.92	31.36	97.28	1.43	0.23	0.805
S4	120.8	14.1	29.2	69.1	69.1	1.26	0.17	0.572
S5	120.8	10.85	50.18	92.92	92.92	3.82	0.57	0.769
S6	120.8	11.99	43.07	92.94	92.94	0.46	0.07	0.769
S7	120.8	12.83	37.52	84.92	84.92	3.07	0.43	0.703
S8	120.8	11.3	46.88	83.33	83.33	0.87	0.12	0.69
S9	120.8	13.69	32.26	96.61	96.61	2.19	0.35	0.8
S10	120.8	10.64	51.14	93.19	93.19	7.68	1.16	0.771
S11	120.8	10.23	54.58	102.81	102.81	2.02	0.36	0.851
S12	120.8	10.33	54.01	105.47	105.47	0.96	0.19	0.873
S13	120.8	9.5	58.42	93.51	93.51	0.94	0.14	0.774
S14	120.8	13.33	34.18	78.32	78.32	0.67	0.09	0.648
S15	120.8	16.53	13.87	68.71	68.71	9.06	1.19	0.569
S16	120.8	3.36	94.28	103.11	103.11	1.97	0.34	0.854
S17	120.8	2.35	61.83	39.95	101.78	1.54	0.24	0.843
S18	120.8	10.34	53.24	92.44	92.44	1.95	0.29	0.765

S19	120.8	10.96	49.7	96.8	96.8	1.46	0.23	0.801
S20	120.8	12.42	40.29	90.78	90.78	1.36	0.2	0.751
S21	120.8	3.01	47.32	101.99	101.99	1.49	0.23	0.844
S22	120.8	13.87	30.9	83.13	83.13	5.57	0.77	0.688
S23	120.8	10.31	53.91	98.8	98.8	1.74	0.28	0.818
S24	120.8	14.34	27.93	82.33	82.33	1.37	0.19	0.682
S25	120.8	10.48	52.85	98.73	98.73	1.58	0.26	0.817
S26	120.8	7.23	73.32	103.73	103.73	1.14	0.2	0.859
S27	120.8	10.59	51.86	94.15	94.15	2.04	0.31	0.779
S28	120.8	11.19	48.2	94.83	94.83	3.53	0.54	0.785
S29	120.8	3.76	29.24	85.97	85.97	23.16	3.1	0.712
S30	120.8	6.01	81.75	30.85	112.6	2.03	0.42	0.932
S31	120.8	11.09	48.96	98.64	98.64	3.39	0.56	0.817
S32	120.8	12.49	39.45	47.14	86.59	1.96	0.24	0.717
S33	120.8	8.46	63.38	82.51	82.51	4.41	0.61	0.683
S34	120.8	3.23	39.66	47.74	47.74	2.99	0.42	0.395
S35	120.8	3.33	38.99	79.5	79.5	20.21	2.66	0.658
S36	120.8	3.22	42.35	101.46	101.46	6.73	1.04	0.84
S37	120.8	2.48	59.89	103.91	103.91	3.92	0.63	0.86
S38	120.8	2.4	53.96	89.27	89.27	9.75	1.37	0.739
S39	120.8	2.19	67.06	107.52	107.52	3.41	0.6	0.89
S40	120.8	3.56	34.14	101.11	101.11	3.01	0.46	0.837

S41	120.8	3.73	29.82	80.34	80.34	17	2.23	0.665
S42	120.8	4.15	19.89	73.11	73.11	14.26	1.84	0.605

Appendix D2 Prepared shortest duration rainfall data of Woreta metrological Station

T in min													
		15	30	45	60	75	90	105	120	135	150	165	180
T in Hr													
year	24	0.25	0.50	0.75	1.00	1.25	1.50	1.75	2.00	2.25	2.50	2.75	3.00
1987	50.0	18.3	25.8	29.9	32.7	34.6	36.1	37.3	38.2	39.0	39.7	40.3	40.8
1988	108.2	39.7	55.8	64.8	70.7	74.9	78.1	80.6	82.7	84.4	85.9	87.2	88.3
1989	64.3	23.6	33.2	38.5	42.0	44.5	46.4	47.9	49.1	50.2	51.1	51.8	52.5
1990	70.2	25.7	36.2	42.0	45.9	48.6	50.7	52.3	53.7	54.8	55.7	56.6	57.3
1991	64.6	23.7	33.3	38.7	42.2	44.7	46.6	48.1	49.4	50.4	51.3	52.1	52.7
1992	65.8	24.1	33.9	39.4	43.0	45.5	47.5	49.0	50.3	51.3	52.3	53.0	53.7
1993	62.4	22.9	32.2	37.4	40.8	43.2	45.0	46.5	47.7	48.7	49.6	50.3	51.0
1994	68.0	24.9	35.1	40.7	44.4	47.1	49.1	50.7	52.0	53.1	54.0	54.8	55.5
1995	48.0	17.6	24.7	28.8	31.4	33.2	34.6	35.8	36.7	37.5	38.1	38.7	39.2
1996	72.4	26.5	37.3	43.4	47.3	50.1	52.3	53.9	55.3	56.5	57.5	58.4	59.1
1997	38.5	14.1	19.9	23.1	25.2	26.7	27.8	28.7	29.4	30.0	30.6	31.0	31.4
1998	40.5	14.9	20.9	24.3	26.5	28.1	29.3	30.2	31.0	31.6	32.2	32.7	33.1

1999	47.5	17.4	24.5	28.5	31.1	32.9	34.3	35.4	36.3	37.1	37.7	38.3	38.8
2000	37.6	13.8	19.4	22.5	24.6	26.0	27.1	28.0	28.7	29.3	29.8	30.3	30.7
2001	54.2	19.9	27.9	32.4	35.4	37.5	39.1	40.4	41.4	42.3	43.0	43.7	44.2
2002	74.1	27.2	38.2	44.4	48.4	51.3	53.5	55.2	56.7	57.9	58.9	59.8	60.5
2003	79.6	29.2	41.0	47.7	52.0	55.1	57.4	59.3	60.8	62.1	63.2	64.2	65.0
2004	73.8	27.1	38.1	44.2	48.2	51.1	53.3	55.0	56.4	57.6	58.6	59.5	60.3
2005	58.2	21.3	30.0	34.9	38.0	40.3	42.0	43.4	44.5	45.4	46.2	46.9	47.5
2006	54.3	19.9	28.0	32.5	35.5	37.6	39.2	40.5	41.5	42.4	43.1	43.8	44.3
2007	63.5	23.3	32.7	38.0	41.5	44.0	45.8	47.3	48.5	49.6	50.4	51.2	51.9
2008	61.5	22.5	31.7	36.8	40.2	42.6	44.4	45.8	47.0	48.0	48.8	49.6	50.2
2009	55.6	20.4	28.7	33.3	36.3	38.5	40.1	41.4	42.5	43.4	44.2	44.8	45.4
2010	70.0	25.7	36.1	41.9	45.7	48.5	50.5	52.2	53.5	54.6	55.6	56.4	57.2
2011	66.0	24.2	34.0	39.5	43.1	45.7	47.6	49.2	50.4	51.5	52.4	53.2	53.9
2012	57.5	21.1	29.6	34.4	37.6	39.8	41.5	42.8	43.9	44.9	45.7	46.3	47.0
2013	80.0	29.3	41.2	47.9	52.3	55.4	57.7	59.6	61.1	62.4	63.5	64.5	65.3
2014	60.0	22.0	30.9	35.9	39.2	41.5	43.3	44.7	45.9	46.8	47.6	48.4	49.0
2015	80.0	29.3	41.2	47.9	52.3	55.4	57.7	59.6	61.1	62.4	63.5	64.5	65.3
2016	68.9	25.3	35.5	41.3	45.0	47.7	49.7	51.3	52.7	53.8	54.7	55.5	56.3